Barton Springs
Edwards Aquifer
CONSERVATION DISTRICT

The BSEACD Trinity Aquifer Sustainability Model: A Tool for Evaluating Sustainable Yield of the Trinity Aquifer in Hays County, Texas

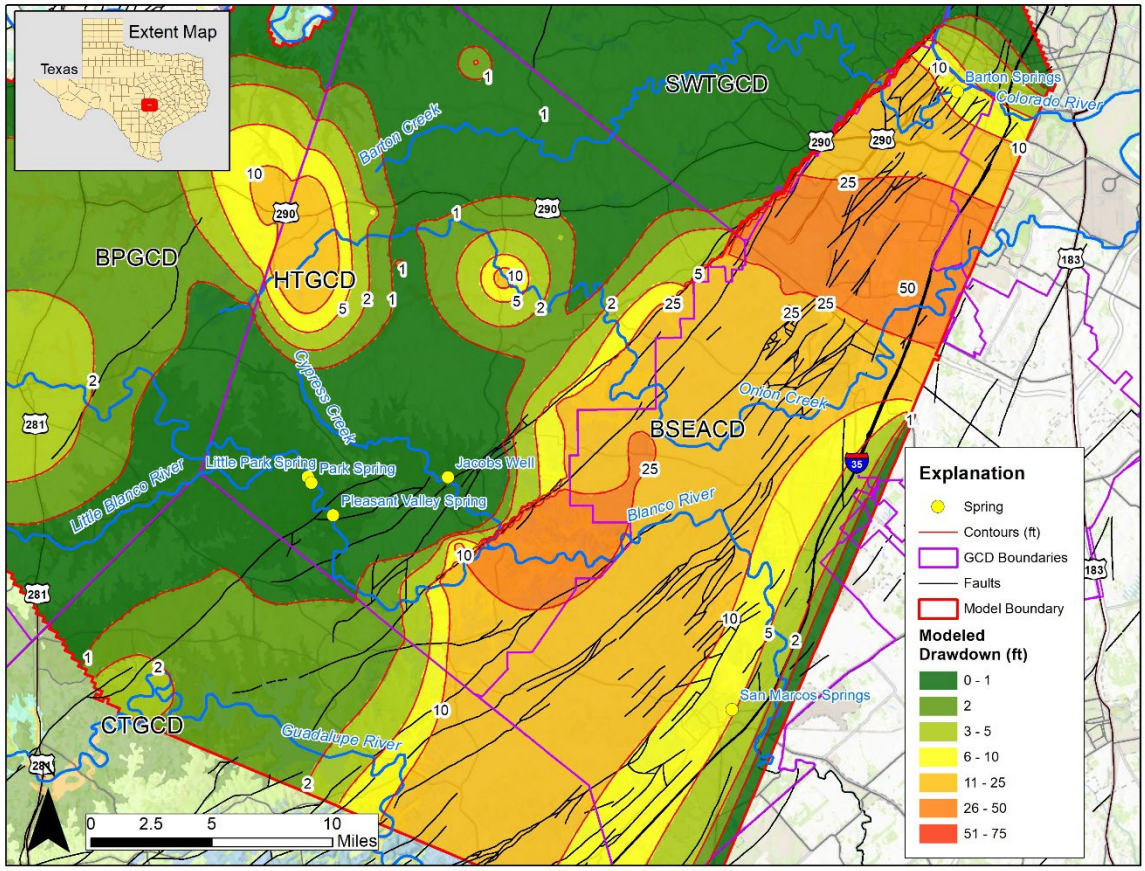

BSEACD Report of Investigations 2023-0717
July 2023

Barton Springs/Edwards Aquifer Conservation District
1124 Regal Row
Austin, Texas

The BSEACD Trinity Aquifer Sustainability Model: A Tool for Evaluating Sustainable Yield of the Trinity Aquifer in Hays County, Texas

Jeffery A. Watson, P.G., and Brian A. Smith, Ph.D., P.G.
Barton Springs/Edwards Aquifer Conservation District

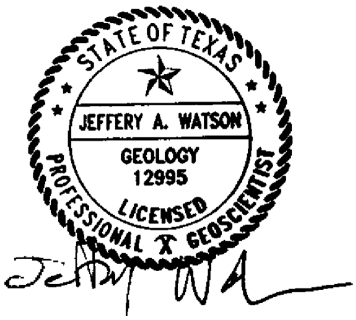

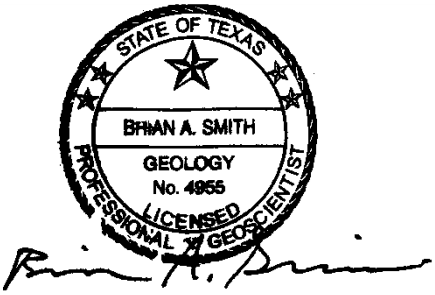

BSEACD Report of Investigations 2023-0717

July 2023

Barton Springs/Edwards Aquifer Conservation District
1124 Regal Row
Austin, Texas

Disclaimer

All of the information provided in this report is believed to be accurate and reliable; however, the Barton Springs/Edwards Aquifer Conservation District and the report's authors assume no liability for any errors or for the use of the information provided.

Cover. Modeled drawdown map for predictive model scenario C-1: recurrence of 10-year drought of record with 2020 pumping.

Contents

List of Figures

List of Tables

List of Abbreviations

BFZ	Balcones Fault Zone
BSEACD	Barton Springs/Edwards Aquifer Conservation District
cfs	Cubic feet per second
cfd	Cubic feet per day
CTGCD	Comal Trinity Groundwater Conservation District
GHB	General Head Boundary (MODFLOW package)
gpm	Gallons per minute
HFB	Horizontal Flow Barrier (MODFLOW package)
HTGCD	Hays Trinity Groundwater Conservation District
JWS	Jacob's Well Spring
Kh	Horizontal hydraulic conductivity
Kv	Vertical hydraulic conductivity
Kgrl	Lower Glen Rose Formation (Cretaceous)
PVS	Pleasant Valley Spring
SWTCGCD	Southwest Travis County Groundwater Conservation District
TAS	Trinity Aquifer Sustainability model
TDS	Total dissolved solids
TWDB	Texas Water Development Board

Abstract

The Trinity Aquifer in Hays County is an important groundwater resource which is the only available source of drinking water to people living in central and western Hays County, and is the source of ecologically, culturally, and economically important springs within the Blanco River Basin. Pumping has increased in recent years as a result of rapid population growth, putting increasing strain on this critical groundwater resource. Numerical groundwater models are a useful tool for simulating impacts of different pumping and/or recharge conditions, and thus are a valuable tool for guiding the groundwater planning process. This report documents development of the Trinity Aquifer Sustainability model (TAS), a transient numerical groundwater model developed by the Barton Springs/Edwards Aquifer Conservation District to guide development of a policy framework for sustainable management of the Trinity.

The TAS utilizes MODFLOW USG, a modular finite-difference flow model, for simulating hydraulic head (water level) and springflow in the Trinity Aquifer. The conceptual model for the TAS consists of the three hydrostratigraphic units in the Middle Trinity Aquifer (from top to bottom): the Lower Glen Rose, Hensel, and Cow Creek. Regional groundwater flow is generally from west to east over the study area. Springs discharge from the Middle Trinity Aquifer as artesian springs within the Blanco River basin upstream of the Balcones Fault Zone, including Pleasant Valley Spring and Jacobs Well Spring, and as gravity-fed seeps and small springs along some reaches of the Pedernales River. Recharge enters the model in portions of the Blanco River and Onion Creek Basins. Pumping is represented as both discreet (non-exempt) pumping wells and as distributed, non-discreet polygons (exempt). Faults associated with the Balcones Fault Zone displace hydrostratigraphic units downward from west to east, and act as barriers to lateral groundwater flow.

The TAS was calibrated over a 13-year transient simulation period from 2008-2020 using a combination of manual parameter adjustments and automatic calibration using the PEST software package. Head calibration targets consisted of water level measurements from monitoring wells throughout the study area with 4128 observations. Springflow calibration targets consisted of a combination of manual springflow measurements and monthly-averaged continuous USGS flow gage measurements. Sensitivity analyses for specific model parameters were performed to evaluate the impact of individual parameter uncertainties on overall model performance. Horizontal hydraulic conductivity, general head boundary head elevation, and recharge were determined to be the most sensitive of the parameters evaluated for impacting head calibration statistics. Storage parameters had minimal sensitivity to calibration statistics.

Predictive models were constructed from the calibrated TAS model to evaluate the impact of different pumping and drought scenarios on aquifer water levels and spring discharge. These predictive models indicate that increases in pumping across the study area have the potential to result in significant decreases in water levels and significant reductions in springflow. Predictive scenarios approximating the 1950's drought of record show that drought also has an important impact on water levels and springflow, especially when coupled with increased pumping. These predictive model scenarios, and others planned for future development, will be a valuable tool for guiding Trinity Aquifer groundwater management policymaking for the Barton Springs/Edwards Aquifer Conservation District.

Introduction

Rapid growth in central Texas is placing significant demand on water resources. With groundwater being the primary source of water supply in central and western Hays County, studies of the Trinity Aquifers are being conducted to better understand potential impacts to the aquifers, to users, and to ecological resources from this increased demand. Significant increases in water demand in conjunction with frequent droughts could cause significant lowering of water levels in wells plus decreasing flow from springs that are the sources of water to many of the streams that cross the Hill Country. Decreased flow in these streams can lead to degraded water quality that can impact ecological and economic resources. Decreased flow can also lead to less recharge in the Edwards Aquifer and ultimately impacts to the endangered species that live in San Marcos Springs and Barton Springs. In addition to data that have been collected over many years, numerical models are one of the best tools for predicting responses to increased pumping and drought on the Trinity Aquifers.

The Middle Trinity Aquifer is the primary groundwater resource for the central and western portions of Hays County which includes large portions of BSEACD. However, specific groundwater availability numbers and policies for the study area in BSEACD are lacking. This is primarily due to the complexity of the groundwater system, recent increases in demand, and lack of historic water-level, pumping, and water-quality data.

This lack of data, and the need for BSEACD to understand the hydrogeology of the Trinity Aquifers within and adjacent to the BSEACD boundaries was recognized more than 15 years ago and has culminated in studies that have significantly increased our understanding of the system (Wierman et al., 2010; Wong et al., 2014; Hunt et al., 2017a; Smith et al., 2018; Martin et al., 2019; Hunt et al., 2020). Thus, the science and understanding of the system (conceptual model) has reached a level that enables development of regional and local-scale numerical models with some confidence. Although a regional groundwater availability model (GAM) for the Trinity Aquifers of the Hill Country has been developed by the Texas Water Development Board (TWDB) (Jones et al., 2011), that model covers a very large area and only covers a small portion of the BSEACD boundaries. The model utilizes a large cell size (1 mile by 1 mile) which does not provide adequate detail to meet the needs of the BSEACD.

To fill in these key modeling gaps, BSEACD Aquifer Science staff began development of the Trinity Aquifer Sustainability Model (TAS) in 2019 (previously called the “BSEACD In-house Model”). A calibrated steady state version of the TAS was completed in late 2020 (Hunt and Smith, 2020). Construction of a transient version of the TAS began in 2021. This report presents the first phase of transient TAS model construction and presents a preliminary set of predictive model simulations which can be used to inform the BSEACD Trinity sustainable yield policymaking efforts, and have been established as a priority for the BSEACD. A second phase of improvement/refinement of the TAS and building out new predictive scenarios will continue in conjunction with ongoing Trinity sustainable yield policymaking efforts.

Study Area

The study area covers the Middle Trinity Aquifer within Hays County and portions of Travis, Comal, and Blanco Counties (Figure 1). The study area traverses two major physiographic provinces in central Texas: the eastern edge of the Edwards Plateau (also known as the Hill Country) and the western edge of the Gulf Coastal Plains (also known as the Blackland Prairies) defined by the prominent Balcones Escarpment. These provinces are underlain by Cretaceous strata and various geologic structures (Hill and Vaughn, 1898).

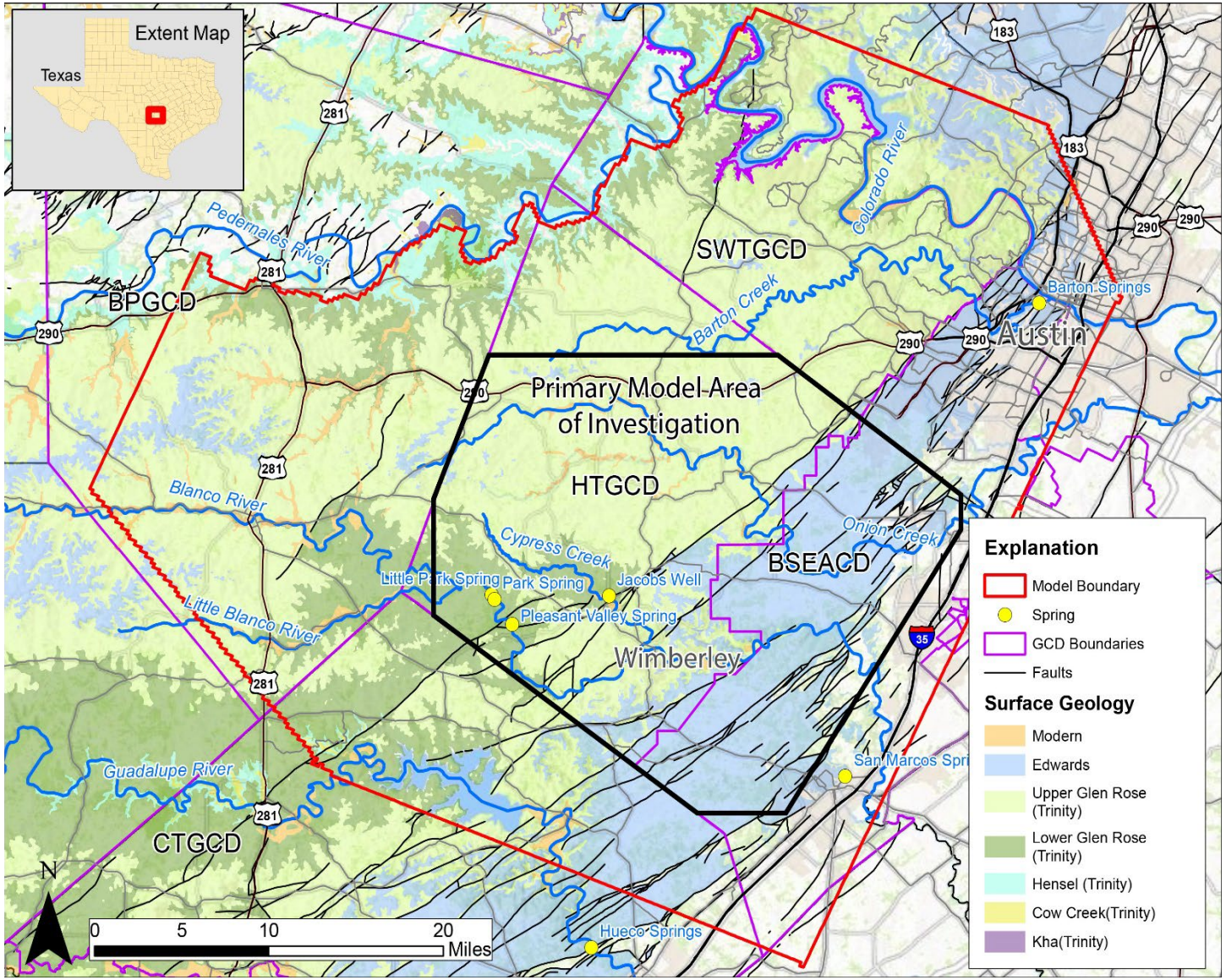

Figure 1. Map of study area and TAS model domain boundary and key points of interest and primary model area of investigation.

Purpose and Model Objectives

Area of Focus for Model Investigation

The primary area of focus for the TAS model is approximately coincident with Hays County extending from the Hays/Blanco County line in the west to IH-35 in the east (Figure 1). Model cells and boundary conditions along the margins of the model domain have been extended well outside this main area of interest to reduce the influence of margin boundary conditions on modeling results. This area of focus was selected because it encompasses the most critical portions of the Trinity Aquifer for recharge and pumping as it pertains to groundwater availability within BSEACD jurisdictional boundaries. Thus, refined modeling of this area will necessarily produce more accurate estimates of groundwater budgets and simulated impacts from pumping under different scenarios.

Steady-State vs. Transient

In a steady-state model, the hydrologic parameters, computed heads, and fluxes are constant in time and are inherently simpler than transient models. Transient models include parameters such as recharge, water levels, pumping, and spring discharge that all vary over time. Development of the TAS model began with completion of a steady-state model which allowed evaluation of hydrogeologic questions and modeling objectives such as average flow patterns, average flow rates, and long-term pumping effects (Hunt and Smith, 2020). The steady-state model was adequate for evaluating the aquifer under conditions that approximate steady state. However, in reality these conditions are rare as the groundwater system is subject to many stressors that change on different temporal scales, such as changes in recharge quantity due to individual storm events or longer-term changes in climatic conditions (e.g., shifts between El Niño/La Niña conditions due to the El Niño Southern Oscillation), or changes in the amount of groundwater production due to seasonal or multi-year changes in water demand. Because the Trinity Aquifer is subject to these temporally variable factors, it was determined that the model should be advanced to a transient model to better evaluate the sustainability of the Middle Trinity Aquifer. Some questions being considered in developing this model are:

- How will an increase in groundwater pumping, both on a local and regional scale, impact Trinity water levels and aquifer storage both on short-term (monthly-yearly) and long-term time scales (multi-decadal)?
- To what extent can various pumping regimes in the confined, BSEACD portion of the Trinity Aquifer impact springflow for important Trinity springs discharging upgradient in the Blanco River basin, and how do these impacts compare to more localized impacts within Hays Trinity Groundwater Conservation District (HTGCD)?
- How will Trinity Aquifer water levels and springflow be affected under a recurrence of a drought of record or even greater magnitude drought which appears increasingly likely due to climate change? What are the extent of these impacts when also accounting for increased groundwater production due to increased water demand?

Conceptual Model

A conceptual groundwater model is a synthesis of all of the relevant hydrogeologic data and studies which establishes a framework or understanding for how a given aquifer or groundwater system works. A numerical groundwater model must be informed by a good conceptual model in order to provide accurate simulations of groundwater flow. This section presents the conceptual model for the Middle Trinity aquifer which was used as a basis for the TAS.

Hydrogeologic Framework

The focus of the TAS groundwater modeling effort is the Middle Trinity Aquifer, which is composed of the Cow Creek, Hensel, and Lower Glen Rose geologic units which are part of the Trinity Group (Figure 2 and Figure 3). These units generally dip from west to east and thicken to the east. The lithology of the Middle Trinity appears to have subtle differences in southwestern Travis County from Hays County to the south due to increased clastic sediment input to the north that may have influenced geologic facies and thicknesses of the Lower and Middle Trinity Aquifers (Hunt et al., 2020).

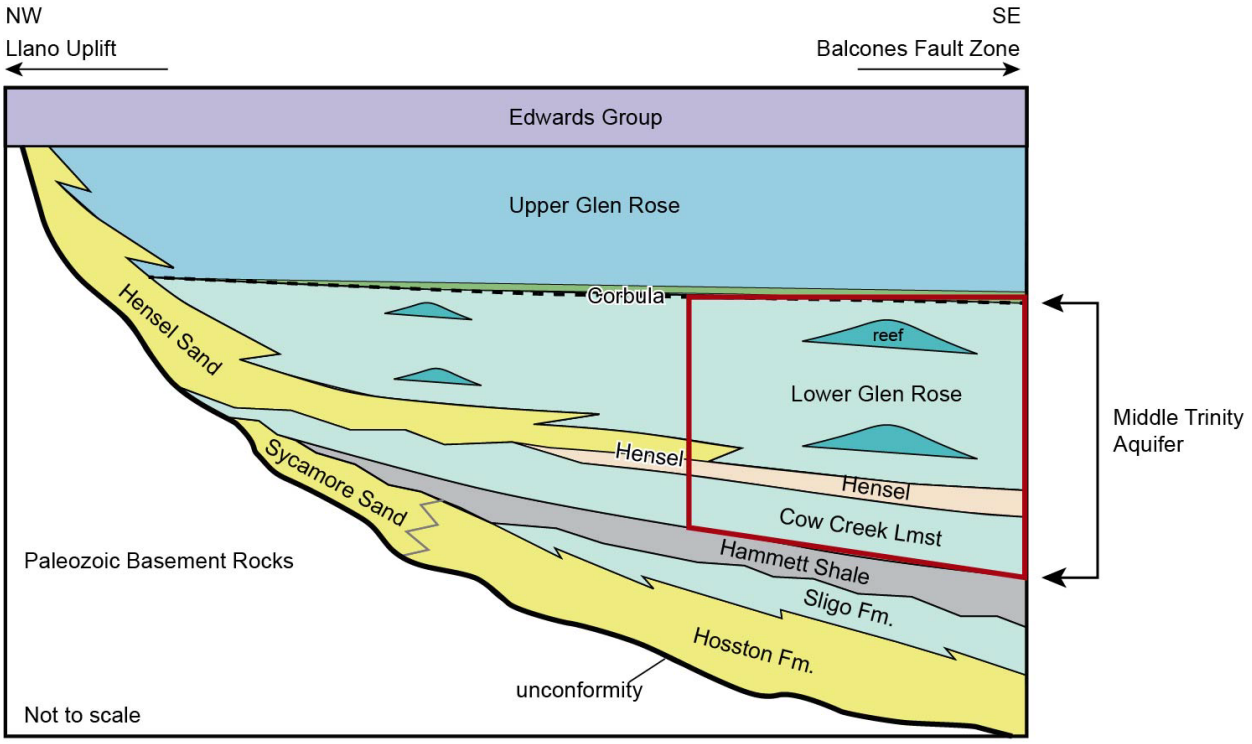

Modified from Striiklin et al., 1971; Loucks, 1977; Barker et al., 1994; Kerans and Loucks, 2002, and Rose, 2016.

Figure 2. Schematic lithostratigraphic cross-section from west to east through the study area. Red box denotes Middle Trinity units modeled in the TAS. Modified from Hunt and Smith (2020).

The Middle Trinity Aquifer is underlain by the Hammett Shale, which separates it hydraulically from the underlying Lower Trinity Aquifer. The Lower Trinity is not presently understood to be in connection with the Middle Trinity in the model domain and is not part of this modeling effort. The top of the Hammett Shale forms the bottom of the model domain and is considered a no-flow boundary. Evaporite-rich deposits near the base of the Upper Glen Rose form an aquitard between the Middle Trinity Aquifer and the Upper Trinity Aquifer (Figure 3). The Upper Trinity and Edwards Aquifers are not considered to significantly influence the Middle Trinity and are not explicitly part of this model.

The Cow Creek is the most prolific aquifer unit within the Middle Trinity and most commonly targeted for well production. It is composed of a carbonate grainstone in the upper section grading to a fine-grained dolomitic sand in the lower section. It is about 75 ft thick in Hays County and thins within western Travis County to about 50 ft. Well-developed conduits, solution-enlarged fractures, and other karst features are commonly observed in the upper section of the Cow Creek. Of note is Jacobs Well Spring (JWS), a prolific karst spring which is sourced from a large cave/conduit system developed in the top of the Cow Creek with over 1 mile of cave passage presently mapped by cave divers (Wierman et al., 2010).

The overlying Hensel abruptly changes facies near the Blanco/Hays County line from being predominantly a relatively thick clastic unit of about 70 ft thickness to the west in Blanco County, to a relatively thin silty marine dolomite of about 30 ft to the east of Blanco County (Broun et al., 2020). The Hensel appears to be semi-confining to the east of this facies transition where it is a silty dolomite. The Lower Glen Rose is composed of more massive limestone units with locally well-developed reefs or bioherms in Hays County which appear largely absent within southwestern Travis County.

Within Hays County, all of these units, other than the Hammett, are fractured and show some degree of karstification. The highest level of karstification occurs within the Blanco River watershed in western Hays County where the Lower Glen Rose is exposed at the surface and has many mapped caves and sinkholes. Within southwestern Travis County the degree of karstification appears less well-developed than in Hays County.

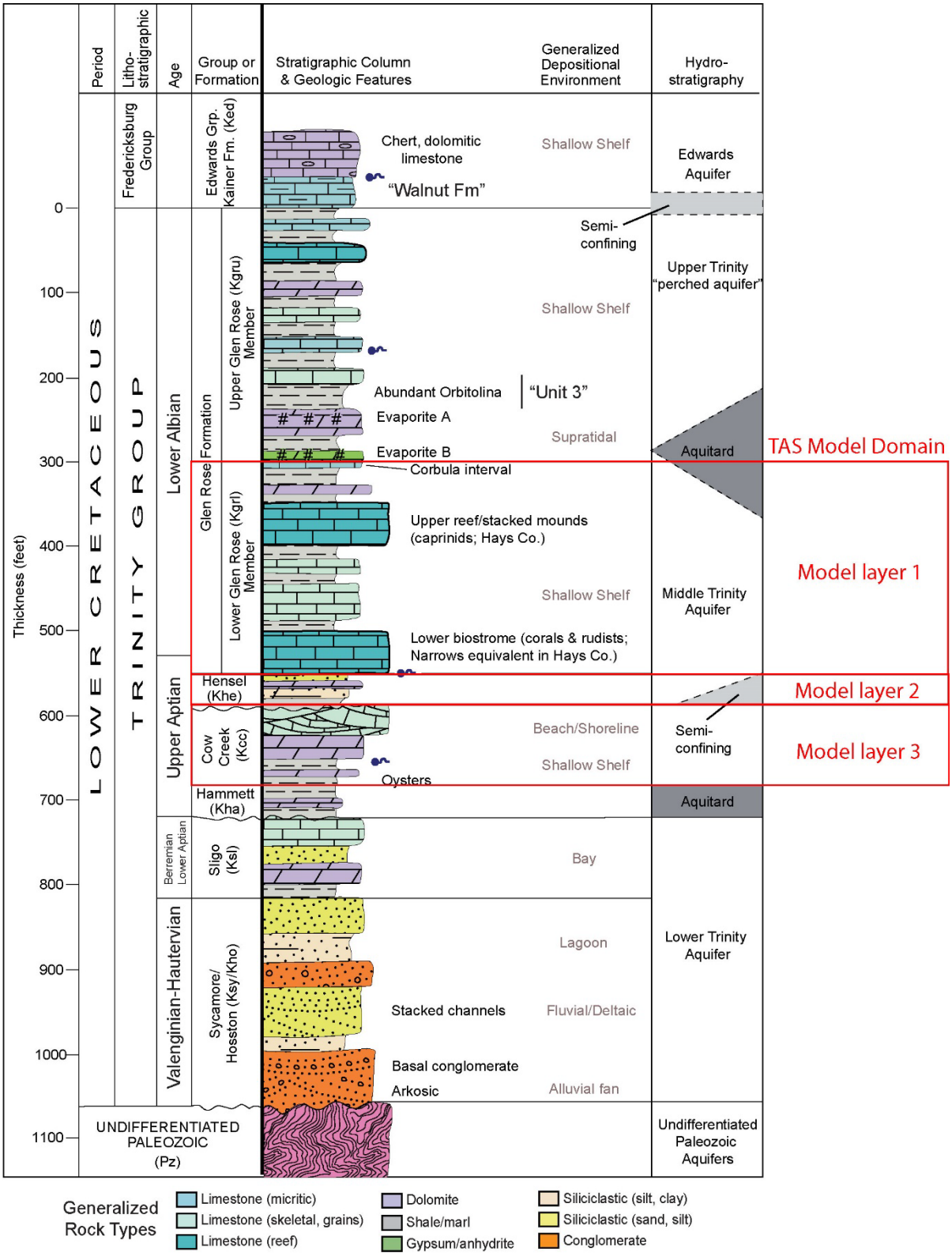

Figure 3. Lithologic and hydrostratigraphic column of Trinity Group in the study area.

Hydrostratigraphy and Model Layers

The Middle Trinity Aquifer is generally described as a single aquifer composed of the Cow Creek, Hensel, and Lower Glen Rose hydrostratigraphic units (Wierman et al., 2010). However, in some locations within the study area hydraulic heads and groundwater geochemistry may vary between the Cow Creek and Lower Glen Rose, suggesting that the Hensel is acting as a leaky aquitard and providing some level of separation between the Cow Creek and Lower Glen Rose. The transient model presented in this report conceptualizes the Middle Trinity as containing three layers, one for each of the three hydrostratigraphic units in the Middle Trinity Aquifer (Figure 2).

Structure

Middle Trinity units generally have an eastward depositional and structural dip off the Llano Uplift (Figure 4). Structural gradients dramatically steepen to the southeast due to the Balcones-age faulting. Faults play a critical role in the geometry and potentially the flow paths within the Middle Trinity Aquifer. Faulting has created a horst structure within the Blanco River watershed that has uplifted the Middle Trinity geologic units and allowed for the incision and erosion of those units. This generally coincides with the mapped extent of the Lower Glen Rose (Figure 1) in Hays County. East of the Mount Bonnell Fault, normal faulting has resulted in deep confinement of the Middle Trinity Aquifer within the Balcones Fault Zone (BFZ). However, the en-echelon nature of the faulting has resulted in relay-ramp structures that provide lateral continuity of the geologic units in Hays County (Hunt et al., 2015). This faulting geometry has resulted in multiple faults with relatively less throw. For example, throw on the Tom Creek Fault diminishes from about 250 ft near the Travis County line to about 25 ft at the Blanco River. Accordingly, the influence of the Tom Creek Fault on the direction of groundwater flow is likely to decrease along strike from north to south (Figure 5).

In southwestern Travis County, the Bee Creek and Mount Bonnell Fault Zones appear to be at least partial barriers to groundwater flow and partially compartmentalize the Middle Trinity Aquifer. Between these two faults, the dip of the units is to the east-northeast and appears to influence the direction of flow down structural dip (Figure 4 and Figure 5).

Faults and fractures have also provided secondary porosity and permeability that have resulted in development of a karstic aquifer system consisting of sinkholes, caves, and conduits. Certain beds and bedding planes are more susceptible to dissolution thereby creating zones of high porosity and permeability that are laterally extensive. The area contains many karst features that appear to be fracture controlled. In addition, fractures are central to the conduit system feeding JWS and Pleasant Valley Spring (PVS) (Hunt et al., 2013).

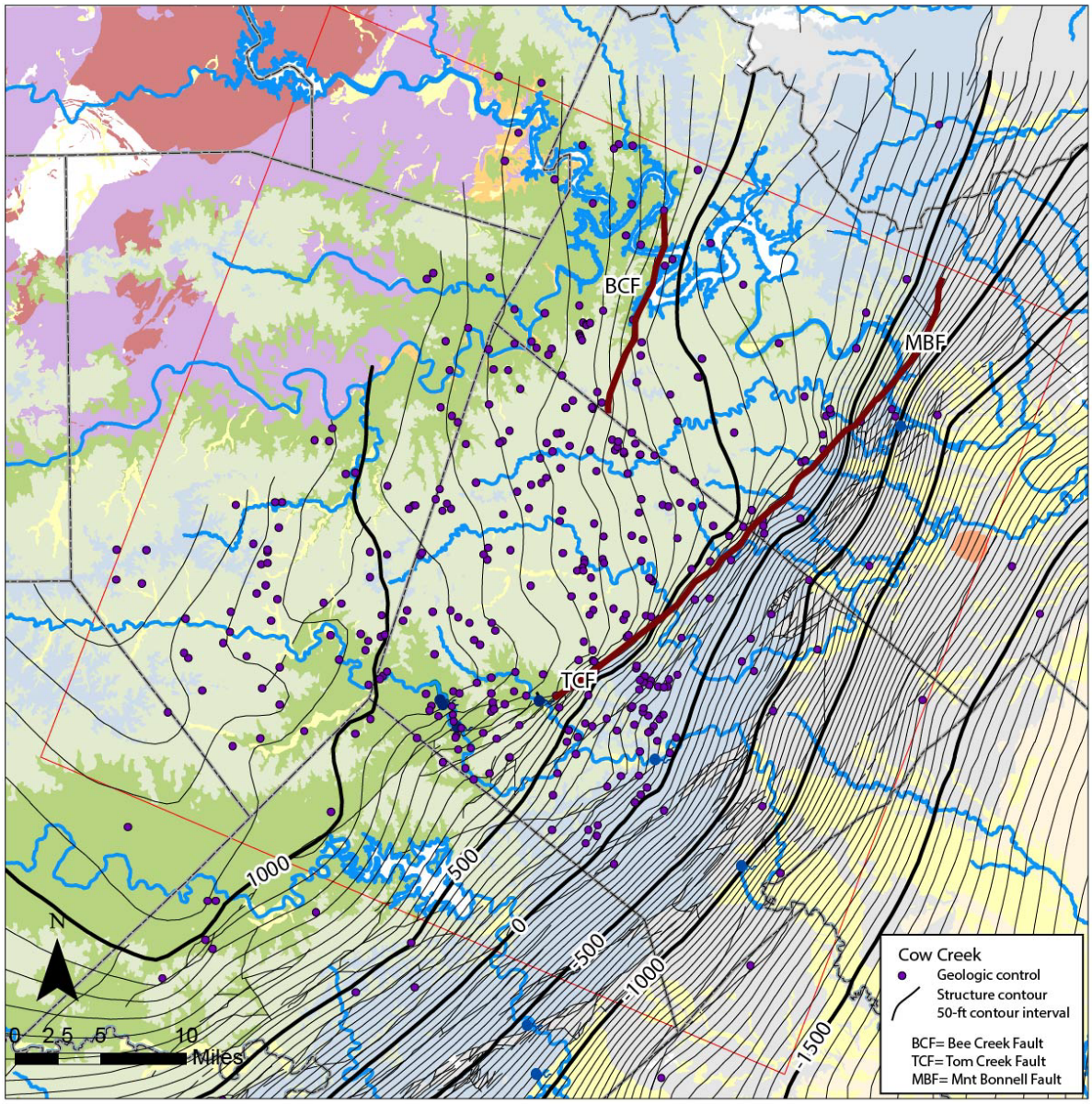

Figure 4. Structure contour map of the top of the Cow Creek Formation. Units are in ft-msl. Modified from Hunt and Smith (2020).

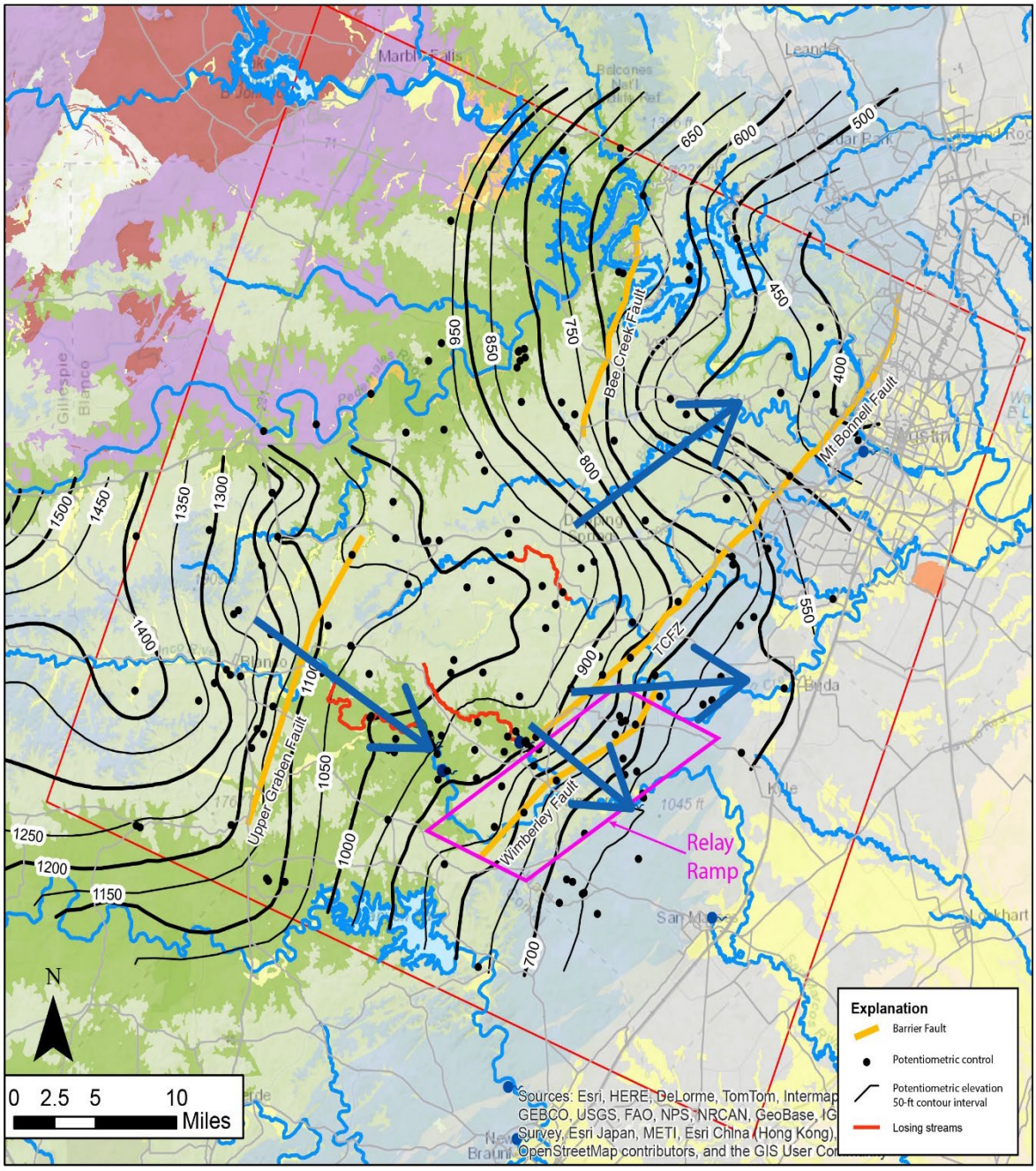

Figure 5. Potentiometric map of the Middle Trinity Aquifer from 2018-2019, representing average hydrologic conditions throughout the study area. Modified from Hunt and Smith (2020). Arrows represent generalized flow directions. Units are in ft-msl.

Groundwater Flow

For this modeling effort, the Middle Trinity geologic units are considered to be a single aquifer referred to as the Middle Trinity Aquifer (Figure 3). Regional groundwater flow at the scale of the study area is conceptualized as having minimal intra- or inter-aquifer flow. In other words, significant inter-aquifer flow does not occur between the Middle Trinity and the Edwards or Upper Glen Rose (above) or Lower Trinity (below) units at the regional (study area) scale.

Previous potentiometric maps (Mace et al., 2000; Hunt and Smith, 2010; Watson et al., 2014) are similar to the composite 2018-2019 potentiometric map provided in Figure 5 (Hunt et al., 2019a; Hunt et al. 2020a). Groundwater flow within the Middle Trinity Aquifer is generally from Gillespie and Blanco Counties into Hays County. The overall flow direction is from west to east, with potentiometric gradients generally following structure contour gradients that reflect depositional dip and, in some cases, faulting or other structures (Figure 4). Water-level gradients in central Hays County are relatively flat in the area between Onion Creek and Cypress Creek, two streams with documented flow losses along reaches coinciding with the flat gradients. North of Onion Creek in Hays and Travis Counties, the gradients steepen to the northeast into southwestern Travis County. Thus, groundwater flow in the Middle Trinity in southwestern Travis County is predominately to the northeast and appears derived mostly from Hays County.

A potentiometric trough is located upgradient from JWS in Cypress Creek (Hunt et al., 2009; Watson et al., 2014). The trough coincides with losing stream reaches in the Blanco River basin, and with the JWS conduit as mapped by cave divers with over 1 mile of cave passage (Wierman et al., 2010). Such potentiometric troughs are common within the karstic aquifers, such as the Edward Aquifer (Hunt et al., 2007). In central Hays County, some portion of groundwater flow in the Middle Trinity bypasses major Middle Trinity springs (PVS and JWS) to the southeast and into the BFZ where gradients generally increase (Figure 5).

Within the study area, steepening potentiometric gradients coincide with several mapped faults, indicating that the faults are likely acting as barriers to groundwater flow (Figure 5). These include the Bee Creek and Mount Bonnell Faults in Southwestern Travis County, and the Western Graben Fault in Blanco County (Figure 5). Within Hays County, the Tom Creek Fault Zone (TCFZ) is associated with steepening gradients north of Cypress Creek, and smaller gradients south of Cypress Creek (Figure 5). This suggests that south of Cypress Creek, the TCFZ is less of a barrier to lateral groundwater flow and allows groundwater to bypass the fault zone and flow into deeper confined portions of the Middle Trinity. Hunt et al., (2015) suggest that this increased groundwater flow is facilitated by a relay ramp structure which transmits water across fault blocks and may provide an important source of water to the confined Middle Trinity Aquifer within the BSEACD.

Further to the southeast along the southeast boundary of the model domain, where the Middle Trinity dips deeper and is faulted deeper into the subsurface, there are only a few Trinity wells within 2 miles of the model boundary. Knowledge of flow in the deep aquifer systems is from studies by Hoff and Dutton (2017). These studies indicate that freshwater in the Edwards Aquifer (hydropressured groundwater) flows into a deep system until it reaches higher heads in the highly saline Edwards. These higher heads are due to geopressures that result from sediment accumulation in the Gulf of Mexico Basin. Where these two pressure systems meet, the buildup of pressure is relieved by cross formational flow, either through the rock matrix or along faults. Hoff and Dutton (2017) postulate that these conditions likely apply to

other aquifers such as the Trinity and Carrizo-Wilcox. This suggests that Middle Trinity groundwater flows a considerable distance to the east, miles outside of the model domain boundary.

Hydraulic Properties

Middle Trinity hydraulic properties from aquifer tests have been combined for the region by the BSEACD and appended to data from Hunt et al. (2010) (Figure 6 and Figure 7). The interquartile values presented in Figure 7 provide boundaries or ranges for the model parameters. Additional aquifer parameter results from a large-scale aquifer test in central Hays County are summarized in Table 1 (BSEACD, 2017, 2018a). Separate calculated aquifer parameters were estimated by Oliver and Pinkard (2018) based on the same aquifer test data using different methods and analytical solutions (Table 2).

Few aquifer parameters from aquifer tests exist for southwestern Travis County. However, an analysis of specific capacity tests shows that Middle Trinity wells in Travis County are four times less productive than Middle Trinity wells in Hays County (Hunt et al., 2020).

A range of hydraulic conductivity values from slug testing from two multiport monitor wells in Hays County (Hunt et al., 2016b) is presented in Figure 7. A multiport well in southwestern Travis County indicates that where equivalent Middle Trinity units are saturated (note the Lower Glen Rose is unsaturated), hydraulic conductivity values are more than an order of magnitude higher and lower than zones in Hays County (Hunt et al., 2020). For example, in the southwestern Travis County multiport well, the Hensel and Cow Creek have hydraulic conductivity values of 43 and 21 ft/d, respectively. The equivalent zones in the Rolling Oaks multiport well for the Hensel are 0.3 ft/d and for the Cow Creek between 243 to 917 ft/d (Hunt et al., 2020).

Table 1. Aquifer parameters and pumping used in the individual well and regional drawdown assessment. Pumping values from WRGS (2017) and aquifer parameters from BSEACD (2018a). Table from Hunt and Smith (2020).

	Bridges #1*	***Bridges #2****	***Bridges #3****	***Bridges #4****	***Odell #1****	***Odell #2****	***Odell #3****
Pumping Rate (gal/min)	645	148	48	66	95	560	175
Transmissivity (ft^2/d)	363	204	187	187	187	538	187
Hydraulic Conductivity (ft/d)* **	6.6	3.7	3.4	3.4	3.4	9.8	3.4
Storativity	9.45E-05	5.03E-05	4.82E-05	4.82E-05	4.82E-05	9.88E-05	4.82E-05

*Parameters from evaluation A-C, Table 6 BSEACD, 2018.
**Parameters from evaluation D, Table 6, BSEACD, 2018.
***Assumed thickness is isolated to Cow Creek. About 55 ft thick.

Table 2. Aquifer parameters estimated using TTIM analytical model by Oliver and Pickard (2018). Table from Hunt and Smith (2020).

Unit	***Thickness (ft)***	***Horizontal K (ft/d)***	***Vertical K (ft/d)***	***Vertical Anisotropy***	***Specific Storage (ft^{-1})***
Upper Glen Rose	470	1.0E-03	1.0E-05	1.0E-02	1.5E-05
Lower Glen Rose	195	2.5E-01	1.0E-01	4.0E-01	1.0E-06
Hensel	45	1.0E-04	1.0E-05	1.0E-01	1.0E-06
Cow Creek	75	4.0E+00	4.0E-01	1.0E-01	8.0E-07
Hammett	50	1.0E-07	1.0E-09	1.0E-02	1.0E-06

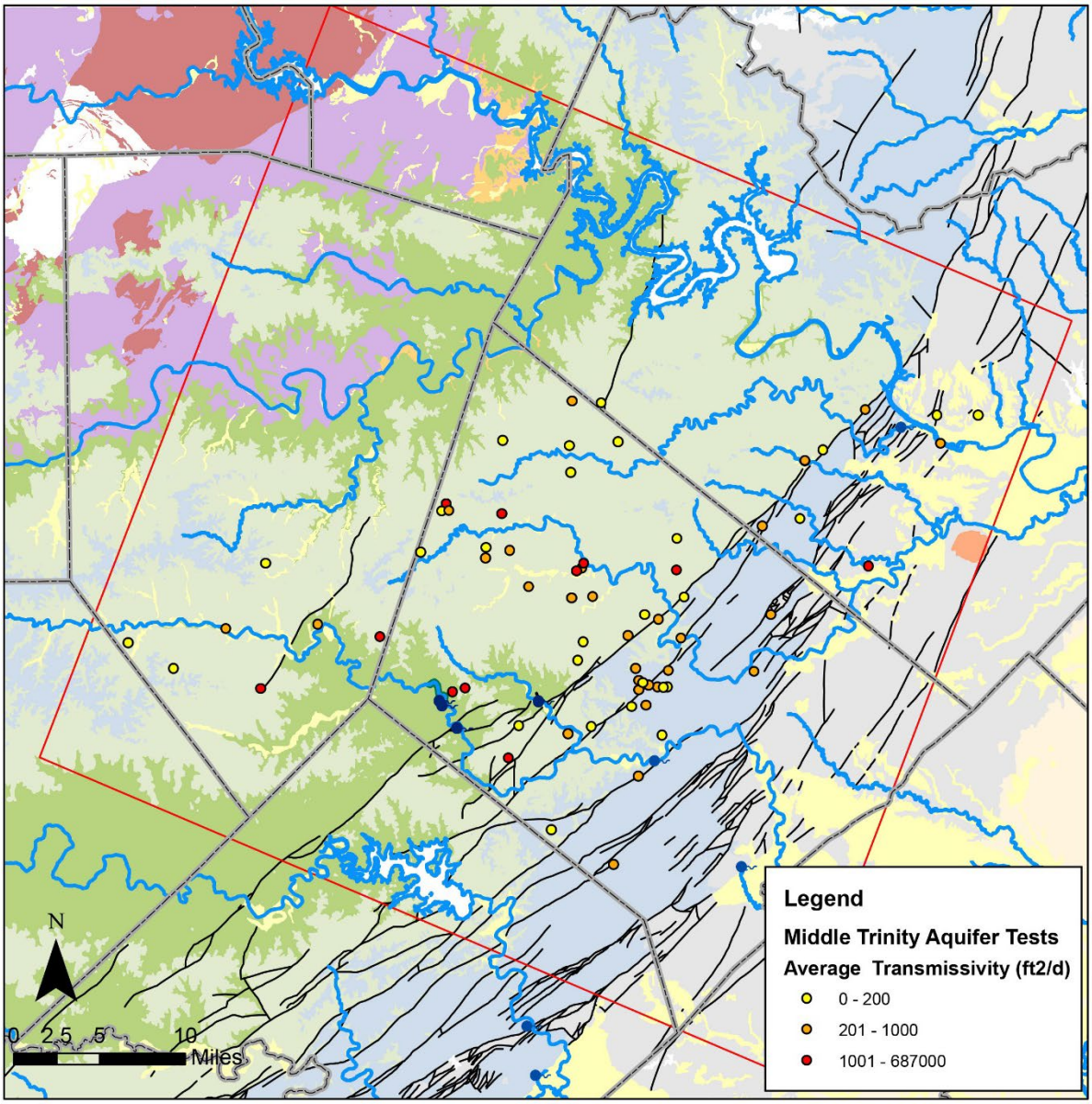

Figure 6. Map of Middle Trinity wells with aquifer-test data in and corresponding calculated transmissivity values. Color corresponds to the interquartile range of the average of the transmissivity results from each test (ft^2/d). Modified from Hunt and Smith (2020).

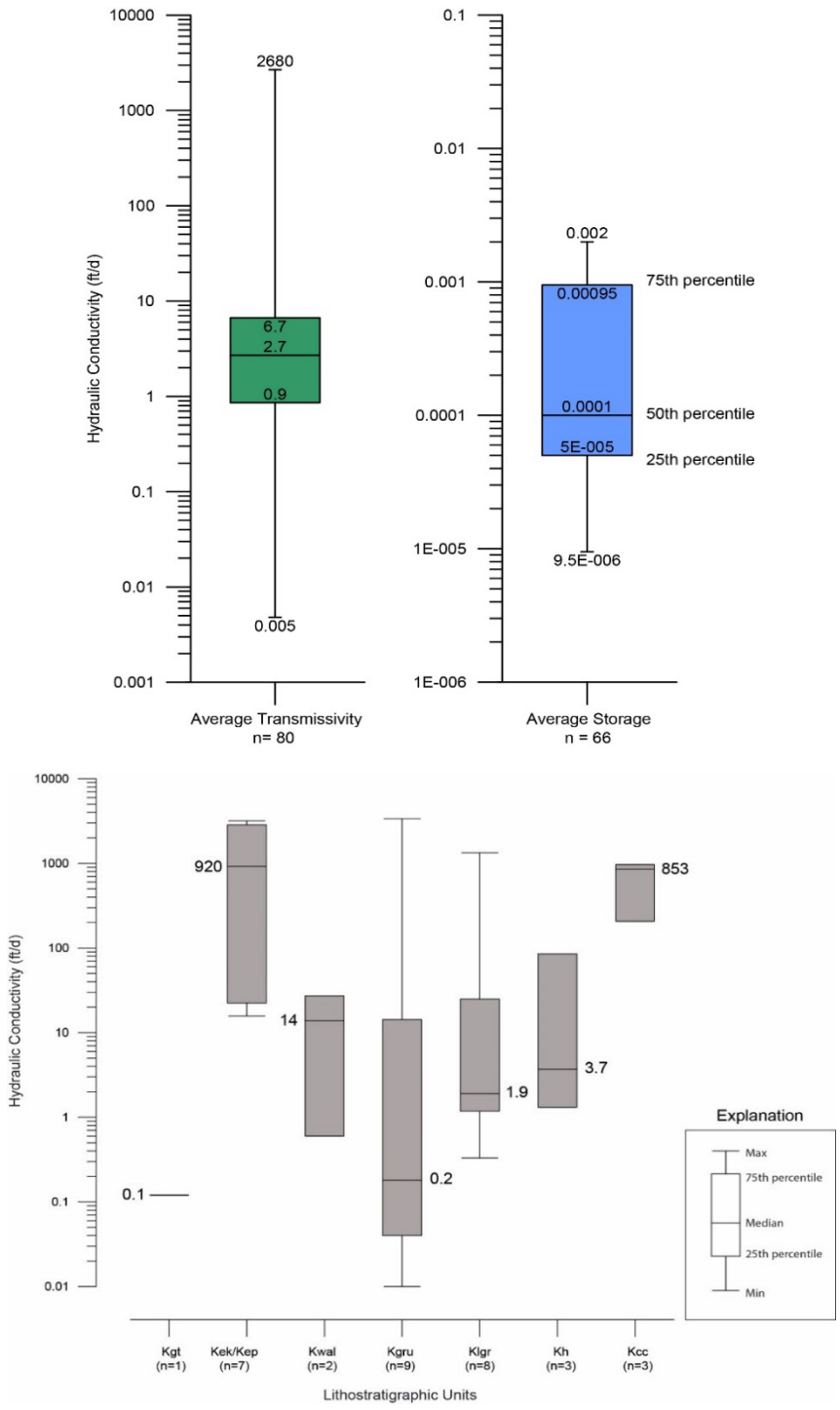

Figure 7. Whisker plots of average hydraulic conductivity and storativity results from Middle Trinity Aquifer tests shown in Figure 6. Values are from either Hays County (top), or calculated hydraulic conductivity from slug testing from the Ruby Ranch and Antioch multiport wells in Hays County (bottom) (Hunt et al., 2016b). The Cow Creek (Kcc) zones have values similar to the Edwards Aquifer (Kek/Kep). Modified from Hunt and Smith (2020). See Figure 3 for additional geologic unit abbreviations.

Estimated Water Budgets

Recharge

Recharge to the Middle Trinity Aquifer is conceptualized to have the components described below. Note that deep water table and confined aquifer conditions in the Middle Trinity allow a simple recharge conceptualization that does not include evapotranspiration.

Regional lateral inflows: Jones et al. (2011) wrote: "The primary sources of inflow to the Hill Country portion of the Trinity Aquifer System are rainfall on the outcrop, and seepage through headwater creeks, ….". This concept can be refined to state that recharge generally occurs in the outcrop of the aquifer units. Regional inflows into the study area are sourced from recharge from Gillespie and Blanco Counties to the west where the thick, sandy Hensel facies and the sandy limestones of the Glen Rose are exposed (Wierman et al., 2010). Groundwater then flows to the east and southeast into the study area (Hunt et al., 2019a; Hunt et al., 2020). A portion of the groundwater flowing into Hays County discharges to PVS and JWS, with another portion bypassing these springs and continuing to the east and into the BFZ. Another portion of the regional inflow also flows to the northeast into southwestern Travis County and continues toward Williamson County.

Vertical leakage: Recharge passing through overlying units, such as the thin remnants of the Edwards and Upper Trinity, and into the Middle Trinity of the Hill Country was historically conceptualized to be a significant source of water (Ashworth, 1983; Jones et al., 2011). For the TAS conceptual model, recharge to the Middle Trinity through the Upper Glen Rose is assumed to be localized within specific watershed catchments. For example, recharge to the Middle Trinity along reaches of Onion Creek occurs through the thin and fractured Upper Glen Rose (Hunt et al., 2016a) and could occur in other stream areas. Thus, recharge through, or leakage from, thin and fractured Upper Trinity (Upper Glen Rose) likely does occur west of the Tom Creek Fault Zone (TCFZ). However, the magnitude and spatial distribution of this vertical leakage is poorly constrained.

East of the TCFZ/Mount Bonnell Fault Zone where the Middle Trinity is deeply confined, vertical leakage from the Edwards or Upper Trinity in the BFZ is not considered significant (Wong et al., 2014; Smith et al., 2015). Because of the Hammett Shale, upward vertical leakage is not thought to occur from the underlying Lower Trinity Aquifer. However, it is possible some localized vertical or lateral leakage into the Middle Trinity could occur within the BFZ either due to juxtaposition of Lower Trinity and Middle Trinity Aquifer units by faulting, or through hydrologic connection via faults and fractures associated with the BFZ.

Upland recharge: Diffuse and discrete recharge is known to occur where the Lower Glen Rose, Hensel, and Cow Creek units are exposed at the surface in both Hays and Travis Counties. In Hays County, this occurs generally within the horst block where most of the Lower Glen Rose outcrop occurs. Discrete upland recharge is known to occur in karst features in the Lower Glen Rose, such as Raccoon Cave near Wimberley. In southwestern Travis County, Middle Trinity units are exposed along the Pedernales and Colorado valleys. There are presently no documented discrete karst recharge features in southwestern Travis County.

Estimates of upland recharge is 10 to 25 % of rainfall on an annual basis within the Cypress Creek Watershed (Gary et al., 2019), while other regional modeled values of diffuse recharge are about 4 to 6%

of annual rainfall (Jones et al., 2011). Diffuse upland recharge is estimated to be 22 to 28% of rainfall for the nearby karstic Edwards Aquifer (Hunt et al., 2019b).

Stream recharge

Discrete and diffuse recharge to the Middle Trinity Aquifer has been documented along stream and river channels in portions of Hays County (Figure 5**,** Table 3). This has not been incorporated previously in Trinity Aquifer numerical models but is a significant recharge process for the aquifer. Jones et al., (2011) estimated up to 13 in/yr of recharge along the losing portion of Cibolo Creek near San Antonio (about 34% of average annual precipitation). For comparison, the nearby Edwards Aquifer has up to 75% of its recharge derived from losing streams with the remaining 25% occurring in the uplands—those numbers vary based upon hydrologic conditions (Hunt et al., 2019b). Hunt et al., (2016a) documented a potentiometric mound which coincides with losing reaches of Onion and South Onion Creeks in the vicinity of Dripping Springs, suggesting that stream losses along these reaches are recharging the Middle Trinity Aquifer across a thin overlying layer of the Upper Glen Rose. To reflect the elevated recharge entering the Middle Trinity Aquifer along losing stream reaches, elevated recharge coefficients have been applied to portions of the model recharge domain that coincide with losing stream reaches within the Blanco and Onion Creek basins. This is discussed in more detail in subsequent sections of this report.

In addition to direct stream recharge accounting for a significant portion of the recharge water budget, springflow and heads within the Trinity Aquifer often display a quick response to rainfall events in recharge areas. This “flashy” behavior is characteristic of many karst aquifer systems (including the Edwards Aquifer), and is caused by fast-moving subsurface flow through conduits, solution-enlarged fractures, and other secondary porosity features within karstified portions of the Trinity Aquifer. Within the Blanco basin in the study area, springflow and head responses to recharge events also appear to depend on antecedent surface and subsurface hydrologic conditions. For example, when Blanco River flow is higher, springflow and head responses to rainfall/storm events are generally more pronounced than when baseflow conditions are lower, showing a distinctive inflection of springflow responses at ~40 cubic feet-per-second (cfs) (Figure 10). Because Blanco River baseflow is primarily sustained by Middle Trinity springs and has a relatively large catchment area, Blanco River flow, as reported at the Wimberley Gage (USGS gage ID: 08171000), provides a useful proxy for overall antecedent hydrologic surface and subsurface conditions within the study area. For the TAS model conceptualization, data from this Blanco River gage has been used to regulate how much recharge from rainfall enters the model domain for each stress period of the calibrated and predictive model simulations.

The creeks in southwestern Travis County, such as Barton Creek, are net gaining streams due to seep and spring flows from the Upper Trinity aquifer. The Pedernales River and the Colorado River west of the Bee Creek Fault appears also to be gaining streams. Heads in the aquifer are above the river and lake levels in that area (Hunt et al., 2020). However east of the Bee Creek Fault along the Colorado River there is potential for leakage from Lake Travis into the Middle Trinity Aquifer (Figure 8). Aquifer units are exposed to the lake and the heads in the aquifer are below the average lake level. Along the Colorado River, east of Mansfield Dam and within Lake Austin, a pass-through lake, there is variable potential for discharge or recharge with the aquifer depending on heads in the aquifer (Hunt et al., 2020).

Few studies have characterized the surface-groundwater interaction of the Guadalupe River and Canyon Lake with the Middle Trinity Aquifer. A recent exception is student course work done on the Guadalupe

River directed by Marcus Gary at UT Austin (UT Austin, 2019). That study documents significant loss of about 30 cfs and recharge in the Lower Glen Rose along the Guadalupe River between about Highway 281 and Canyon Lake.

Little is known about the surface-groundwater interactions of Canyon Lake, which is reported to have a normal level of about 909 ft-msl. Elevations for the river bottom of the lake are presented in Austin et al., 2001. The fractured and faulted Middle Trinity Aquifer is exposed in the drainage basin of the Guadalupe River and Canyon Lake and thus has the potential for recharge. However, the Guadalupe River is overall a gaining stream upstream of Canyon Lake (Wierman et al., 2019)

Table 3. Summary table of Onion Creek and Blanco River gain-loss reach characteristics from Hunt et al., 2017b based on Smith et al., 2015 and Hunt et al., 2016a. Losing reaches indicated on Figure 5. Note that losing reaches such as South Onion Creek, Cypress Creek, and the Little Blanco River, as well as possibly other streams, are not well quantified, but are potential sources of additional recharge.

Reach Name	Creek	Length (mi)	Generalized Flow (cfs)	Geology	Comments
Upper Gaining	Onion	13	30	Edwards hilltops, Upper Glen Rose	Shallow Upper Trinity and gravity springs
	Blanco	32	10	Edwards's hilltops, Upper Glen Rose	Shallow Upper Trinity and gravity springs
Trinity Recharge Zone	Onion	5	-3 net; (up to -15)	Thin fractured Upper Glen Rose	Burns Swallet recharge feature
	Blanco	11	-10	Lower Glen Rose, Hensel, and Cow Creek	Saunders Swallet recharge feature in Cow Creek
Lower Gaining	Onion	17	85	Upper Glen Rose	Shallow Upper Trinity and Emerald and Camp Ben McColluch Springs
	Blanco	27	75	Lower Glen Rose and Upper Glen Rose	Upper and Lower Glen Rose springs; Middle Trinity artesian springs: PVS and JWS

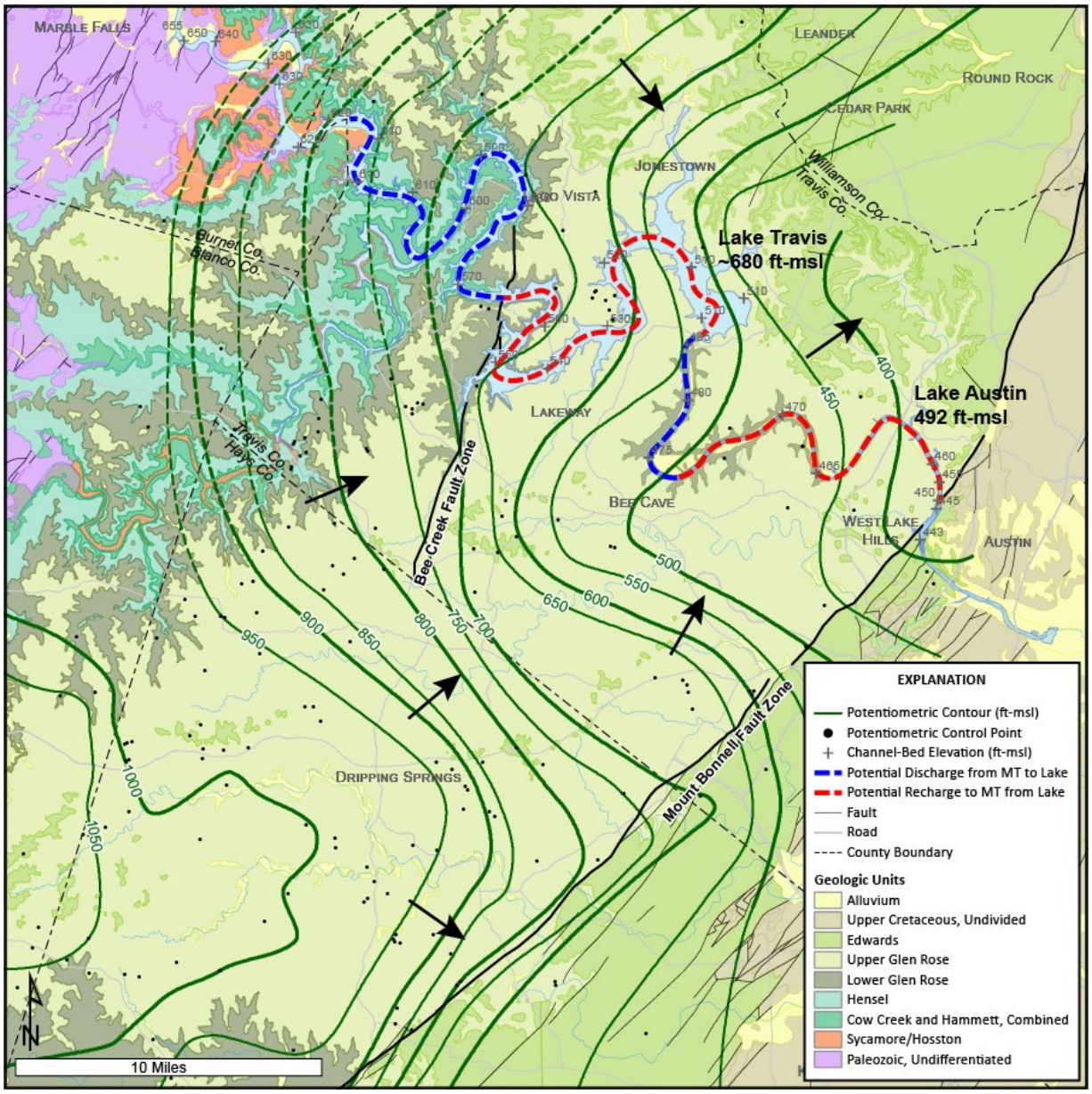

Figure 8. Map of hydrogeologic interactions between the Middle Trinity Aquifer and lakes in southwestern Travis County. Figure from Hunt et al., (2020a).

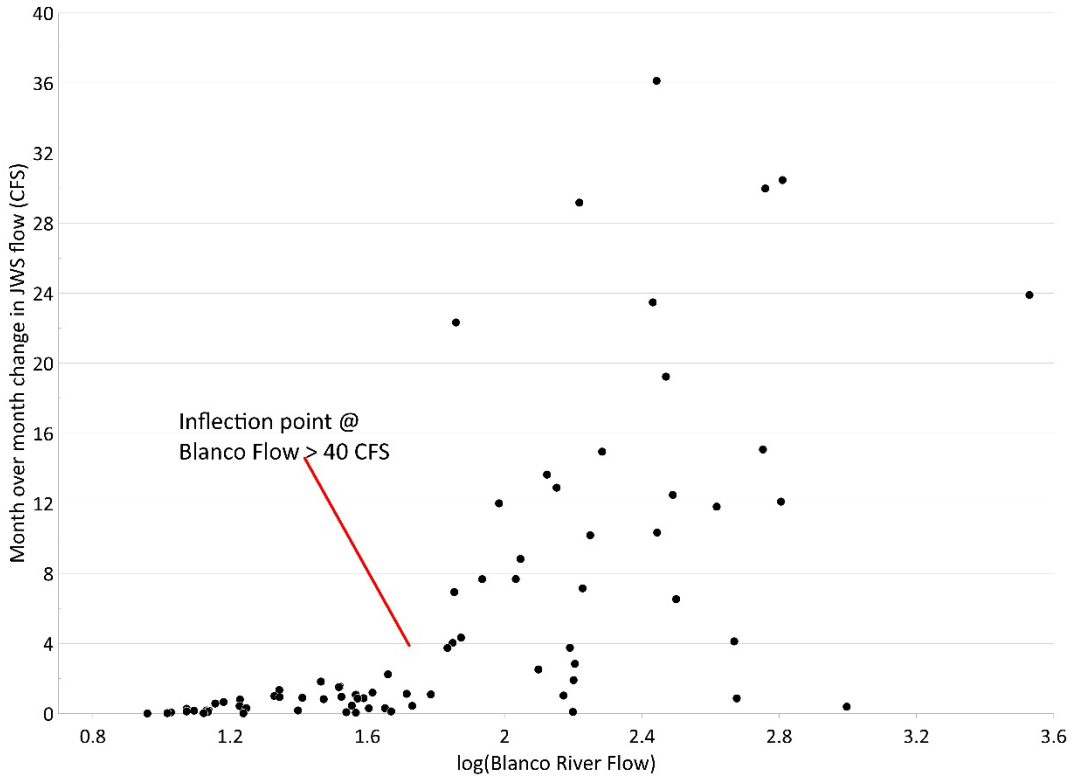

Figure 10. Monthly average JWS flow responses (positive flow responses only) versus log of Blanco River flow. Larger springflow responses occur generally when the log of Blanco River flow is above ~1.7 (which corresponds to a flow value of ~40 cfs).

Discharge

Discharge from the Middle Trinity Aquifer occurs as springflow, pumping, and lateral outflow from the study area. The first two sources can be measured and estimated, while the latter source is not quantifiable. Lateral outflow occurs in the eastern and northeastern portion of the study area. The southeastward groundwater flow in the Middle Trinity in Hays County is conceptualized as continuing some miles east of the model boundary, and then flowing vertically into the overlying units outside of the model domain (Hoff and Dutton, 2017). Flow directions in southwestern Travis County are conceptualized as oriented toward the northeast with a portion of the flow potentially discharging into the Colorado River and a portion of flow bypassing the Colorado and continuing to the northeast toward Williamson and Bell Counties.

Springflow

PVS and JWS are the major natural discharge locations from the aquifer (Table 4 and Table 5). Other notable springs in the area include Miller Spring and the Park Spring complex, which discharge along the Blanco River and upstream from PVS.

Springflow measurements at PVS indicate flows ranging from 10 to 54 cfs with an estimated median value of 20 cfs. During dry hydrologic conditions (drought), baseflows in the Blanco River at Wimberley (USGS

gage: 08171000) are mostly derived from PVS about 12 miles upstream of the gage. At the end of the 1950s drought of record, springflow from PVS may have decreased to as low as 0.8 cfs (Gary et al., 2019).

JWS has transitioned from a perennial spring to an ephemeral spring due to increased pumping and capture in the last decade. Historic measurements during the drought of record vary from 0.2 to 2.6 cfs (Gary et al., 2019). Since 2005, measured daily flow values at JWS range from 0 to greater than 150 cfs. The range of monthly mean flows reported by the U.S. Geological Survey is 0 to 55 cfs with an average of 8.1 cfs and a median of 3.3 cfs (USGS gage: 08170990). Some of the higher flow values are likely biased high, as they include storm runoff in Dry Cypress Creek (Gary et al., 2019).

Additional small-flow springs occur along the Pedernales and Colorado Rivers and their tributaries at locations such as Reimers Ranch, Westcave Preserve, Hamilton Pool, and Deadhead Springs (Hunt et al., 2020). However, these springs are not gaged, have flows orders of magnitude smaller than PVS and JWS, and have small, localized springshed areas compared to the larger springsheds of PVS and JWS.

Table 4. US Geological Survey streamflow gages of interest for quantifying Middle Trinity springflow. Table from Hunt and Smith (2020).

USGS Springflow Gage	*Link*	*Comment*
Blanco River @ Fischer Store Rd. (Pleasant Valley Spring)	https://waterdata.usgs.gov/monitoring-location/08170950	Blanco river gage downstream of PVS, but within the river. Baseflows would primarily be all the springflow such as PVS, Park, and Miller Springs. After rainfall flows include surface runoff.
Blanco River @ Valley View Rd.	https://waterdata.usgs.gov/monitoring-location/08170905	Gage upstream of Blanco River Middle Trinity Spring run. When reporting 0 cfs flow, all flow at downstream Fischer Store gage represents cumulative Middle Trinity Springflow.
Jacob's Well Spring	waterdata.usgs.gov/monitoring-location/08170990	Gage at the spring within Cypress Creek. Peak storm flows from runoff. Very rarely flows from Cypress Creek upstream of gage location.
Blanco River at Wimberley (RR12)	https://waterdata.usgs.gov/monitoring-location/08171000	Longest period of record for Blanco River downstream of all springs. Baseflows are primarily springflow.

Table 5. Springflow statistics of JWS and PVS in Hays County. Median value is used to eliminate surface flow influence on average values. Table updated from Hunt and Smith (2020).

Springs	*Median (cfs)*	*Median (cfd)*	*Comment*
Pleasant Valley Spring	20	1,728,000	Estimated from available manual springflow measurements
Jacob's Well Spring	3.3	285,120	From USGS gage 08170990 period of record, daily average flow, April 2005-February 2023
Other Springs	?		Miller and Park Springs
Total	23.4	2,021,760	

Pumping

Pumping from the Middle Trinity Aquifer occurs from wells throughout Blanco, Hays, and portions of Travis County that are classified either as permitted or exempt wells (Figure 11). Permitted wells are often large-capacity wells that are metered and managed by BSEACD, HTGCD, or Blanco-Pedernales Groundwater Conservation District (BPGCD). Southwestern Travis County Groundwater Conservation District (SWTCGCD) is a relatively new GCD which has only recently established rules and begun to issue production permits on a temporary basis. As such, metered pumping data is not available from SWTCGCD over the 2008-2020 TAS calibration period. Exempt wells are generally small-capacity private wells used for domestic water-supply, irrigation, and stock needs. Pumping from exempt wells is estimated, while permitted wells are metered (Table 6). Table 7 presents large pumping centers, defined as having permits greater than 50 million gallons per year permitted by a groundwater conservation district.

Table 6. Summary of annual pumping within study area. No data were available for Comal County. Total pumping estimates for SWTCGCD are provided from Hunt et al., 2020. Table from Hunt and Smith (2020).

	PERMITTED PUMPAGE (GAL)	PERMITTED AC-FT/YR	2018 ACTUAL PERMITTED PUMPAGE (GAL/YR)	2018 ACTUAL AC-FT/YR	2018 ACTUAL PERMITTED (CFD)	ESTIMATED EXEMPT (GAL/YR)	EST. EXEMPT AC-FT/YR	ESTIMATED EXEMPT (CFD)	TOTAL ACTUAL PERMITTED PUMPAGE + EXEMPT	TOTAL ACTUAL AND EXEMPT (AC-FT/YR)	TOTAL PERMITTED AND EXEMPT	TOTAL PERMITTED AND EXEMPT (AC-FT/YR)
HTGCD	1,205,443,381	3,699	631,782,570	1,939	231,390	1,216,727,634	3,734	445,626	1,848,510,204	5,673	2,422,171,015	7,433
BSEACD	492,481,557	1,511	212,571,252	652	77,854	206,035,587	632	75,460	418,606,839	1,285	698,517,144	2,144
BPGCD	185,000,000	568	140,000,000	430	51,275	325,851,000	1,000	119,343	465,851,000	1,430	510,851,000	1,568
SWTCGCD	NA	NA	NA	NA	NA	NA	NA	NA	523,484,691	1,607	NA	NA
TOTAL (GAL)	1,882,924,938		984,353,822			1,748,614,221	5,366		3,256,452,734		3,631,539,160	
TOTAL (AC-FT)		5,778		3,021								
TOTAL (CF)	251,711,289		131,589,403			233,756,498			435,325,858		485,467,786	
TOTAL (CFD)	689,619.97		360,518.91		360,518.91	640,429			1,192,674		1,330,049	

Table 7. List of permitted pumping and pumping centers within study area greater than 50 MGY. Table from Hunt and Smith (2020).

Name	*GCD*	*Ddlat*	*Ddlong*	*Annual Permit Amount (Ac-ft)*	*Annual Permit Amount (gal)*	*2018 Production (gal)*	*Comment*
Dripping Springs WSC	HTGCD	30.15288	-98.086395	1125	366,582,375	158,425,300	
Wimberley WSC	HTGCD	29.982824	-98.12232	645	210,173,895	158,728,000	
Rocking J Ranch	BPGCD	30.04659	-98.40154		185,000,000	140,000,000	average annual production
Needmore LLC (Trinity)	BSEACD	29.97083	-98.03445	552.3	179,965,440	12,086,000	
Wimberley Springs Partners Ltd.	HTGCD	30.033889	-98.146111	500	162,925,500	13,153,000	
Onion Creek Country Club (Trinity)	BSEACD	30.1466	-97.80799	391	127,410,000	120,547,000	
Woodcreek Phase II - Aqua Texas	HTGCD	30.033676	-98.139574	339	110,463,489	89,179,600	
Woodcreek Phase I - Aqua Texas, Inc	HTGCD	30.024547	-98.114723	321	104,598,171	76,953,900	
Caliterra	HTGCD	30.171263	-98.087996	208.7	68,005,104	26,188,500	

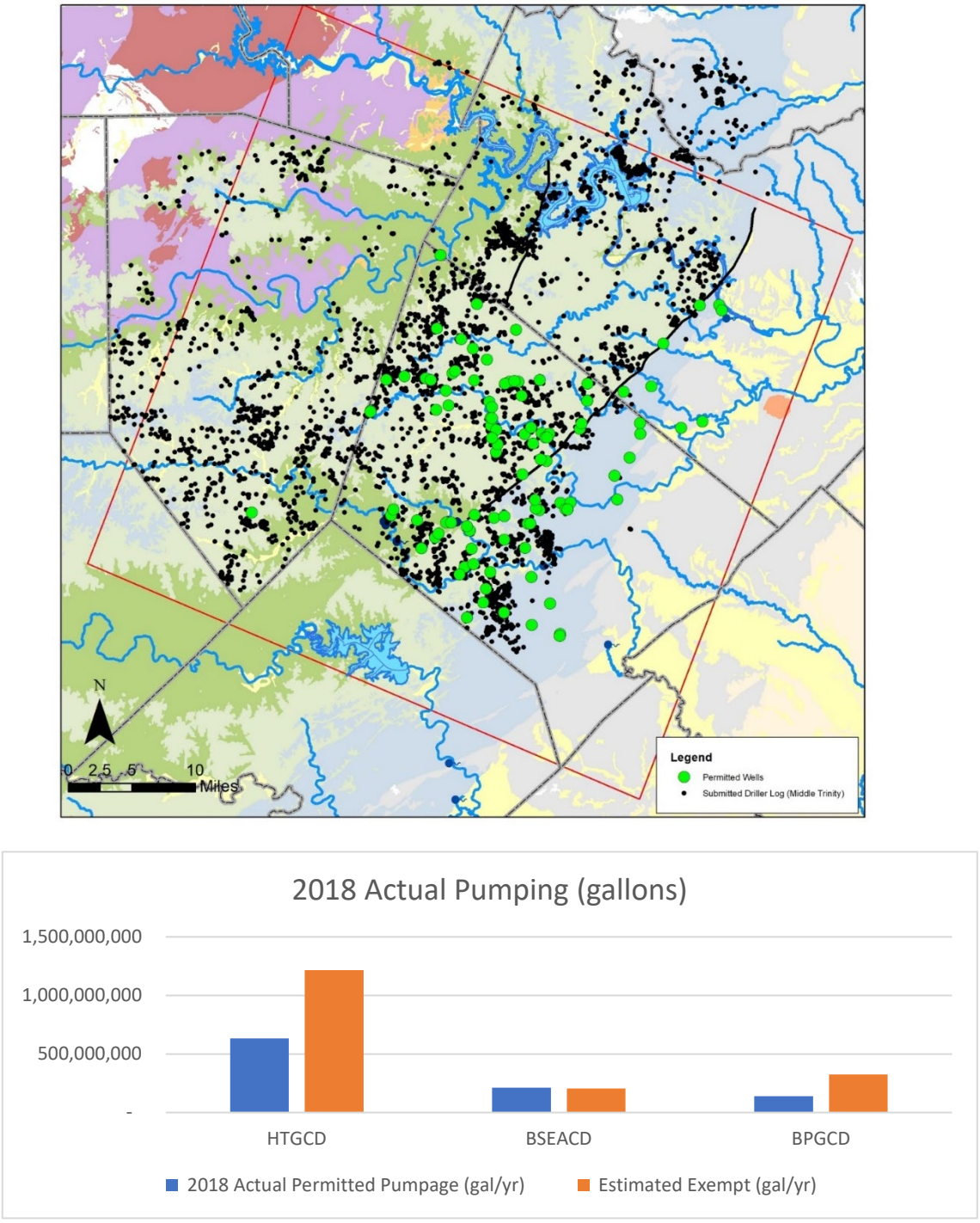

Figure 11. (top) Map of permitted pumping wells (green circles). Also shown as small black circles are the more than 2,000 Middle Trinity wells from the SWDR database within the region. This is a minimum number of wells for the area as many other wells exist that are not registered on the SWDR database. (Bottom) Metered permitted and estimated exempt pumping from 2018 for the three groundwater conservation districts in the area. Figure from Hunt et al., (2020a).

Conceptual Model Summary

A regional conceptual model that extends outside of the study area and includes additional overlying aquifers is provided in Figure 12. Figure 13 and Figure 14 provide more detailed and comprehensive conceptual models for Hays County and southwestern Travis County, respectively.

In Hays County, the Middle Trinity Aquifer can be characterized as two interconnected aquifer zones: 1) the Middle Trinity to the west, and 2) the BFZ Middle Trinity to the east (Figure 13). The geologic units of the Middle Trinity Aquifer to the west are variably exposed and hydrogeologically characterized by generally higher hydraulic conductivities and faster water level responses to recharge events, losing and gaining streams, significant springs, and more developed karstification and conduit flow than the BFZ Middle Trinity. Relay-ramp structures likely provide lateral geologic and hydrologic continuity from the western Hays County Middle Trinity into the BFZ Middle Trinity (Hunt et al., 2015). The BFZ Middle Trinity is more deeply confined and dominated by matrix, fracture, and locally karstic porosity and permeability. Geochemistry in the BFZ Middle Trinity is commonly fresh to brackish and dominated by evaporite mineralogy and older groundwater. The natural discharge areas from this system are unknown (Hunt et al., 2017a; Smith et al., 2018). However, Hoff and Dutton (2017) suggest that southeastward groundwater flow in the Middle Trinity continues east, then flows vertically into the overlying units. This vertical flow occurs at least several miles east of the TAS model boundary.

Aquifer characteristics of Comal County are broadly similar to Hays County. The Guadalupe River is a losing river upstream of Canyon Lake and has significant areas of the karstic Middle Trinity units exposed in the watershed. Little is known about the surface-groundwater interaction of Canyon Lake, but it has the potential to provide recharge to the Middle Trinity Aquifer. This portion of the model domain is outside of the primary area of investigation for the TAS.

In southwestern Travis County, the Middle Trinity Aquifer is compartmentalized and depleted in places. West of the Bee Creek Fault Zone the Middle Trinity is unconfined with locally diffuse recharge and limited lateral inflows. Wells tend to be low yielding but produce fresh groundwater. Between the Bee Creek and Mount Bonnell Fault systems the Middle Trinity Aquifer is compartmentalized by faults which limit lateral inflow. Groundwater tends to be very old and brackish and Middle Trinity wells have relatively low yields. Hydraulic conductivity is an order of magnitude lower than in Hays County. The Pedernales and Colorado Rivers west of the Bee Creek Fault Zone are locations of diffuse discharge for the Middle Trinity Aquifer. However, Lake Travis may provide recharge to the Middle Trinity in some reaches. Lake Austin may also have potential for leakage to the Middle Trinity Aquifer. However, the influence of these lakes appears to be localized and groundwater flow may continue beneath the river system to the northeast toward Williamson County (Hunt et al., 2020). While southwestern Travis County is outside the main area of investigation for the TAS, it is still included in the model domain.

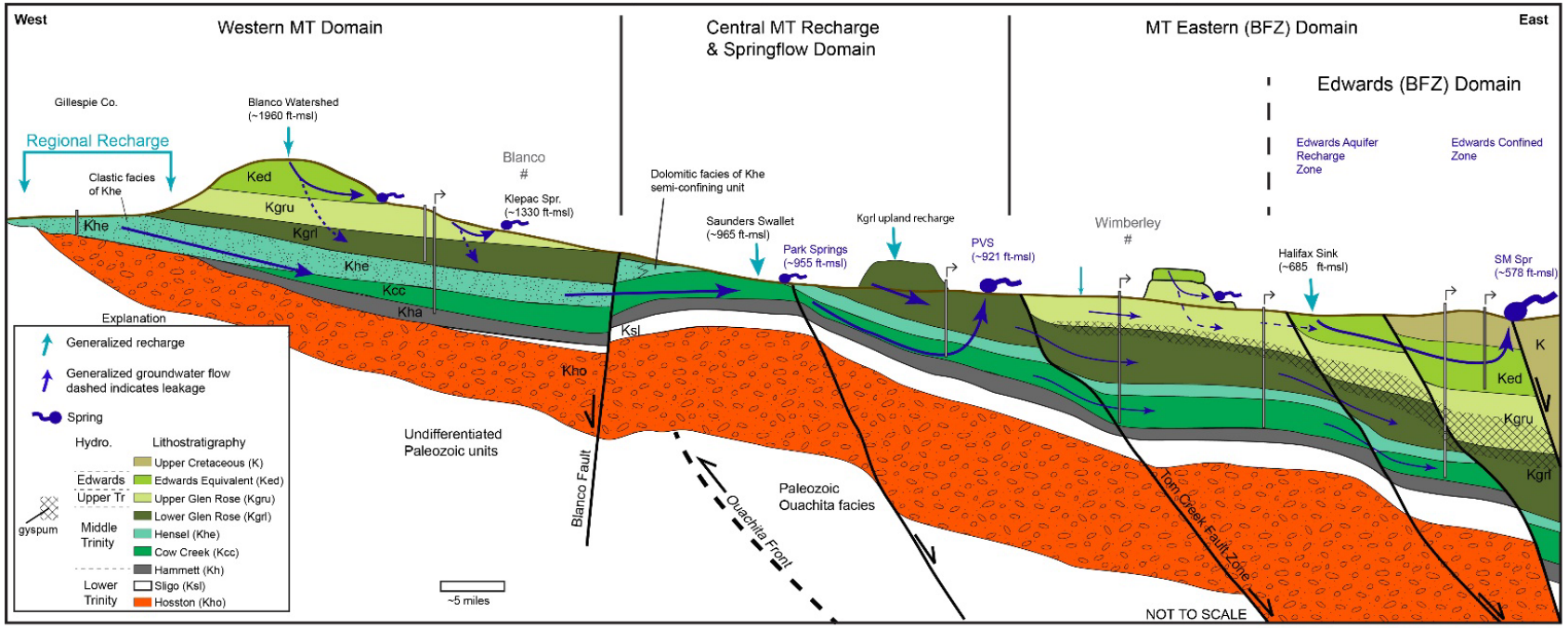

	Western MT Domain	Central MT Recharge & Springflow Domain	MT Eastern (BFZ) Domain	Edwards (BFZ) Domain
Structure	Depositional dip east (~3 degrees?) off Llano Uplift. Fractures trend BFZ.	BFZ horst block exposes MT rock units. Minor BFZ faults and signficant fractures throughout and associated with springs. Anticline structure north of Cypress. Depositional dip slope in western area from Narrows to Burnett Ranch (Park Springs).	Steep structural gradients from BFZ faults, and relay-ramps. Faulting appears to locally compartmentalize. Highly fractured.	
Hydrostratigraphy	Hensel clastic and thick in west, Cow Creek and Hammett Shale pinch out near headwaters of Blanco River. Middle Trinity relatively thin and thickens to east.	Hensel transitions to thinner confining unit. Lower Glen Rose has localizezd patch reefs with high porosity and is Karstic. Cow Creek is locally exposed within Blanco, is karstic and transmits water to PVS and JWS.	Cow Creek and Lower Glen Rose are primary aquifers. Hensel is locally confining. Lower Kgru and upper Kgrl contain confining units.	Edwards Group is highly karstic, uppermost Kgru are in hydrologic communication with overlying Edwards.
Recharge	Regional inflows from Hensel outcrop in Gillespie County--could be flux boundary? Dominated by diffuse recharge and leakage from overlying units. Recharge as a percentage of rainfall <3-5% (previous modeling studies).	Focused recharge to MT in Blanco River documented up to 10 cfs (Hunt et al., 2017). See new gages between Hwy 281 and Burnett Ranch. Diffuse and discrete recharge to Lower Glen Rose units in uplands--could be represented as a high percentage of rainfall (up to 25%). Kgru is relatively thin and likely provides diffuse and focused recharge to Kgrl.	Lateral inflows of MT along relay ramps from the west. Possible leakage, or induced leakage from overlying Kgru.	Majority of recharge from losing streams. Uplands also provide signicant recharge. Some lateral inflows from Kgru possible. Blanco flow loss ~20 cfs (Hunt et al., 2017).
Groundwater Flow	Middle Trinity dominated by diffuse and locally fracture flow. Middle Trinity relatively old (Klepac and Rhoden wells), while Kgru springs young water. Assume diffuse flow dominates MT with local fracture flow.	Middle Trinity dominated by karstic and fracture flow with some diffuse. Middle Trinity groundwater relatively young. Assume relatively fast flow dominates MT.	Dominated by diffuse and locally fracture (karstic) flow. Compartmentalized system. Middle Trinity groundwater is relatively old. Assume relatively slow flow dominates.	Dominated by karst and fracture flow. Rapid groundwater flow.
Discharge	Discharge from MT from limited pumping (BPGCD data) and lateral outflow. Spring discharge is largely from Ked and Kgru, which sustains Blanco River baseflows (~10 cfs gaining)	Discharge from MT from pumping (HTGCD data), major springs (PVS, JWS) and lateral outlfow. Spring discharge is largely from Cow Creek artesian springs. Springflow up to 75 cfs (Hunt et al., 2017), but newer gage data shows more potential sprinflow. HTGCD pumping data....	Discharge from MT from pumping (HTGCD and BSEACD data), and lateral outlfow (unknown).	Discharge from Edwards from pumping (BSEACD, EAA data), and spring discharge at BS and SM.

Figure 12. Hydrogeologic summary and conceptual model of the Middle Trinity Aquifer for Blanco and Hays Counties. Prepared for Martin et al., (2019).

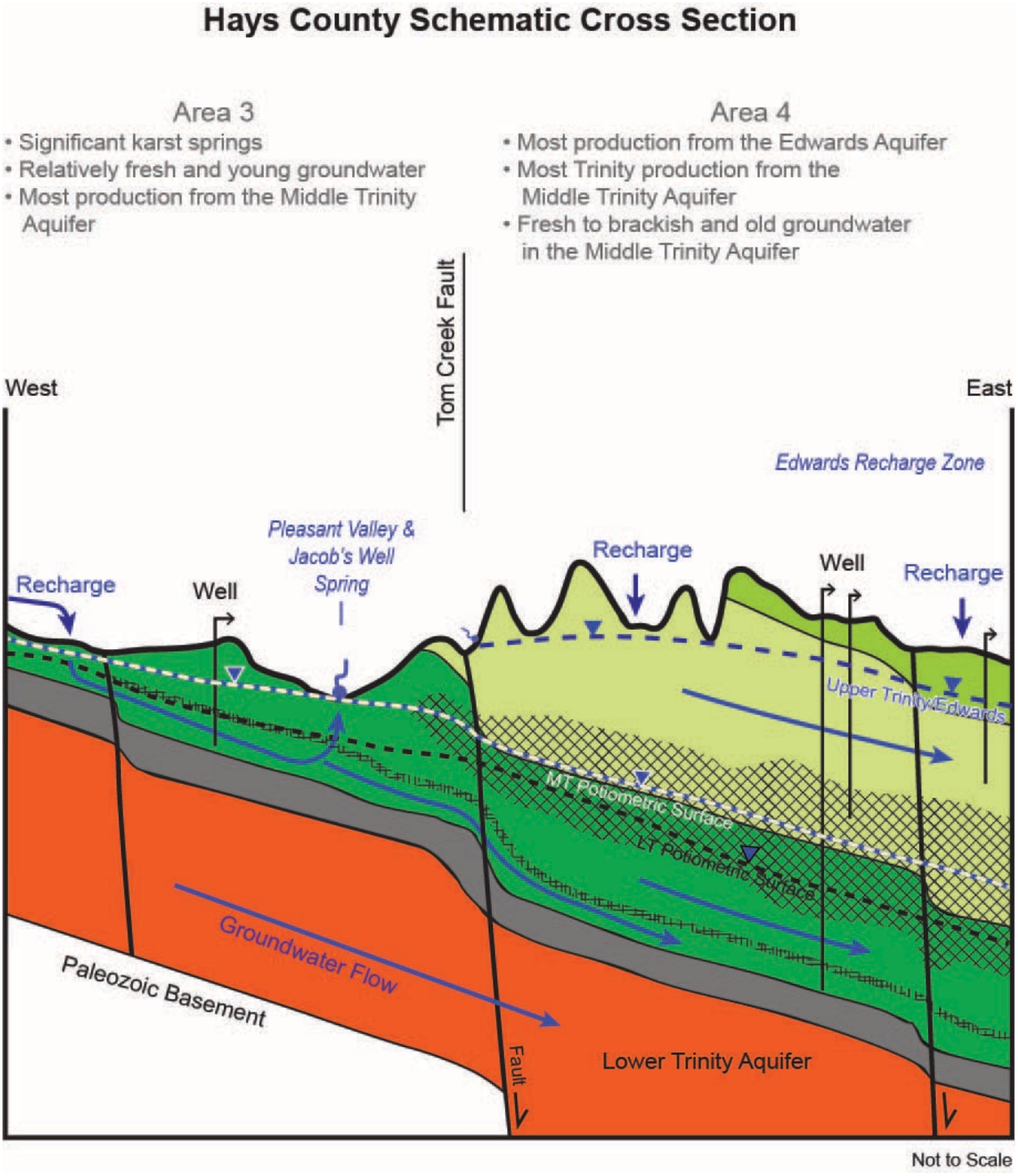

Figure 13. Conceptual model for Hays County. Modified from Hunt et al., (2017a) and Hunt et al., (2020). Figure from Hunt et al., (2020a).

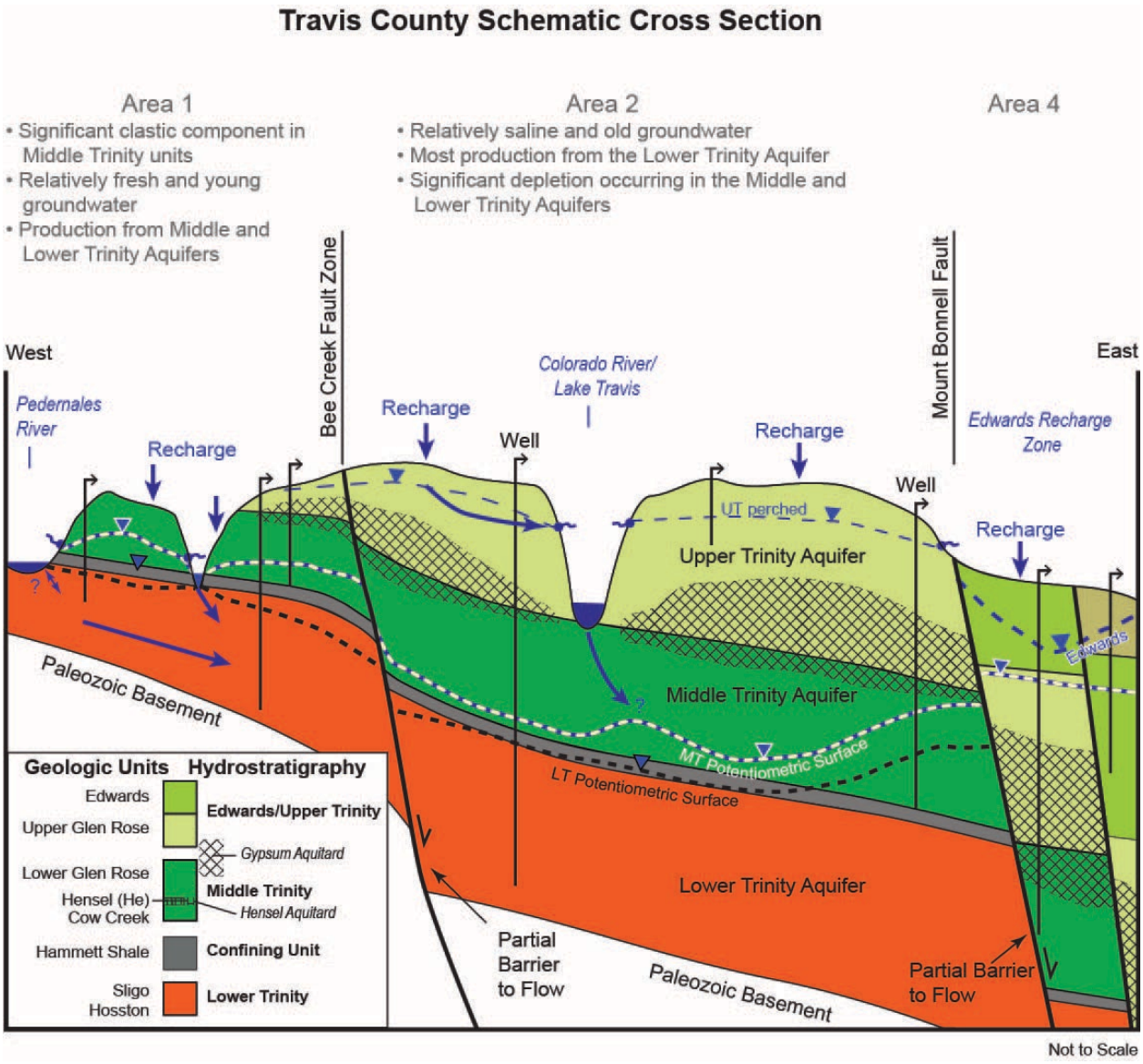

Figure 14. Conceptual model of southwestern Travis County. Modified from Hunt et al., (2020). Figure from Hunt et al., (2020a).

Data Limitations

Abundant hydrogeologic data exist for the study area to develop a conceptual groundwater model. However, there are some areas where additional data would better inform the conceptual model and future numerical modeling. These include:

- Intra-aquifer flow within the Middle Trinity is poorly constrained. Multiport well data and aquifer tests have shown heterogeneities and head differences of units that comprise the Middle Trinity Aquifer. For example, head differences exist between the Lower Glen Rose and the Cow Creek, with the Hensel acting as a local aquitard (Wong et al; 2014; BSEACD, 2017). In other areas, head differences between the units are minor to non-existent. Thus, the vertical hydraulic conductivity of the Hensel may spatially vary significantly, and rendering a 3D model may introduce more errors than a simple 2D model without additional intra-aquifer data.

- The hydraulic functioning of many mapped faults in the area is largely unknown, particularly for faults downgradient of the Mt Bonnell/TCFZ in the BFZ Middle Trinity Aquifer. These downgradient faults have the potential to create locally compartmentalized fault blocks that are partially hydraulically separated from the rest of the aquifer. Middle Trinity water level data is sparse in this downgradient portion of the BFZ Middle Trinity, making evaluation of the hydraulic influence of faults a challenge.

- Inter-aquifer flow from the Lower Trinity and overlying Upper Trinity into the Middle Trinity Aquifer is poorly constrained. Although thought to be minimal, there could be some vertical or lateral flow occurring locally around or across faults.

- The hydrologic relationships of lakes Travis, Austin, and Canyon to the Middle Trinity Aquifer are largely unknown. The river/lake systems may behave as either a source or sink to the Middle Trinity depending upon location and hydrologic conditions (Hunt et al., 2020). However, these lakes fall outside the main area of interest for the TAS.

Model Architecture

Specifics on model code, model grid, and boundary condition architecture, as well model calibration procedures, are presented in the sections below.

Model Code

Groundwater Vistas Version 8 (Rumbaugh and Rumbaugh, 2020) was selected as the software that facilitates the use of MODFLOW and plotting of modeling results with a graphical user interface. MODFLOW-USG (unstructured grid) (Panday 2023) was ultimately selected as the modeling code for the TAS model based on the modeling needs and the new features that USG packages within GWV8, such as:

- Ability to change grid size where needed (nested, quadtree etc.).
- Ability to pinch out model layers.
- Connected Linear Network (CLN) for wells producing from multiple layers, linear conduits (karst), and surface streams. CLNs have not yet been incorporated into the TAS model but are under consideration for implementation in future modeling efforts as they will likely provide a better simulation of turbulent conduit flow than using the equivalent porous media approach, especially near springs.

MODFLOW-USG is like any other version of MODFLOW with identical package options. However, the grids are called unstructured because the traditional row and column arrangement of MODFLOW is no longer assumed. Because the grids are unstructured, the model is much more flexible. For example, layers can be pinched out, which is not possible in a traditional grid. Also, cells can connect to cells in different layers as necessary.

Transient Model Development

The final, 3-layer steady-state version of the TAS model (version 2.1) was completed in September 2020 and provided the foundation for construction of the transient version of the TAS model presented in this report. In general, the model grid and overall location and arrangement of boundary conditions has remained relatively unchanged between the steady state and transient versions of the model. The following is a summary of changes that were made between the steady state and transient versions:

- Removal of cells north of the northern drain boundary of the model domain (approximately coincident with the Pedernales River channel).
- The Layer 1 recharge domain was reduced in size to approximately follow the Blanco River and Onion Creek basins upstream of the BFZ to the upstream boundary of the model domain. The recharge domain was further subdivided into different recharge zones with different recharge coefficients for each zone.
- The number of horizontal flow boundary (HFB) reaches used to represent fault flow barriers has been increased and the location of some HFB reaches has been changed.
- Vertical and horizontal hydraulic conductivities (Kh, Kv) applied to model cells have been changed from zone-based to a cell-specific K matrix. PEST software was used to interpolate Kh and Kv between user-specified pilot points to produce this matrix. The range of Kh and Kv values has also been changed.

- Specific storage and specific yield parameter values have been introduced for all cells in the model domain.
- The BSEACD analytic element polygon used to conceptualize exempt pumping has been significantly reduced in size to more closely align with the distribution of known exempt wells.
- The head elevation for steady-state general head boundary (GHB) reaches has been changed.

Specific changes to boundary conditions and hydraulic parameters are covered in more detail in the sections below.

Model Architecture Overview

Model Units

The following model units for locating all model cells and boundary conditions in real space, as well as hydraulic parameters, inputs, and outputs is as follows:

Coordinate system: UTM Z14-feet
Length dimension: Feet
Time Dimension: Days
X Offset: 621,001 feet
Y offset: 10,884,755 feet
Grid rotation: 23 degrees W of N

Parent Grid

Dimensions of the model are 46 miles E-W by 42 miles N-S. Based on the dimensions of the model, the parent grid spacing and number of cells can be estimated (Table 8). It is generally recommended that a model have less than 500,000 total cells (Rumbaugh, 2016). In addition, it should be noted that additional layers may triple the total number of cells, and nested or quadtree grids will add to the total number of cells. For this model, a grid cell size of 1,000 ft by 1,000 ft was selected. Future versions of the model may include nested grid cells with smaller dimensions over key areas of interest such as springs or pumping centers.

Table 8. General approximations of grid dimensions and number of cells for a single layer for a model of 46 miles by 42 miles. Table modified from Hunt et al., (2020a).

Cell Dimensions (ft)	Number of E-W Cells (242, 880 ft)	Number of N-S Cells (221, 760 ft)	Total Cells	Comment
5280	46	42	1,932	Dimensions of the TWDB GAM
1000	243	222	53,861	TAS Model

A summary of the grid construction for the TAS model is presented in Table 9.

Table 9. Summary of TAS model grid construction

Model Units	Length=[Feet]; Time=[days]
Total Cells	165,375
Active Cells	125,943
Cell Dimensions	1000 ft x 1000 ft
Rows	245
Columns	225
Layers	3

Model Top and Bottom Elevations

The top of the Middle Trinity Aquifer surface (Layer 1) was created from surface and subsurface geologic contacts of the Lower Glen Rose (Cockrell et al., 2018). Those data were supplemented with surface contact elevations from the mapped top of the Lower Glen Rose from the Geologic Database of Texas (USGS 2005). In addition, elevations of the Lower Glen Rose outcrops within the drainage basins were added to account for the exposed and eroded surface (Figures 15 and 16).

The bottom of the Middle Trinity Aquifer is defined as the top of the Hammett Shale. Those data were compiled from the geologic subsurface database (Figure 17). The point data were imported into ArcMap and then the geometry was calculated to provide UTM-ft coordinates. Those points were then imported into Goldenware's Surfer software where the UTM-ft data points were gridded and contoured. All data were contoured within Surfer with the Kriging algorithm. Note that the matrix of top and bottom elevations does not cover two small areas in the NW and SE of the model domain and were estimated. However, much of that area in the NW area is an inactive portion of the model.

After import of the surfaces into the model, two locations were identified where the thickness of the aquifer grid after kriging was less than 50 ft. Those included an area upstream and around Pleasant Valley Spring and upstream of Canyon Lake. Isopach data indicate that these areas have thicknesses greater than 100 ft except for several small reaches along the Blanco River where the Cow Creek outcrops on the surface (Wierman et al., 2010). Using a function in Groundwater Vistas, minimum thickness of the layer was set to 150 ft to smooth the layer thickness to not exceed a 1:3 ratio change between adjacent cells.

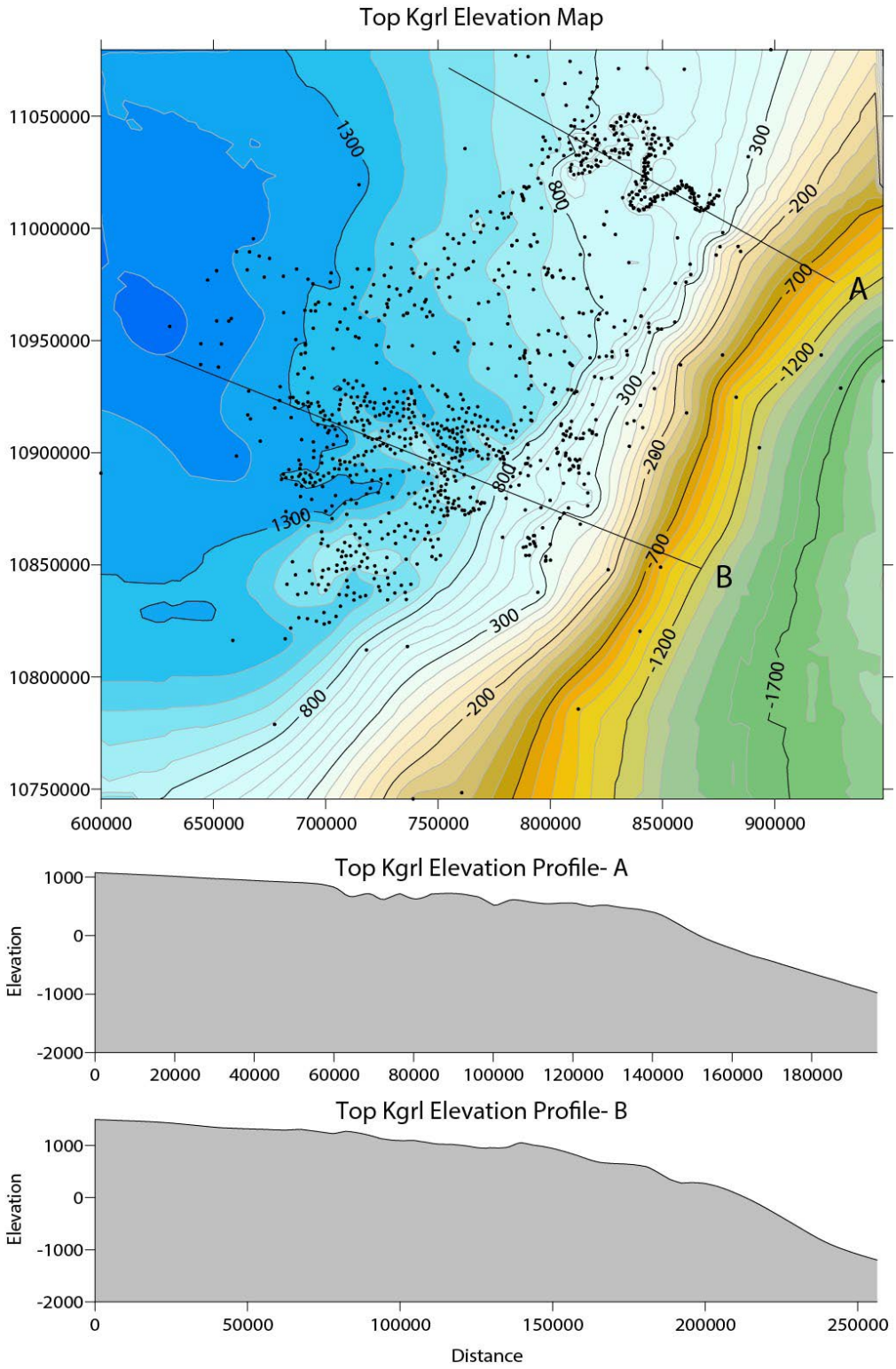

Figure 15. Structure contours and profiles of the top of the Lower Glen Rose (Kgrl), (top of the Middle Trinity Aquifer} and control points. 1,092 data points define the top of the Lower Glen Rose, including 362 subsurface (borehole) control points and 397 map contact control points. The remaining data include the surface elevation where the Lower Glen Rose is exposed along incised rivers and creeks. Units are in feet. Figure from Hunt et al., (2020a).

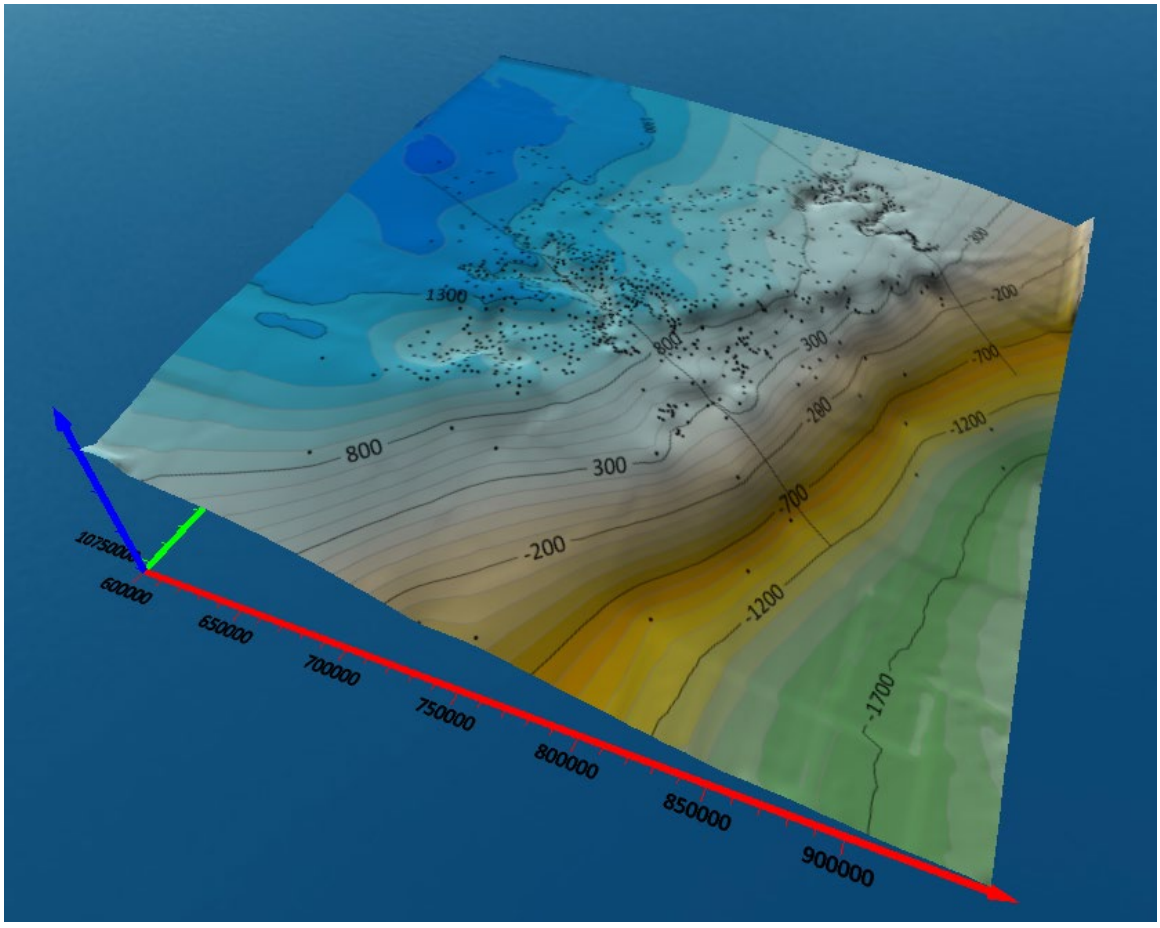

Figure 16. Three-dimensional view of the top of the Lower Glen Rose surface. The deeply incised Colorado River is apparent in the northern portion of the surface with the more broadly incised Blanco River in the middle of the surface. X and Y axes are in UTM-ft coordinates: Zone 14N. The Y-axis (green) represents north. Figure from Hunt et al., (2020a).

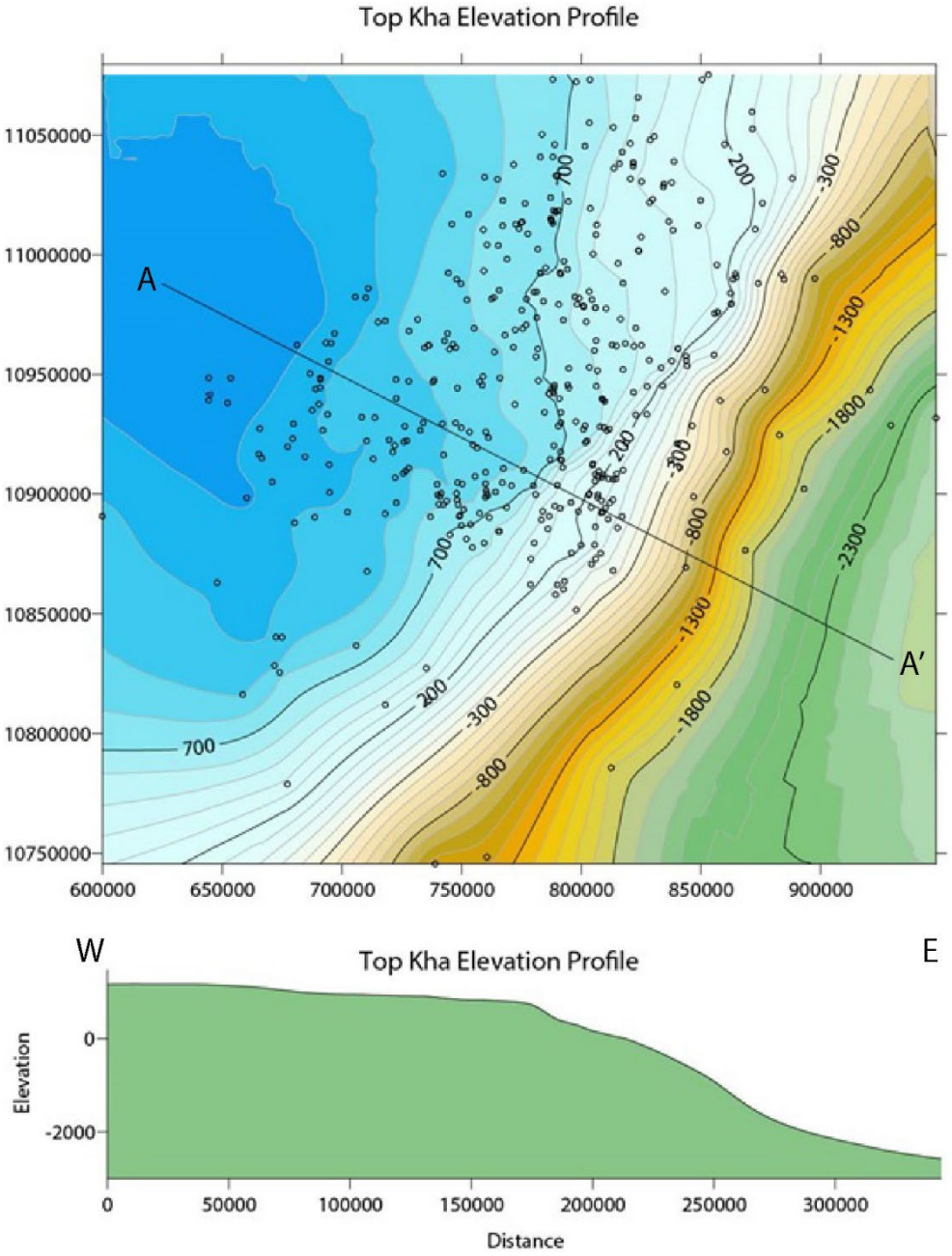

Figure 17. Structure contour of the top of the Hammett Shale (Kha), the bottom of the Middle Trinity Aquifer, and subsurface control points (top); and west-to-east cross section along A-A' (bottom). About 410 data points define the top of the Hammett Shale. The percentage of dip is about 1% across the entire surface from West to East, with a maximum dip of 2% in the BFZ. X and Y axes are in UTM-ft coordinates: Zone 14N. Y-axis represents north in top figure. Figure from Hunt et al., (2020a).

Definition of Layers Within Model Domain Thickness

The three layers for each cell were delineated using the insert grid function and a percentage of the total Middle Trinity thickness at a given location. Percentages for these delineations are as follows:

Layer 1 (Lower Glen Rose):	%70
Layer 2 (Hensel):	%6
Layer 3 (Cow Creek):	%24

For example, one model cell at a location with a total Middle Trinity thickness of 335 ft was subdivided into three layers with the Lower Glen Rose (~230 ft), Hensel (~20 ft), and the Cow Creek (~80 ft). Thus, all three layers are present throughout the active part of the model domain and no pinchouts due to erosion at the surface of any of the layers occurs. This approach was useful for convenient construction of the model grid and computational functionality of the model. However, this model construction differs from known geologic data which indicates that pinchouts of the Hensel and Lower Glen Rose do exist along some reaches of the Pedernales and Blanco Rivers.

Summary of Internal and Perimeter Boundary Conditions

A summary of the internal and perimeter boundary conditions is presented in Table 10.

Table 10. Summary of boundary conditions for the TAS model. Modified from Hunt et al., (2020a).

Boundary Condition/reach # GENERAL HEAD (GHB)	**Name**	**Head (ft-msl)**		**Conductance (ft^2/d)**	**Layer**	**K (ft/d)**
0	Western Inflow	1400		5.44E+5	1-3	5.4E5
1	Northeastern Outflow	350		1.38E+5	1-3	4.1E-1
2	Eastern Outflow	475		2.7E+5	1-3	7.8E-1
DRAINS	**Name**	**Stage (ft-msl)**		**Conductance (ft^2/d)**	**Layer**	**K (ft/d)**
0	Pedernales-Colorado	651-1184		1.3E+1-1.4E+3	3	1
1	JWS	922.84		1.0E+7	3	1.0E+3
2	PVS	922		1.0E+7	3	2.0E+2
4	Park	955		5.0E+7	3	1.0E+4
RIVER	**Name**	**Stage (ft-msl)**	**River Bottom Elevation (ft-msl)**	**Conductance (ft^2/d)**	**Layer**	**K (ft/d)**
0	Lake Travis	680	516 (570 to 490)	1.0E+01	1-3	1.18e-05
1	Lake Austin	492	455 (480 to 450)	1.0E+07	1	3.07E+2
3	Canyon Lake	909	828 (895 to 790)	1.0E+01	1	1.0E+1
Horizontal Flow Barrier (HFB)	**Name**	**Thickness (ft)**				**K (ft/d)**
0	Bee Creek Fault	10			1-3	1E-6
1	Mt Bonnell Fault	1			1-3	7E-6
2	Relay Ramp	1			1-3	1E+3
3	MB Fault-Relay Ramp Transition	1			1-3	1E-2
5	Park Spring Fault	1			1-3	1E-6
6	Graben Upgrad Fault	1			1-3	3.2E-3
7	Tom Creek East	1			1-3	1E-3
8	Wimberley Fault	1			1-3	5E-5
10	Tom Creek West	1			1-3	1

General Head Boundaries (GHB)

General head boundary (GHB) conditions are summarized in Table 10 and shown in Figure 18. GHBs were used to simulate regional lateral groundwater flow entering from upgradient and leaving from downgradient of the model domain as discussed in the conceptual model section earlier in this report.

Western GHB

A GHB head elevation of 1,400 ft-msl for the western boundary was assumed based on the 2018 potentiometric map (Hunt et al., 2019a)(Figure 18).

Eastern and Northeastern GHBs

The eastern boundary is modeled as a GHB with a potentiometric elevation of 475 ft-msl. The elevation was selected through manual calibration of heads in the downgradient eastern portion of the model domain. The eastern GHB boundary is based on the conceptual model indicating southeastward flow east of the model boundary, and then flowing vertically, discharging into the overlying units (Hoff and Dutton, 2017). This vertical flow, if present, likely occurs at least several miles east of the model boundary.

The northeastern boundary is located at about the 350-ft-msl contour based upon the potentiometric mapping of Hunt et al. (2020). This is the area where water leaves the model to the northeast into northern Travis County and flows toward Williamson and Bell Counties.

No-Flow Boundaries

The northern and southern boundaries of the model were considered as no-flow boundaries based on the 2018 and 2019 potentiometric maps (Hunt et al., 2019a and Hunt et al., 2020). These boundaries occur where potentiometric contours indicate a groundwater divide and groundwater flow directions inferred as perpendicular to potentiometric contours are oriented parallel to the no-flow boundary.

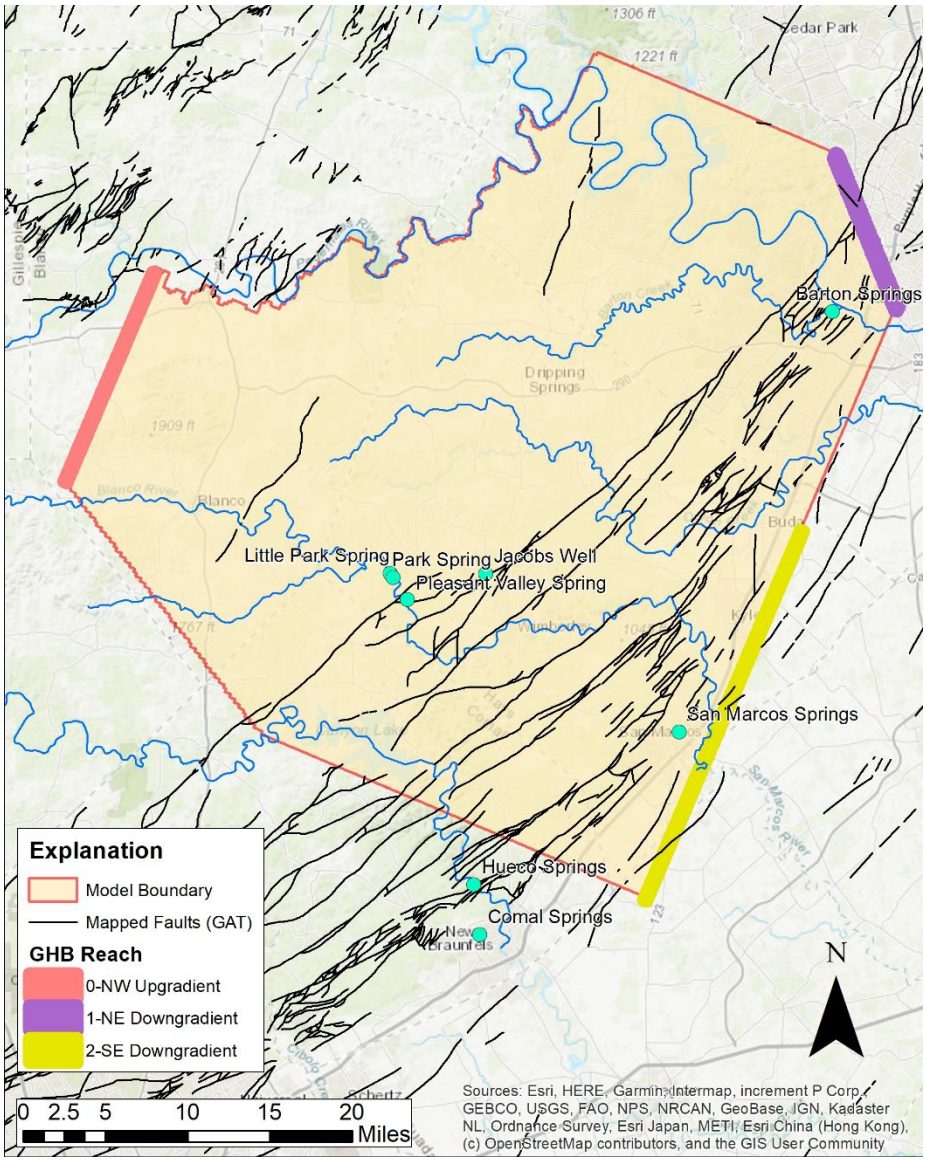

Figure 18. Map of TAS GHB locations for all three model layers.

Fault Barrier Conceptualization: Horizontal Flow Boundaries (HFBs)

Several faults within the model domain are represented as partial groundwater flow barriers using the MODFLOW HFB package. Generally, these flow barriers are faults that coincide with steepening of hydraulic gradients observed in potentiometric maps (Hunt et al., 2020, Hunt et al., 2019a) (Table 8 **;** Figure 19). The most prominent of these barrier faults is the NE/SW trending Mount Bonnell Fault, which is called the Tom Creek Fault in Hays County (TCFZ). As the Mount Bonnell/TCFZ crosses south into Hays County, the hydrologic influence of the faults appears to diminish based on direction and magnitude of head gradients.

Groundwater flow directions are parallel to the Mount Bonnell/TCFZ Fault zone in Travis County and transition to being normal to the TCFZ to the south in Hays County, suggesting that at least some groundwater is moving across the TCFZ in this area. Hunt et al., (2015) describe a relay ramp structure along the fault zone, extending from approximately Onion Creek in the north to the Comal/Hays County line in the south. This area coincides with lower total dissolved solids (TDS) Middle Trinity groundwater, suggesting that fresher groundwater from the upper Blanco Basin may be flowing across the TCFZ into downgradient confined portions of the Trinity. This relay ramp structure has been conceptualized in the TAS model by adding a higher conductivity HFB reach (reach 2) along the TCFZ mapped fault trace extending from approximately Cypress Creek to the Blanco River (Figure 19).

In addition to Mount Bonnell/TCFZ (GHB Reaches 1,3, and 7), other barrier fault HFBs included in the model domain are described below and shown in Figure 19:

- The Bee Creek Fault (HFB Reach 0): A NE/SW-trending fault located in western Travis County.
- The Park Spring Fault (HFB Reach 5): A NE/SW-trending fault intersecting the Blanco River and located just downgradient of the Park Spring complex.
- The Blanco Fault (HFB Reach 6): A NE/SW-trending fault that bounds the upstream extent of Lower Glen Rose outcrop in Blanco County and runs approximately parallel and to the west of the Blanco/Hays County line.
- The Wimberley Fault (HFB Reach 8): A NE/SW-trending fault zone which runs approximately parallel to and downgradient of the TCFZ downgradient of the town of Wimberley

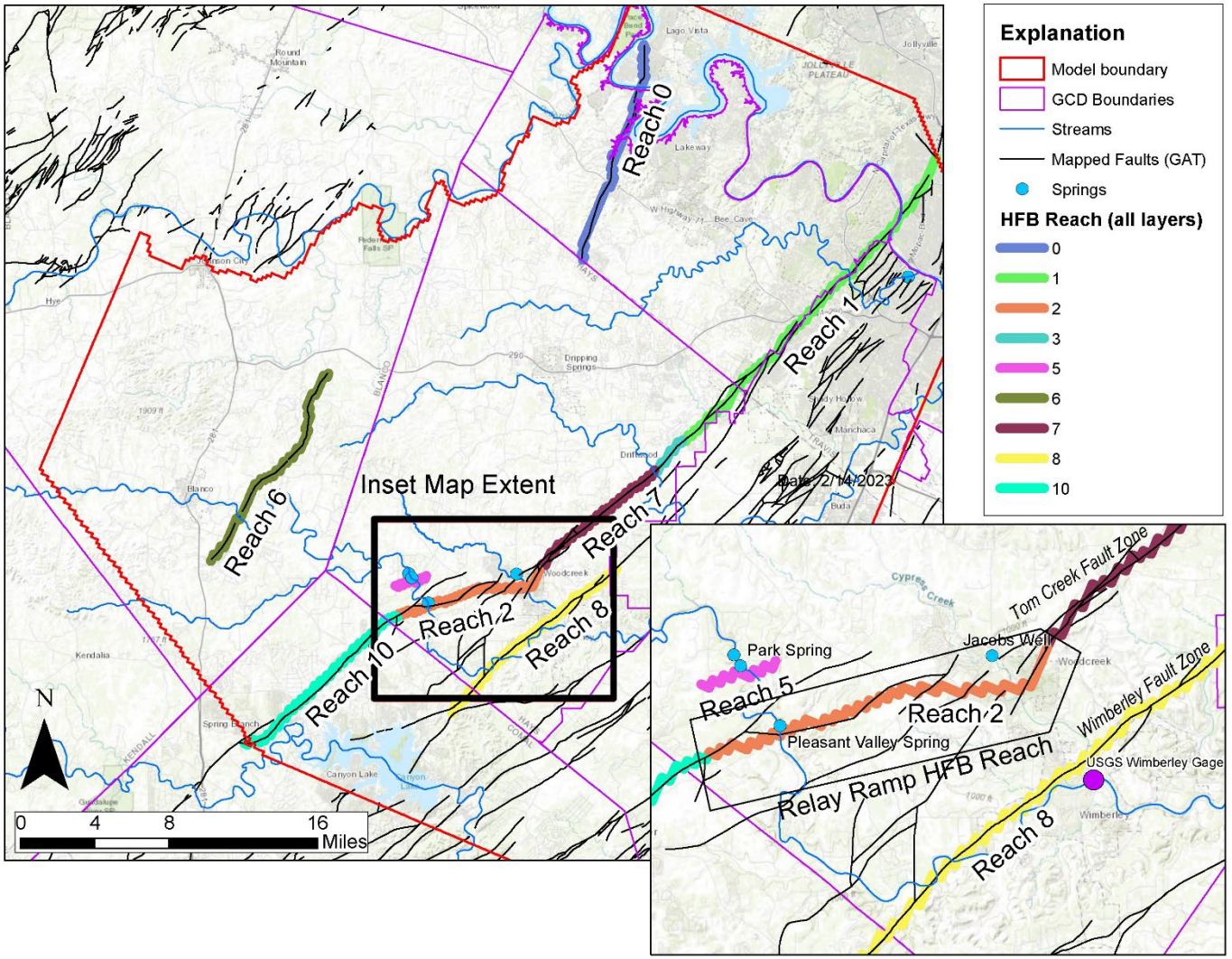

Figure 19. Map of horizontal flow barrier (HFB) reaches for all layers in the model domain (left) and zoomed-in inset map with relay ramp HFB Reach 2 (right).

Drains (Springflow)

Springflow is simulated in the TAS using the MODFLOW drain package. Drains are also used to represent the Pedernales River along the northern boundary of the model and portions of the Colorado River west of the Bee Creek Fault Zone (Table 10**;** Figure 20). In those areas, Middle Trinity heads are above the base of the river channel and result in locally gaining streams (Hunt et al., 2020). Numerous small springs and seeps are known to occur in this area but these features are not discretely modeled.

Major artesian springs of the Middle Trinity Aquifer in Hays County are modeled discretely as individual drain cells within Layer 3 of the TAS model domain (Table 10**;** Figure 20). These are JWS, PVS, and Park Springs, and are simulated with the head (stage) and flux used as calibration targets. Drain flux calibration approach is discussed later in this report.

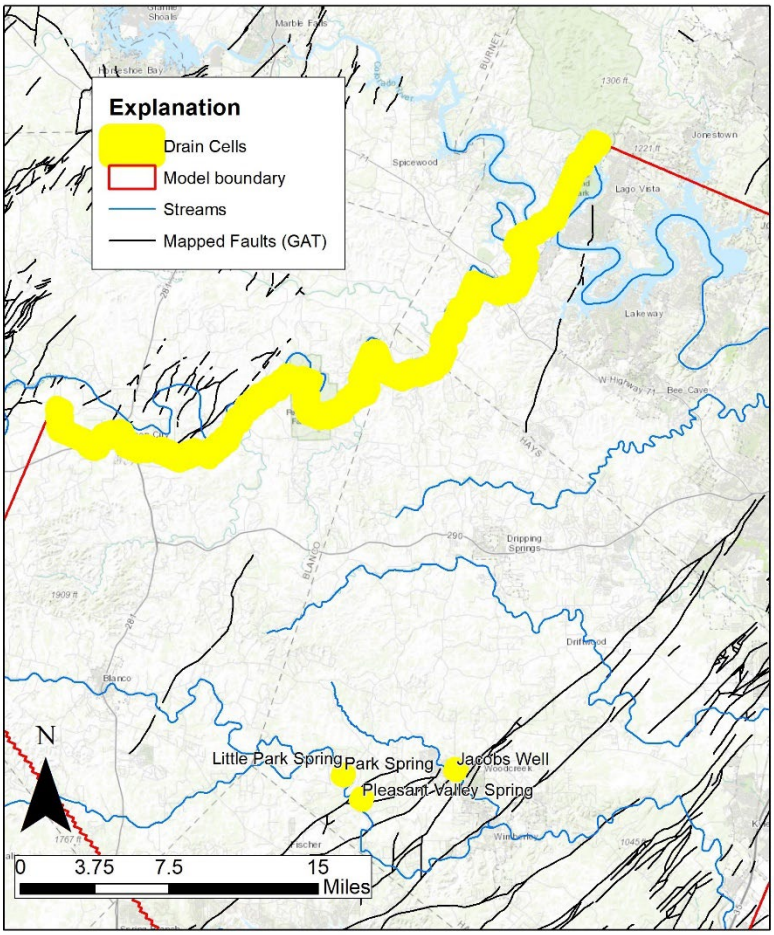

Figure 20. Map of drain cells in Layer 3 of the TAS model domain.

Hydraulic Parameters

Hydraulic Conductivity

Horizontal and vertical hydraulic conductivity (Kh and Kv) were assigned to model cells using a combination of PEST software and manual calibration. Maps of the final TAS Kh/Kv distribution for each model layer are presented in Figure 21-Figure 27. PEST was implemented using pilot point interpolation, with pilot point spatial distribution roughly following the hydraulic conductivity zones established in the steady-state version of the TAS model (Hunt and Smith, 2020). Initial Kh and Kv ranges for PEST parameterization were initially assigned to pilot-point groups based on the conceptual model for groundwater flow in the study area, and known K distribution from observed data from available aquifer testing and multiport slug-test data (Hunt et al., 2010; Hunt et al., 2016b) (Figure 7). These Kh and Kv ranges were later adjusted manually in subsequent PEST runs to improve model performance and calibration statistics.

Manual adjustment of Kh were performed in two areas of the model domain:

1) Layer 3 in the immediate vicinity and upgradient of PVS and JWS (Figure 24).
2) Layer 3 in the eastern, BFZ Middle Trinity portion of the model domain (Figure 23)

Manual adjustment was performed by exporting Kh model cell shapefiles from Groundwater Vistas into ESRI Arcmap and selecting and adjusting Kh attributes for specific cells. For cells in the vicinity of PVS and JWS, a multiplication factor of 3X was applied to the Kh values, increasing them. This was done because increasing Kh in this portion of the model domain increased magnitude of PVS and JWS springflow responses to recharge events, thereby increasing “flashiness” and bringing modeled springflow behavior more in line with observed springflow behavior. In the eastern, confined portion of the model domain, a max Kh of 5 ft/d was applied, with any cells above this value being lowered downward. This was done to increase the magnitude of confined aquifer head variations, bringing them more in line with observed confined Middle Trinity hydrographs.

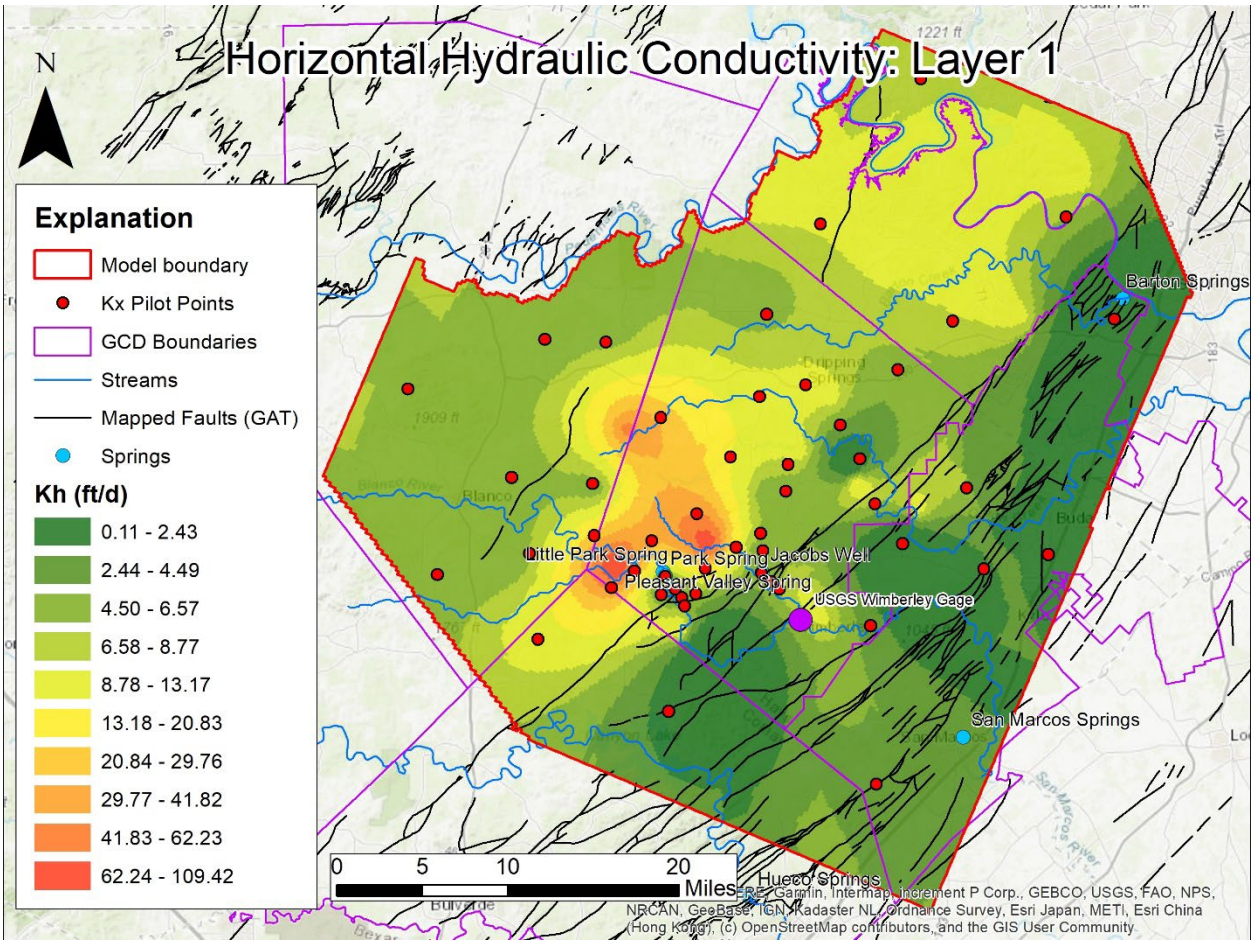

Figure 21. Horizontal hydraulic conductivity (Kh) in Layer 1 of the model domain

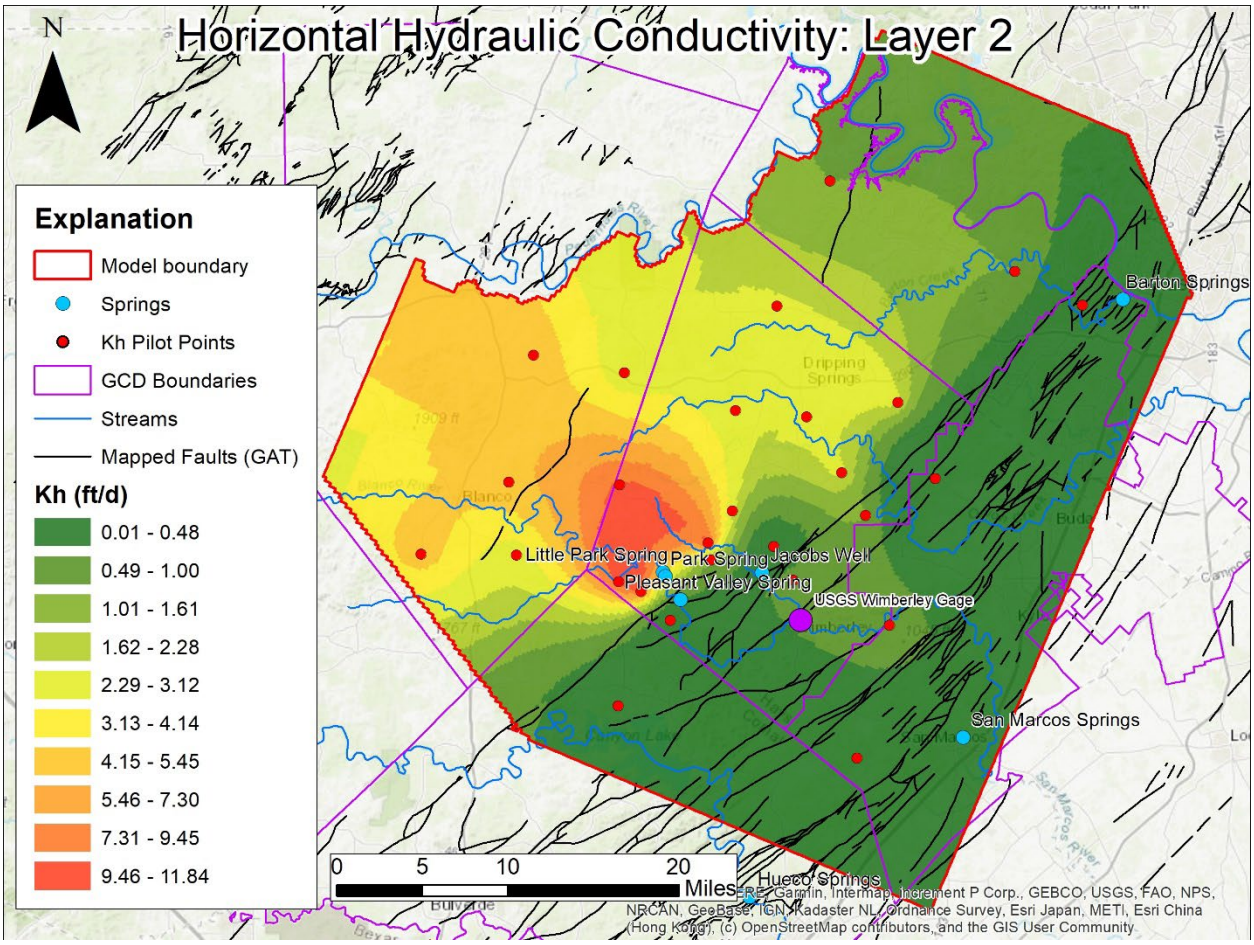

Figure 22. Horizontal hydraulic conductivity (Kh) for Layer 2 of the model domain.

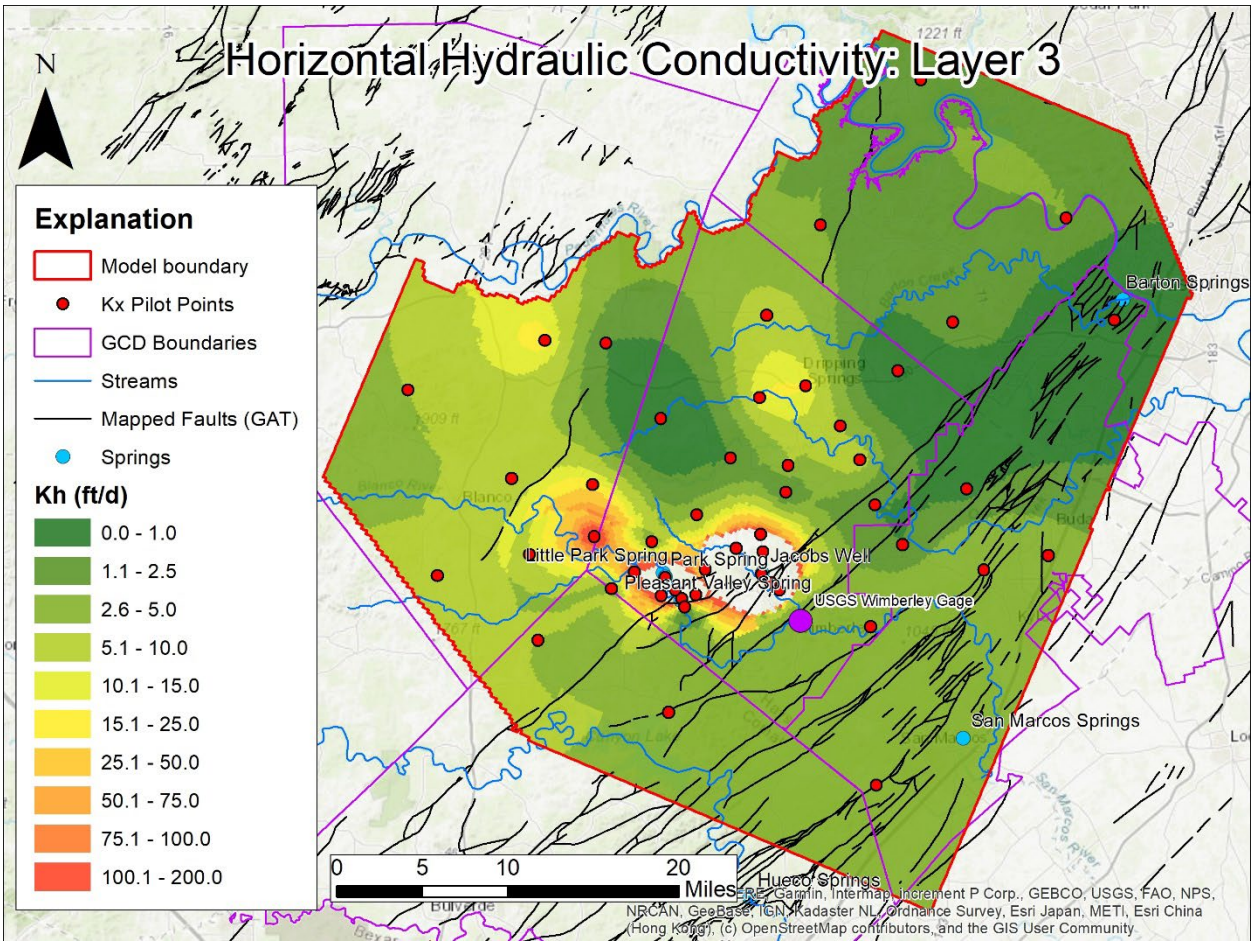

Figure 23. Horizontal hydraulic conductivity (Kh) for Layer 3 of the model domain (excluding model cells with K> 200 ft/d)

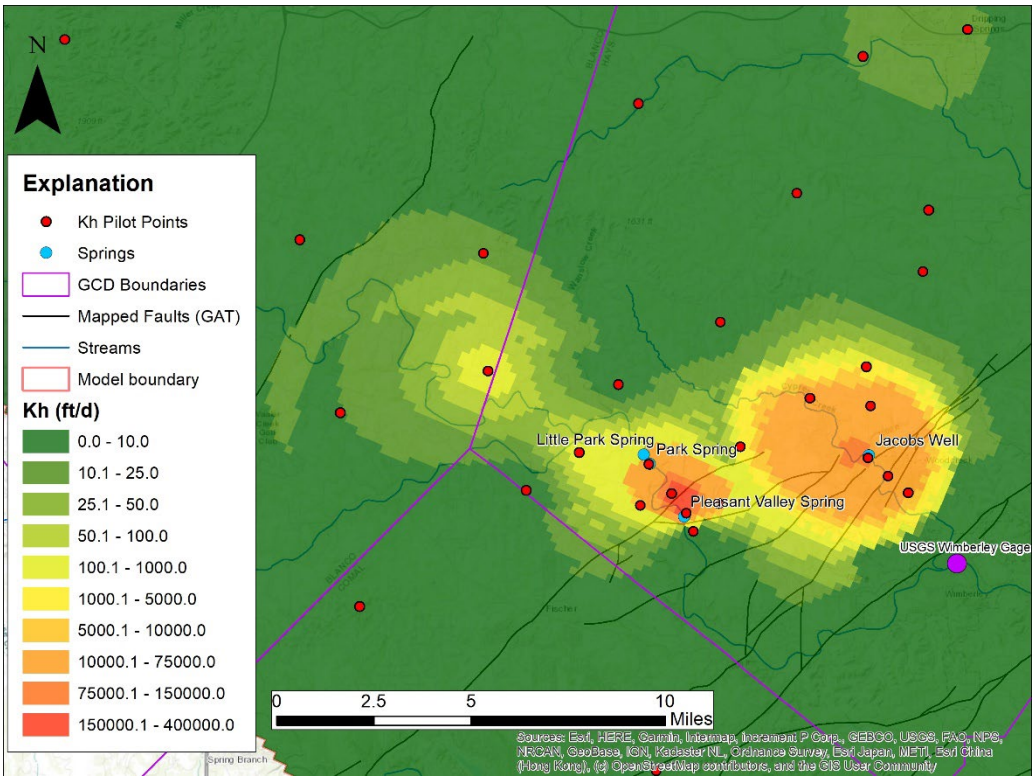

Figure 24. Layer 3 horizontal hydraulic conductivity (Kh) within the model domain in the vicinity of JWS and PVS.

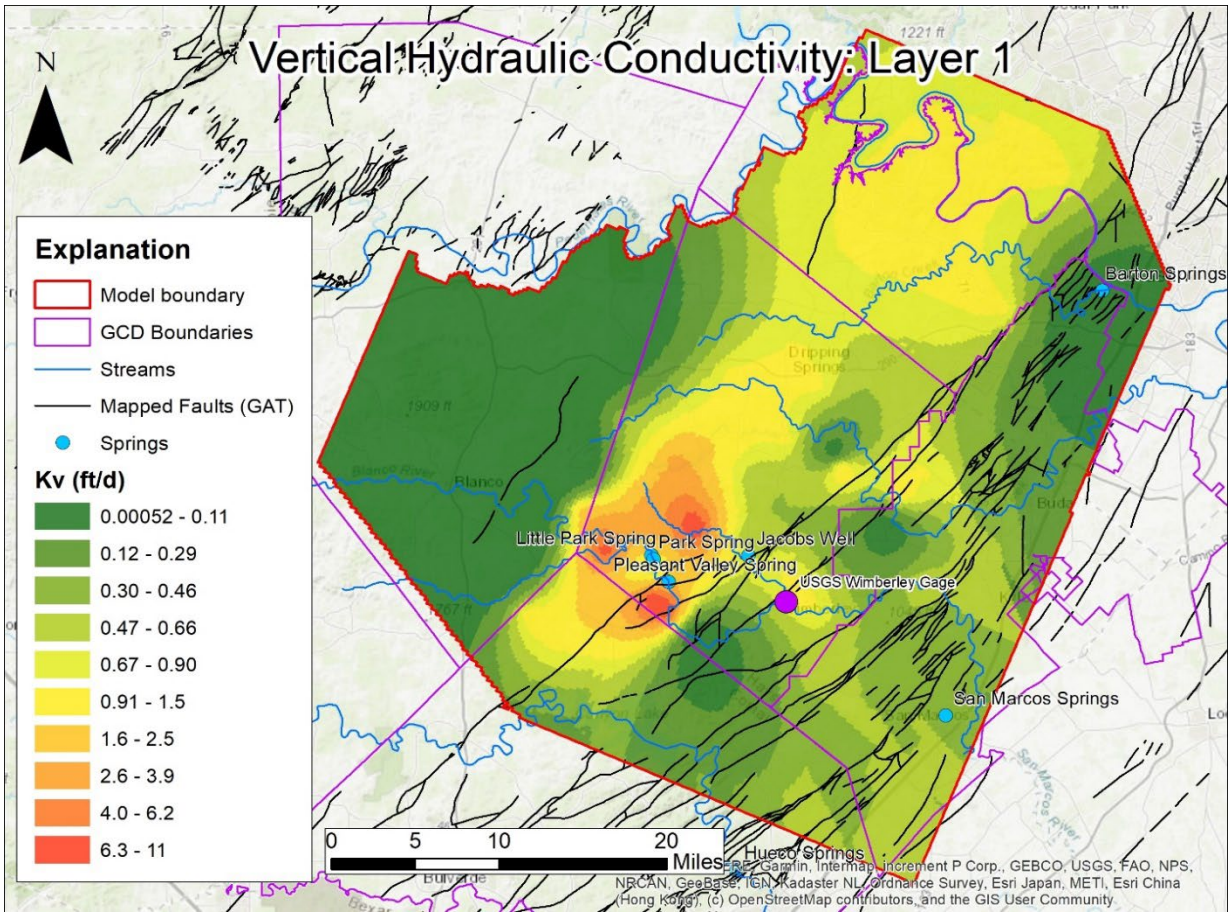

Figure 25. Vertical hydraulic conductivity (Kv) in Layer 1 of the model domain.

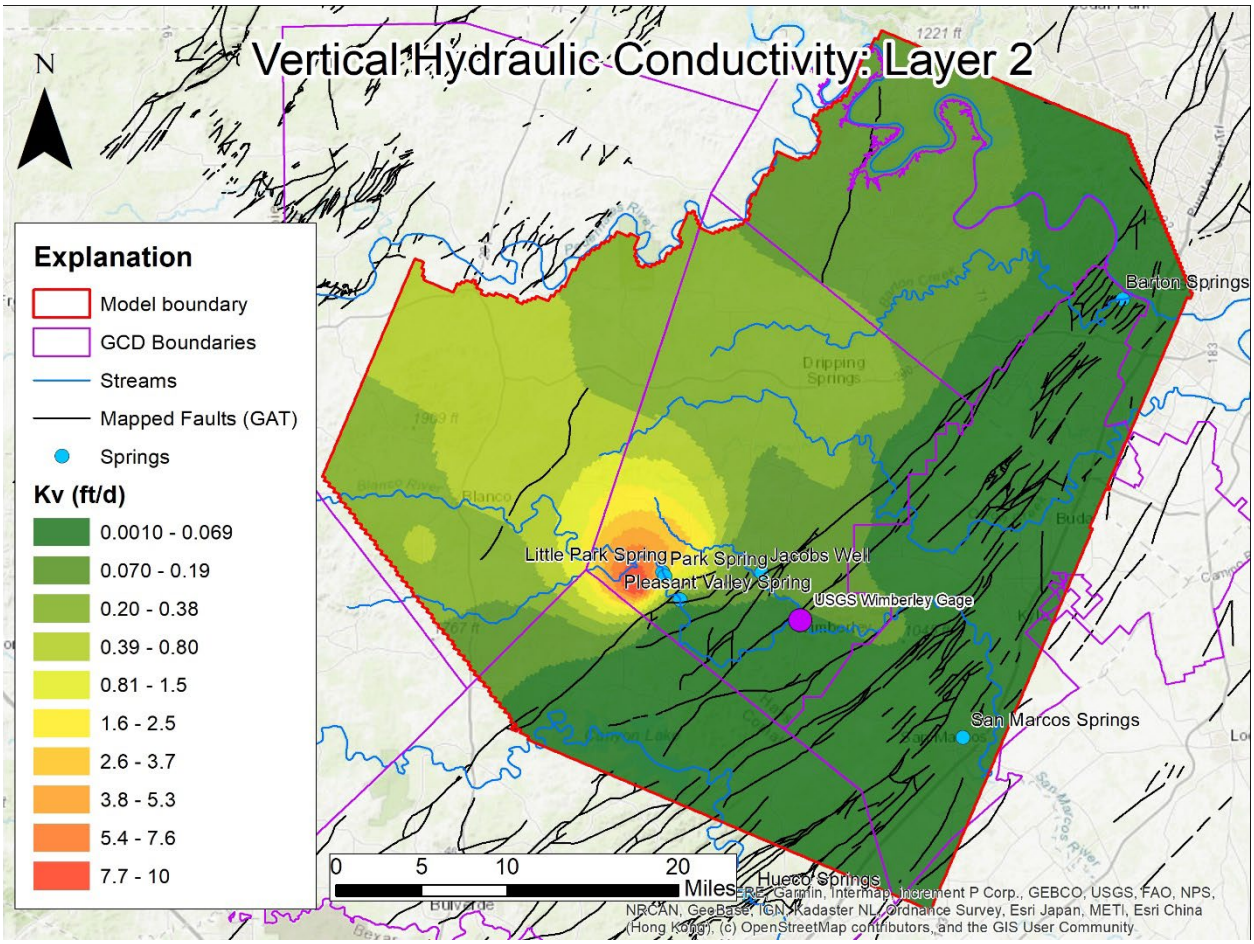

Figure 26. Vertical hydraulic conductivity (Kv) in Layer 2 of the model domain.

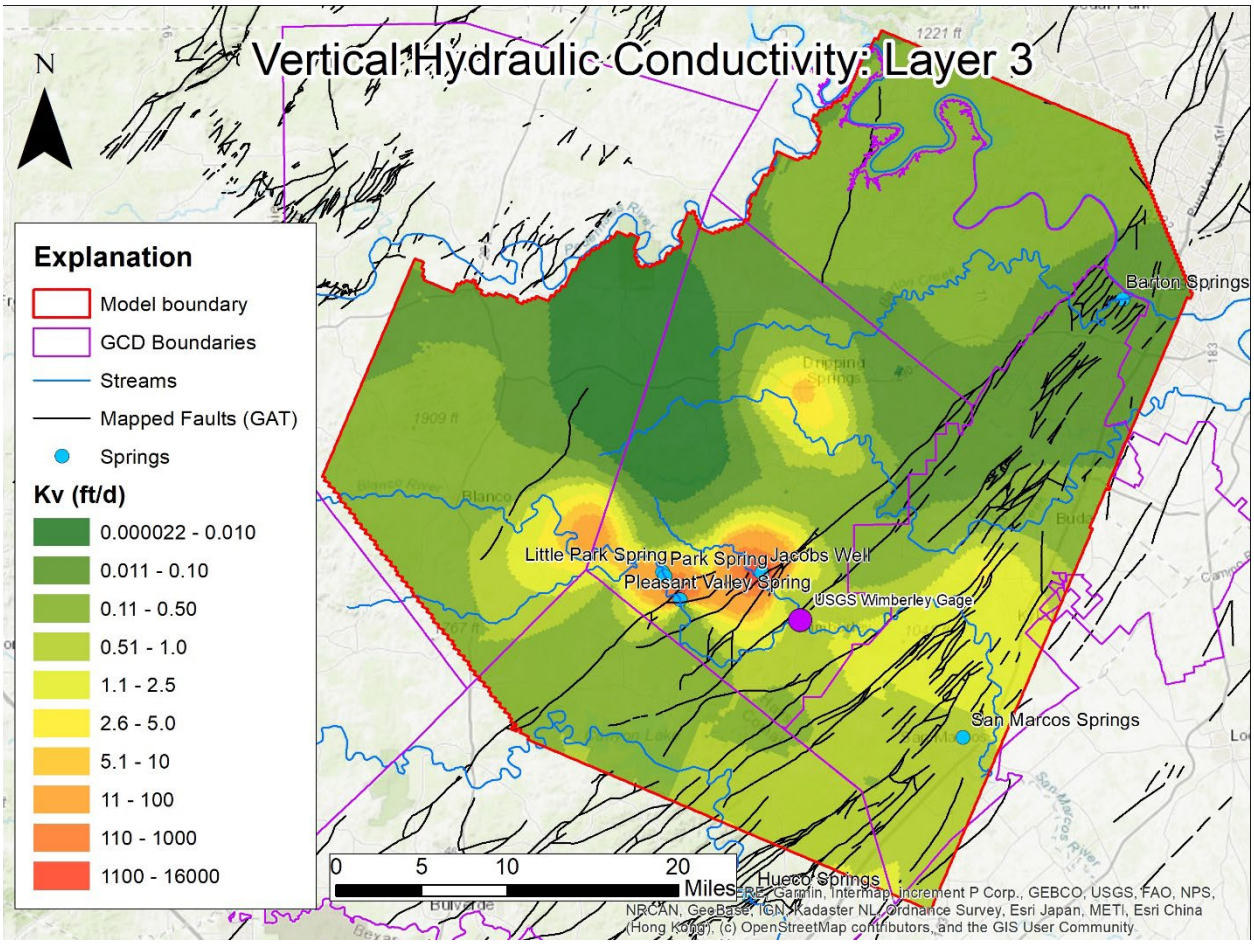

Figure 27. Vertical hydraulic conductivity (Kv) in Layer 3 of the model domain.

Storage Parameters

Storage parameters, specific storage (Ss) and specific sield (Sy), were varied within nine delineated zones in the model domain. For all three layers, storage zones were delineated along the Mt. Bonnell/TCFZ mapped fault, with at least one zone to the west and one zone to the east (Figure 28). This zone distribution was adopted from the hydraulic conductivity zones established in the previous steady state version of the TAS model, which roughly follow the known distribution of hydraulic conductivity within the study area (Hunt and Smith, 2020). Because available data on storage parameters are sparse within the study area, Ss and Sy zone values were automatically selected during PEST calibration constrained to the range of available measured values. This calibration process is discussed later in this report.

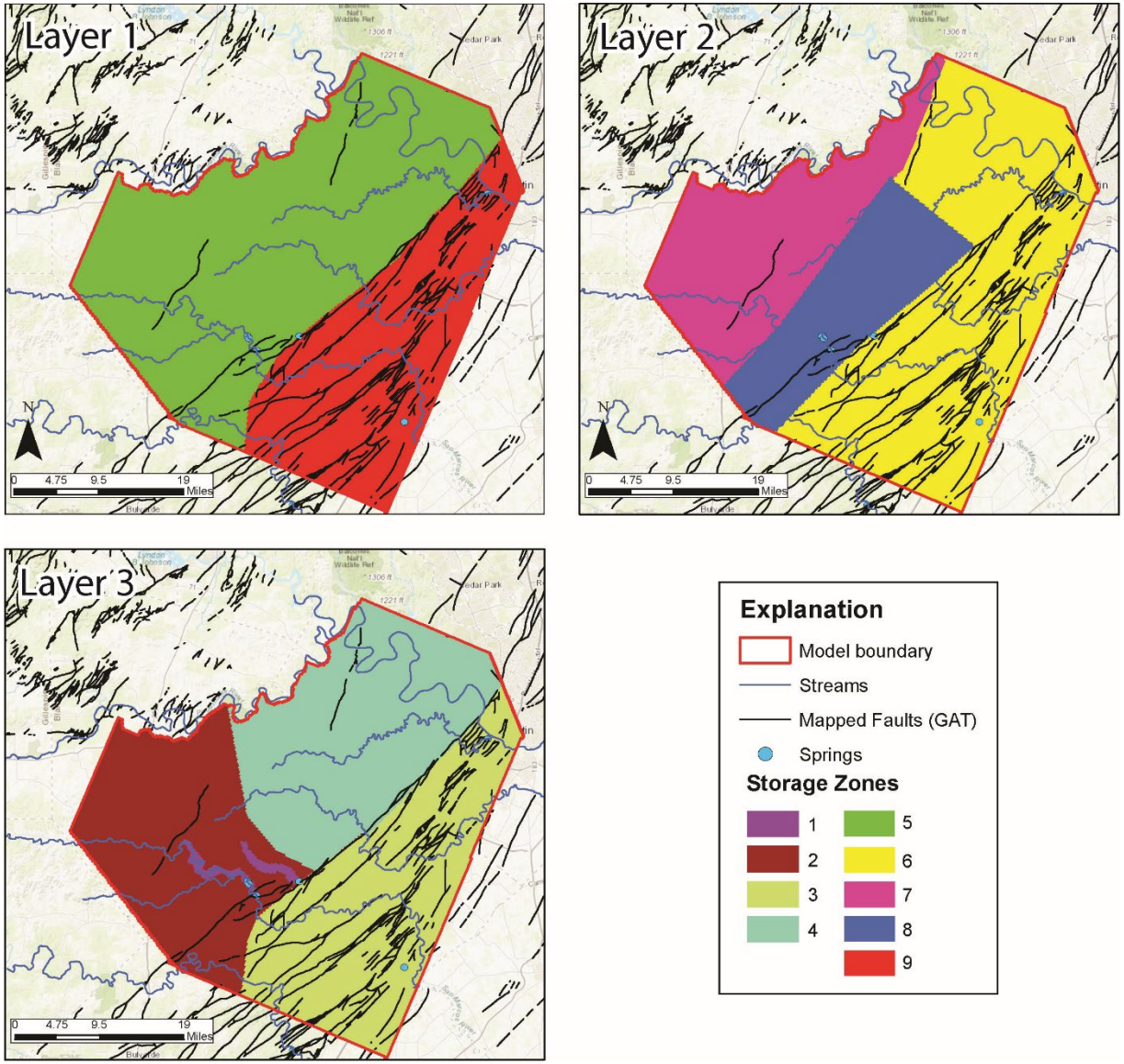

Figure 28. Maps displaying storage parameter zones for all three layers of the model domain.

Rivers

The river package allows for water to enter or leave the groundwater system based upon heads in the aquifer, river or lake, and the assigned conductance. Rivers form head-dependent boundaries within the model and are modeled as different reaches (Table 10**,** Figure 29). In the northern portion of the model, the Colorado River is impounded by two dams creating Lake Travis (~680 ft-msl) and Lake Austin (492 ft-msl). Lake Travis fluctuates according to hydrologic conditions and is used for flood control, water supply, and hydroelectric power. We conceptualize the Colorado River as a river (River Package) rather than a constant level lake. East of the Bee Creek Fault Lake Travis is represented as a specific river reach with the potential to exchange water with the aquifer (Reach 0). Lake Austin occurs as another river reach between Mansfield and Tom Miller dams (Reach 1). Lake Austin is a constant-level lake and generally serves as a pass-through lake and generates some hydroelectric power. Canyon Lake is also represented as a river reach (Reach 3).

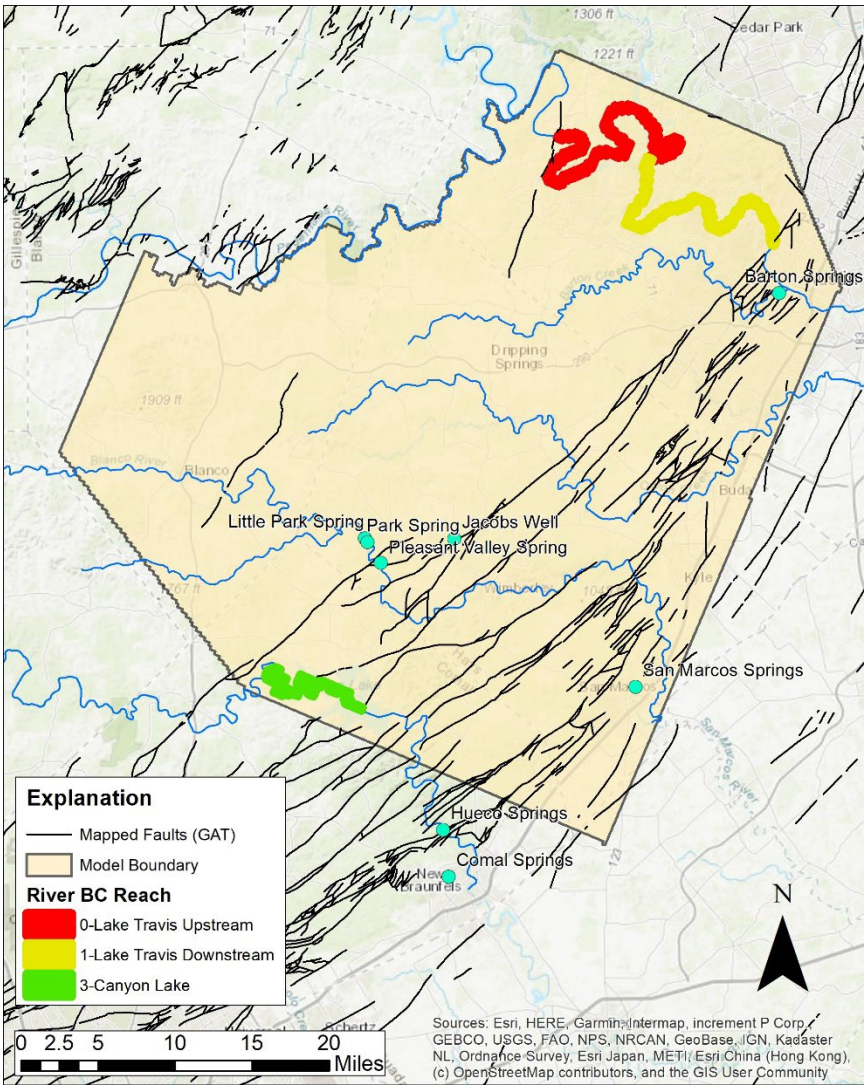

Figure 29. Map of river package boundary cell locations within the model domain.

Recharge

Recharge enters the model domain into the topmost saturated model layer (usually Layer 1 for a given time step) within an area approximately following the upper Blanco River and Onion Creek stream basins, with the downstream extent of the recharge area approximately following the Wimberley Fault within the BFZ. The recharge domain was further subdivided into five different zones, delineated through a combination of mapped fault traces, geologic outcrop, and stream watershed boundaries (Figure 30).

Recharge was calculated as a simple recharge coefficient of total precipitation, and thus does not include separate calculations for atmospheric and unsaturated zone processes such as evapotranspiration. Gridded monthly precipitation data from the PRISM dataset (PRISM 2022) were used to calculate recharge for each cell within the recharge domain depending on that zone's recharge coefficient. As alluded to in the conceptual model outlined earlier in this report, the Trinity Aquifer displays relatively flashy (fast) responses to rainfall/stormflow events occurring in recharge areas. The magnitude of these springflow/head responses is dependent on the amount of rainfall in a given storm event, and the antecedent hydrologic conditions. The Blanco River provides a useful proxy for antecedent Middle Trinity conditions because its baseflow is sustained by karstic Middle Trinity springs.

To simulate these variable springflow/head responses, each zone within the recharge domain was assigned a lower and higher recharge coefficient. Which of these coefficients was applied to a given stress period for a given cell was tied to the amount of average monthly flow as reported at the Blanco River flow gage at Wimberley (USGS gage ID: 08171000). If average monthly Blanco River flow was greater than 40 cfs, the higher recharge coefficient was applied to the monthly precipitation at that model cell (i.e. antecedent conditions were assumed to be "primed" for higher amounts of recharge for that stress period). The lower recharge coefficient was applied to stress periods with monthly average flow below the 40 cfs threshold.

Selection of recharge coefficients was informed by the conceptual model and published literature values (see conceptual model section of this report), and through manual adjustment/experimentation to match volumetric springflow and head calibration targets. High/low recharge coefficient values for each zone are reported in Table 11. The highest coefficients were applied to Zone 6 (up to 15% of total precipitation), which is approximately coincident with a 1-mile buffer of known losing reaches of the Blanco River and Cypress Creek. Zone 1 approximately follows the Blanco River basin upstream of the TCFZ where the Lower Glen Rose outcrops excluding Zone 6 (Figure 30). Zone 3 comprises the upper Onion Creek basin where most recharge to the Middle Trinity within the Onion Creek basin is likely to occur (Hunt et al., 2017b). Zone 2 coincides with the Blanco River basin upstream of Lower Glen Rose outcrop. Zone 5 coincides with the BFZ between the TCFZ and Wimberley faults and within the Blanco Basin and the south side of the Onion Creek Basin. Previous versions of the model excluded the BFZ from the recharge domain but did not simulate adequate head fluctuations in response to recharge events. Thus, Zone 5 was added as a transitional recharge zone with lower recharge coefficients than the upgradient zones in order address this issue and achieve better matching of confined Middle Trinity head responses in the Middle Trinity BFZ portion of the model domain.

Table 11. High flow (Blanco River flow >40 cfs) and low flow (Blanco River flow <40 cfs) recharge coefficients applied to recharge zones.

Recharge zone	Description	High flow coefficient	Low flow coefficient
1	Blanco LGR Outcrop	0.03	0.01
2	Blanco Upgradient LGR Outcrop	0.01	0.005
3	Upper Onion Creek	0.05	0.005
5	BFZ	0.02	0.001
6	Blanco losing stream buffer	0.15	0.01

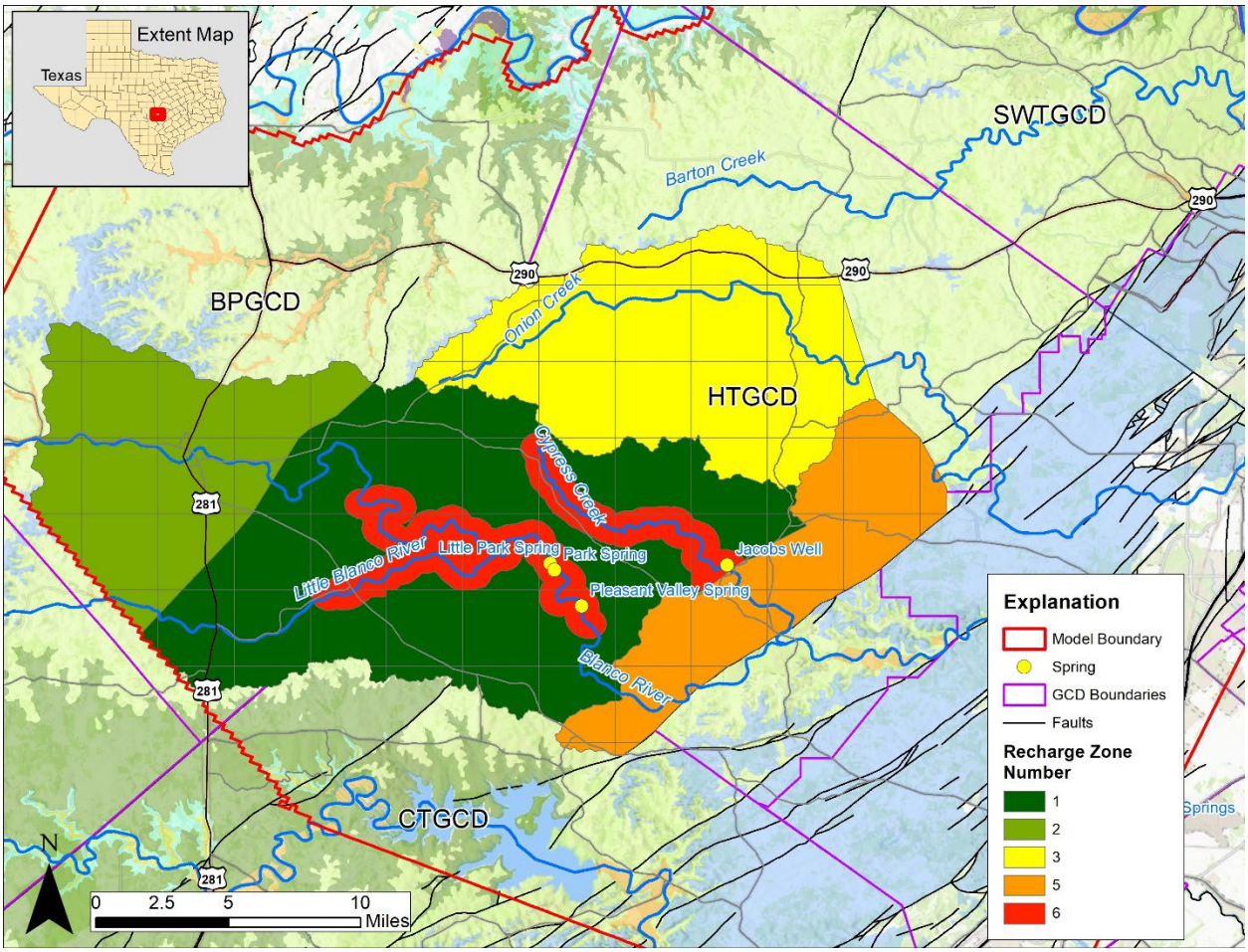

Figure 30. Map of Layer 1 recharge zones within the model domain.

Pumping

Non Exempt

Pumping data for non-exempt wells came from monthly pumping as reported by non-exempt permit holders within HTGCD and BSEACD (data from BPGCD and CTGCD were not available for these modeling efforts). These monthly pumping data are reported as total permitted pumping for an individual permit holder, and do not split pumping based on which well groundwater was pumped from. For permitholders with more than one pumping well, this adds some uncertainty as to where groundwater is being removed from the aquifer. This is particularly true for producers with wells spread over distances greater than the width of a single model cell. To help reduce this uncertainty, monthly reported pumping was split for several of the larger non-exempt permits. Pumping from Wimberley Water Supply Corporation, which has six wells, was split evenly between two point locations, one on each side of the Wimberley Fault, and approximately in the center of the wells located on each side of the fault. Permitted pumping from the Woodcreek Phase II permit was split evenly between the two wells operated by the permit holders.

Non-exempt wells and reported pumping were imported into the TAS model using the analytic element menu in Groundwater Vistas 8. The amount of pumping for each stress period was assigned to either model Layer 1 (Lower Glen Rose), or Layer 3 (Cow Creek), depending on known well completion information. Non-exempt wells screened across all three model layers had all pumping assigned to Layer 3. Future model refinement efforts may include refining non-exempt well pumping to spread it across all three model layers for non-exempt wells known to be screened across both the Lower Glen Rose and Cow Creek.

Exempt

Exempt pumping is represented by hand-drawn analytic element polygons in Groundwater Vistas. These polygons distribute pumping evenly over the area of the cells enclosed by a given polygon boundary. For the BSEACD polygon, GCD boundaries between HTGCD and CTGCD and the distribution of known exempt wells were used to draw a polygon which covers the area where most of the exempt pumping is known to occur. The north boundary of the polygon terminates approximately coincident with Onion Creek and the east boundary terminates along a line that roughly parallels IH-35 and passes just west of Kyle and San Marcos. This generally coincides with the southwestern portion of the district along the western boundary with HTGCD where modeled aquifer units are less deeply buried, and drilling of exempt wells is more economically feasible.

BSEACD and HTGCD analytic element polygons are transient and were assigned monthly pumping values following monthly water use from HTGCD and BSEACD non-exempt pumping data. All of the other GCD exempt pumping polygons are steady state, with a constant rate of negative flux-per-unit area for all stress periods. The percentage of annual exempt pumping assigned to each month is presented in Table 12. A summary of exempt polygon characteristics is presented in Table 13.

All exempt pumping is simulated to be in the Cow Creek (Layer 3) of the model domain. In reality, many exempt wells in the study area are screened across the Cow Creek and Lower Glen Rose formations. It is unknown proportionally how much water is derived from the Cow Creek and Lower Glen Rose in wells screened across both intervals. However, available multiport data generally show that the Cow Creek has significantly higher hydraulic conductivity than the Lower Glen Rose, and thus is likely to be contributing a larger proportion of overall water being produced by a well screened across both intervals (Hunt et al.,

2016b). Refinement of exempt pumping and allocation of some portion of that pumping to the Lower Glen Rose is a goal of future planned TAS modeling efforts.

Table 12-Monthly distribution of assigned exempt pumping for TAS model calibration period.

Month	*Percentage annual exempt pumping assigned*
January	6.4
February	6.0
March	6.2
April	7.3
May	7.9
June	10.2
July	11.6
August	12.1
September	8.7
October	9.3
November	7.4
December	6.4

Table 13. Summary of exempt pumping polygons.

District	*Annual exempt pumping (cfd)*	*Polygon area (ft^2)*	*Layer*	*Comment*
HTGCD	452,000	$1.03x10^{10}$	Layer 3	From 2020 HTGCD Annual report (HTGCD 2020)
BSEACD	44,100	$1.32x10^{9}$	Layer 3	From 2020 BSEACD Annual report (BSEACD 2020)
BPGCD	51,275	$7.57x10^{9}$	Layer 3	
Comal	231,390	$4.2x10^{9}$	Layer 3	Use HTGCD volume/area.
SWTCGCD 1	ND	$8.8x10^{8}$	Layer 3	Use HTGCD volume/area.
SWTCGCD 2	ND	$5.8x10^{9}$	Layer 3	Use HTGCD volume/area

Model Calibration

The TAS model was calibrated using a combination of inverse modeling with the PEST code, and manual adjustment of parameters between PEST iterations. PEST is an automated process that minimizes the "objective function", calculated as follows:

$$\varphi = \sum (w_i r_i)^2$$

Where φ is the objective function, r_i is the residual of a given head or flux target for a given stress period, and w_i is the assigned weight of the target. For the TAS model, the objective function was a combination of head targets (observed monitoring well data), and springflow flux targets from PVS and JWS. Prior to each PEST run, a global weighting factor was applied to the flux targets to ensure that they represented an approximately equal portion of the objective function as head targets. Flux targets are generally much higher in magnitude than head targets, and thus flux residuals tend to be much larger in magnitude and have the potential to overwhelm the representation of head targets in the combined objective function.

Target weighting (w_i in the above equation) was assigned to individual head targets based on their location (whether they were inside or nearby to the main area of investigation). Targets far outside the main area of investigation received lower weighting. Minimum and maximum weighting factors were 0.5 and 1.5, respectively.

Boundary condition parameters adjusted in PEST are shown in Table 14. Manual adjustment of calibration parameters was also made on specific storage/specific yield, drain conductance, GHB conductance, HFB conductance, and Kh. Pilot point interpolation was used in PEST to calibrate Kh (108 pilot points) and Kv (87 pilot points) for all model cells. Pilot point locations are displayed in Figure 21-Figure 24, and a summary of pilot point groups and K ranges is presented in Table 15.

Table 14. Summary of parameters adjusted using PEST code.

PEST Parameter	**Comment**
Specific storage	Zones 1,2,5,7
Specific yield	Zones 1,2,5,7
Drain conductance	For JWS and PVS drain cells
GHB conductance	All reaches
River conductance	All reaches
HFB conductance	All reaches
Kh	Pilot points
Kv	Pilot points

Transient head target statistics for the calibrated model are provided in Table 16. Absolute residual mean and root mean squared error were 34 feet and 47 feet, respectively. These statistics scaled by the total range in head target observations (936 feet) are 4% and 5%, respectively, showing a reasonable agreement with observed versus simulated heads over the 13-year calibration period.

Table 15. Summary of pilot point Kh/Kv minima and maxima used for PEST calibration.

Group (zone)	Layer	Zone description	Number of pilot points		Min/Max (Kv is reported as Kh/Kv anisotropy factor)			
			Kh	Kv	Khmin	Khmax	Kvmin	Kvmax
1	3	High K Spring Run	5	2	1,000*	200,000*	20	10
2	3	High K Watershed	9	3	5	1,000*	20	10
3	3	Western Regional Inflow	4	2	5	20	10	2
4	3	DS Recharge zone	4	4	5	15	10	2
5	3	Rollingwood conf zone	9	4	1	25*	10	2
6	3	SWT Zone	4	3	0.1	2.5	1,000	10
7	3	Downgrad confined	6	5	0.1	5	1,000	10
8	3	Northern Hays Lyr 3	8	6	0.1	8	10,000	10
9	2	Springshed	4	4	2.5	10	10	1
10	2	Hensel confining zone	1	3	0.001	0.1	100	1
11	2	Northern Hays Lyr 2	6	4	0.5	2.5	100	10
12	2	Western Regional Inflo	3	2	5	20	100	10
13	2	Rollingwood conf zone	6	4	0.5	2.5	10	2
14	2	SWT Zone	2	2	0.001	1	1,000	10
15	2	Downgrad confined	4	4	0.001	0.1	1,000	10
16	2	DS Recharge zone	0	3			100	10
17	1	Relayramp upgrad	3	3	2.5	100	1,000	10
18	1	Relayramp downgrad	3	3	2.5	20*	10	1
19	1	Western Regional Inflo	2	2	5	20	10,000	1000
20	1	Downgrad confined	9	9	0.25	5	1,000	10
21	1	High K Watershed	4	5	5	100	1,000	10
22	1	Northern Hays	6	3	0.5	5	1,000	10
23	1	DS Recharge zone	3	3	1	10	100	10
24	1	Rollingwood conf zone	3	4	0.25	25*	10	2

*varies within group, specifies total group minimum/maximum

Table 16. Transient head calibration statistics over calibration period (January 2008-December 2020).

Residual mean	-1.24 feet
Absolute residual mean	34.4 feet
Root mean squared error	46.6 feet
Range of observations	936 feet
Scaled absolute mean	3.7%
Scaled root mean squared error	5.0%

Head targets

A total of 4128 transient head targets from 87 individual wells were compiled from a combination of monitoring well data from TWDB, BSEACD, HTGCD, and BPGCD, and a 2018 synoptic potentiometric map by Hunt et al., (2019a). A map of the Hunt et al., (2019a) observed and simulated contours for the April 2018 stress period is presented in Figure 31. Observed versus simulated hydrographs for selected head targets are presented in Figure 32 through Figure 36.

All head targets represent manual, transducer, or telemetry well water-level measurements referenced to elevation in feet above sea level. Telemetry well data were pulled from the TWDB Automated Groundwater Level Wells Database (TWDB 2023). Raw transducer and telemetry well target data were in 15-, 30-, or 60-minute measurement intervals. These data were processed to match the TAS stress period resolution by calculating mean water level for each monthly stress period where target well data were available over the calibration period.

Each head target has uncertainty associated with measurement error, elevation estimation error, and error associated with averaging water levels over monthly stress periods. Also, interpolation errors may occur within the model space when the head target is not located on a node in a model cell (Anderson et al., 2005). For most targets in the primary area of investigation, elevations were interpolated from the Texas Strategic Mapping (StratMap) Central Texas Lidar Dataset Digital Elevation Model (DEM) rasters (Stratmap 2023), which reports a vertical accuracy of <1 foot for the study area. However, additional errors may occur in interpolating elevation from these DEMs due to uncertainty of target well head GPS coordinates. Measurement errors for e-line and transducer measurements are usually <0.1 foot.

Simulated heads generally performed well matching regional Middle Trinity potentiometric contours, with an overall west-east gradient transitioning to a more south-north gradient in southwest Travis County (Figure 31). Simulated potentiometric gradients steepened from west to east across the BFZ but showed significantly steeper gradients in the Wimberley area than the Hunt et al., (2019a) potentiometric synoptic map. This is likely due to the conceptualization of fault barriers as a linear 2-dimensional HFB boundary, when in reality these fault barriers are 3-dimensional fault zones with complex structure and geometry. However, the HFB conceptualization performs adequately for overall head matching across the BFZ and the more deeply confined Middle Trinity heads within the model domain on a more regional scale. Refinement of the fault barrier conceptualization is a goal for future modeling efforts.

Quality of simulated head matching of target hydrographs varied between different portions of the model domain in the primary area of interest. In the vicinity of JWS and PVS, simulated heads generally matched well with observed heads for low-flow stress periods but were not able to replicate peaks associated with recharge events (Figure 32). This is likely due to high Kh values used to approximate conduit flow in the vicinity of the JWS and PVS spring drain cells which attenuates variations in head. Simulated head matching for BFZ targets was generally good, with an overall matching of head variations with observed data (Figure 33 and Figure 34). Further downgradient in the deeper confined Trinity within BSEACD boundaries simulated head matching generally followed overall variations in head over time but showed more attenuated variations and poorer matching of absolute head (Figure 35). Simulated heads at the Onion Creek Country Club well showed large drops in water levels due to pumping (>250 feet), which is consistent with known Middle Trinity Aquifer drawdown behavior in response to pumping at this location (Figure 35). Simulated heads in the Dripping Springs/Upper Onion Creek area within HTGCD showed poorer matching than other portions of the model domain, with the Henly and Whit Hanks well targets

showing a nearly flat-line simulated head with minimal variability that does not match observed head data (Figure 36). This area is a good target for future model refinement efforts, as it contains large public water-supply system wells and recent monitoring well data has shown large drops in water levels.

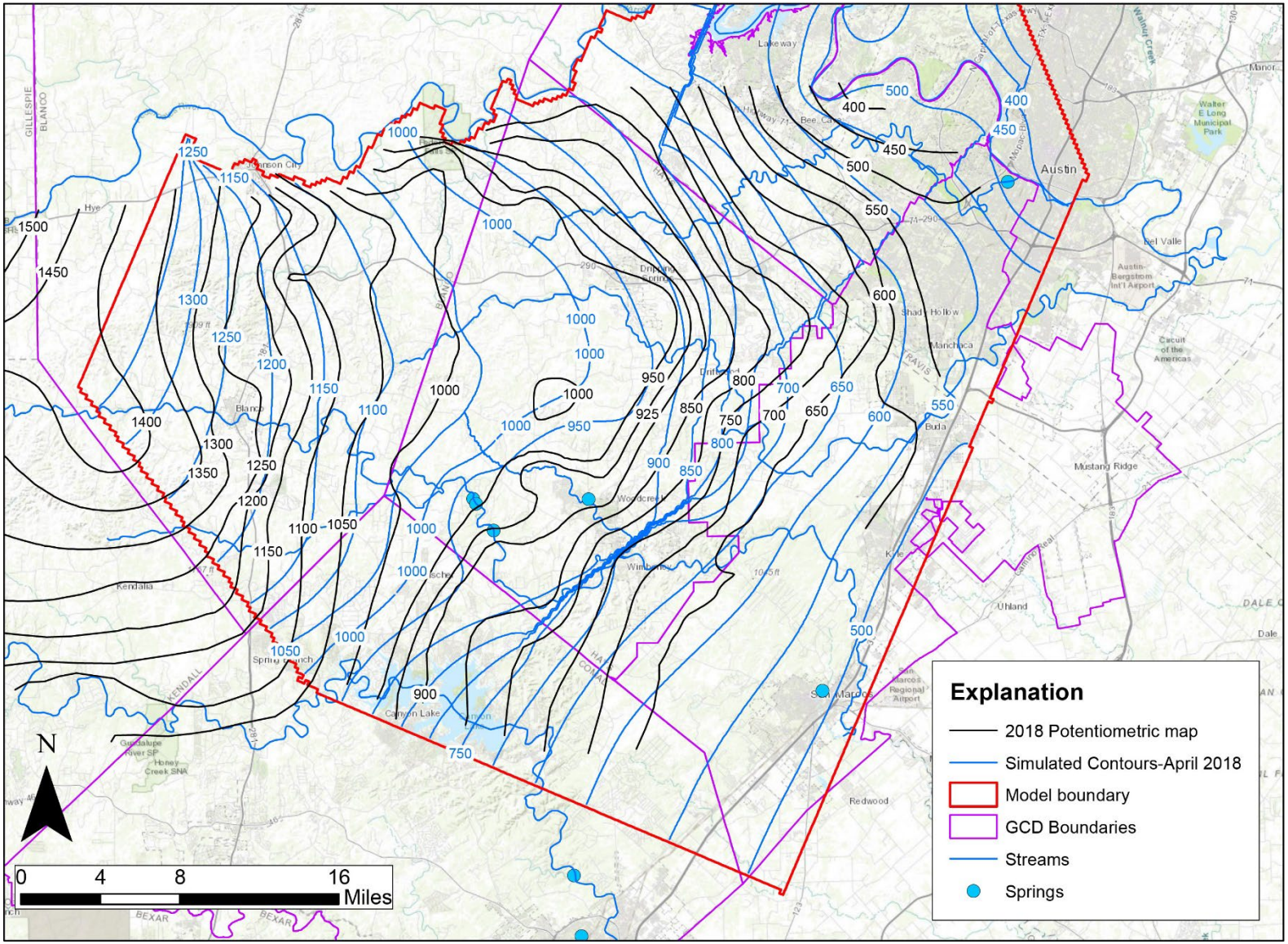

Figure 31. Potentiometric contours from 2018 potentiometric study (Hunt et al., 2019a), and calibrated, simulated heads for April 2018 (stress period 127).

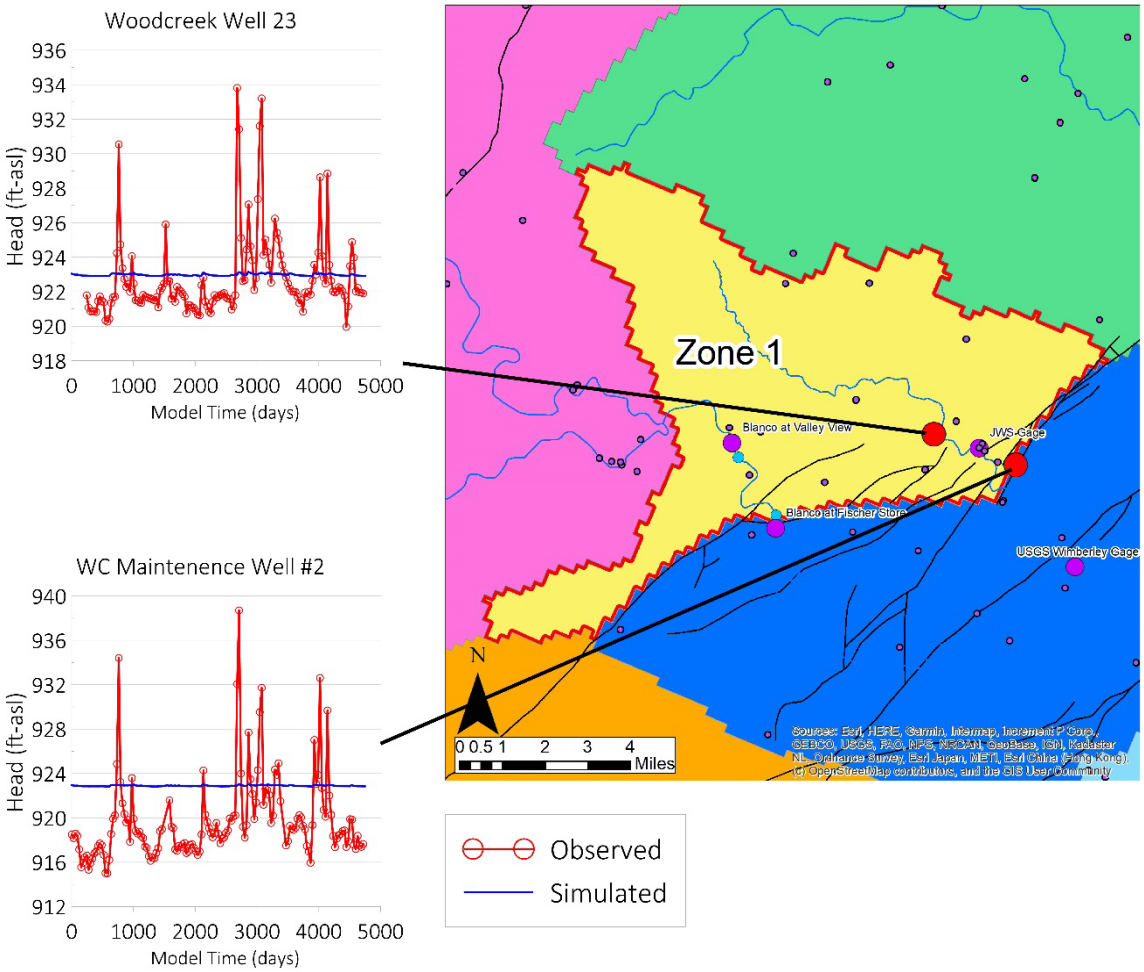

Figure 32. Selected head calibration targets in hydrostratigraphic Zone 1

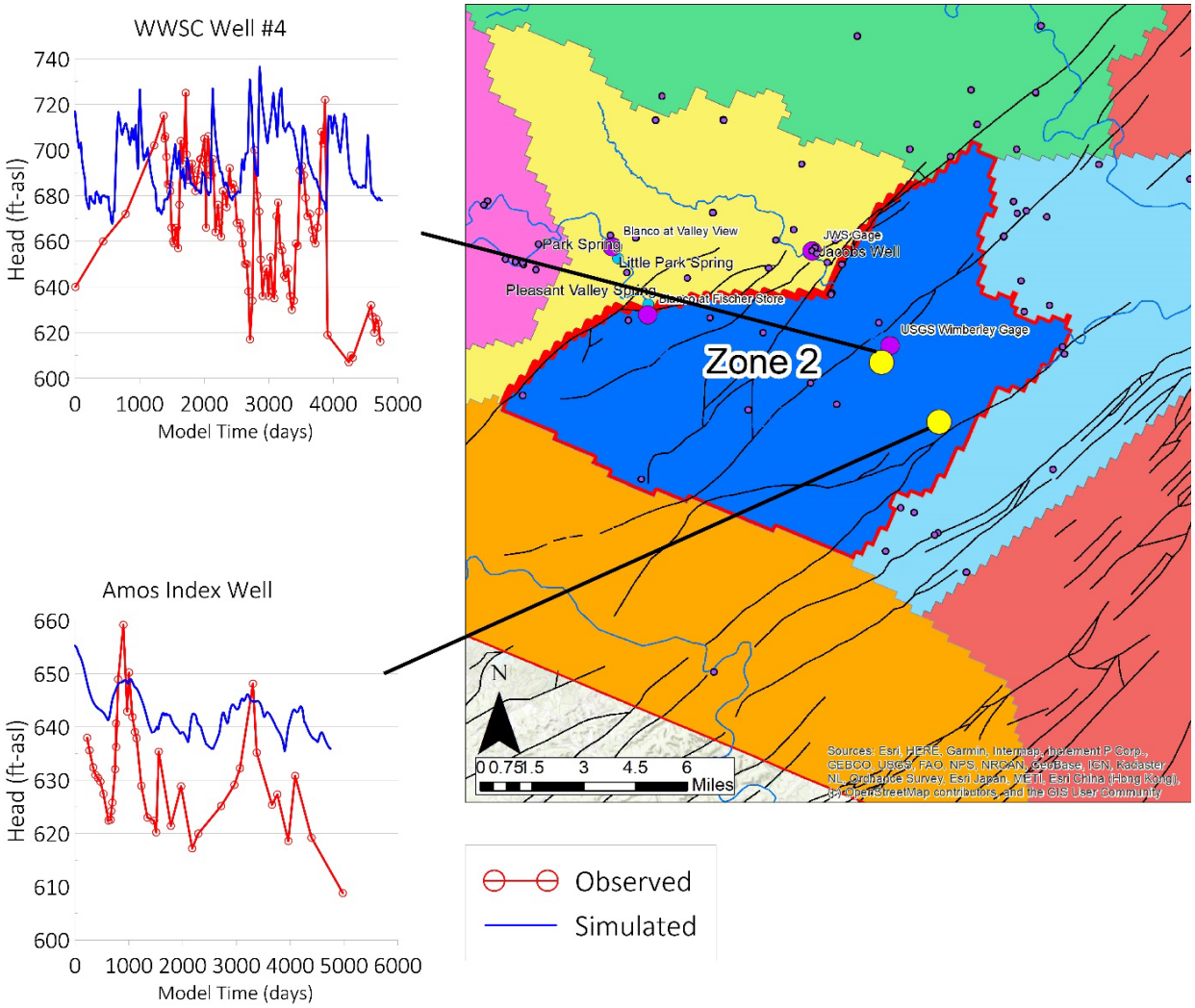

Figure 33. Selected head calibration targets in hydrostratigraphic Zone 2

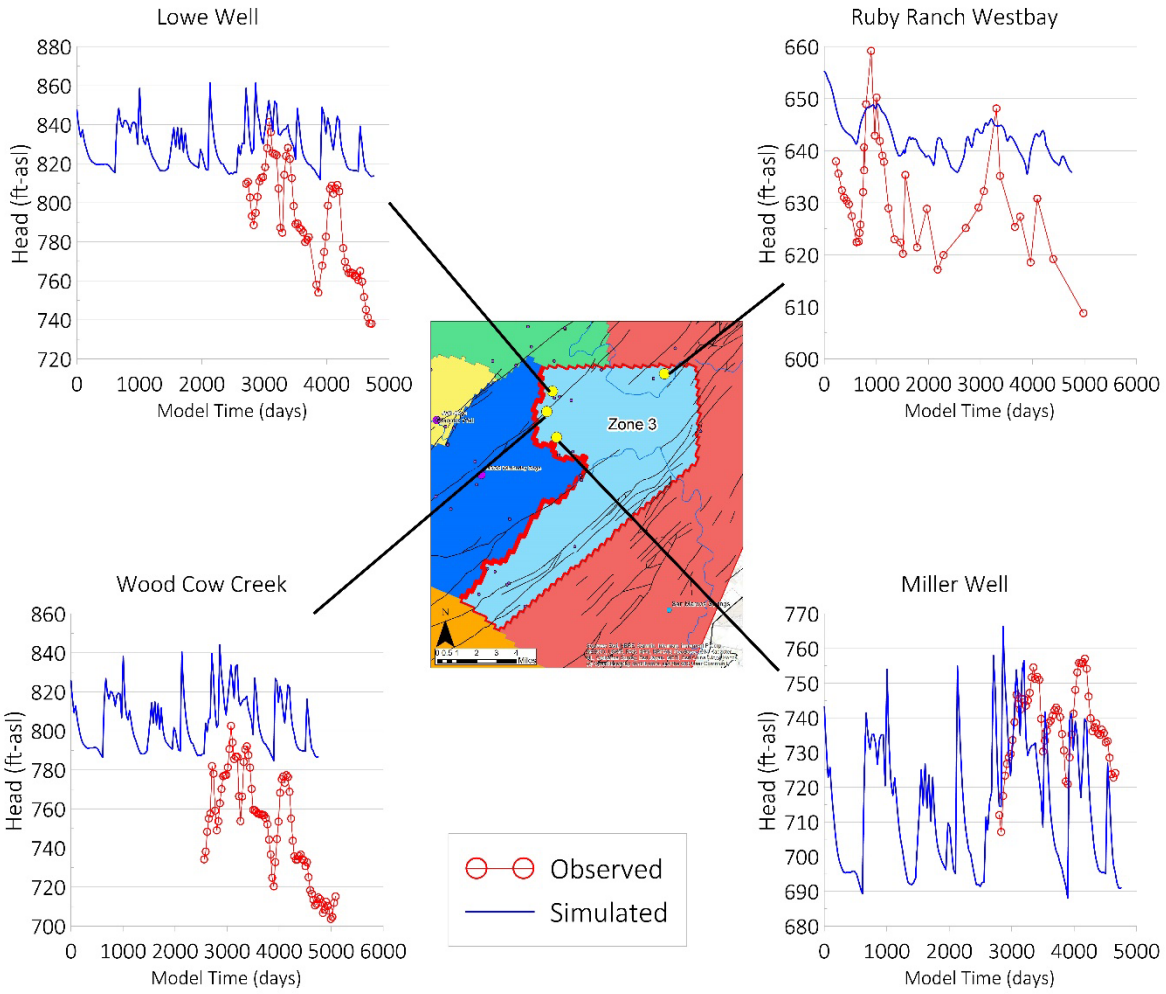

Figure 34. Head calibration targets in hydrostratigraphic Zone 3

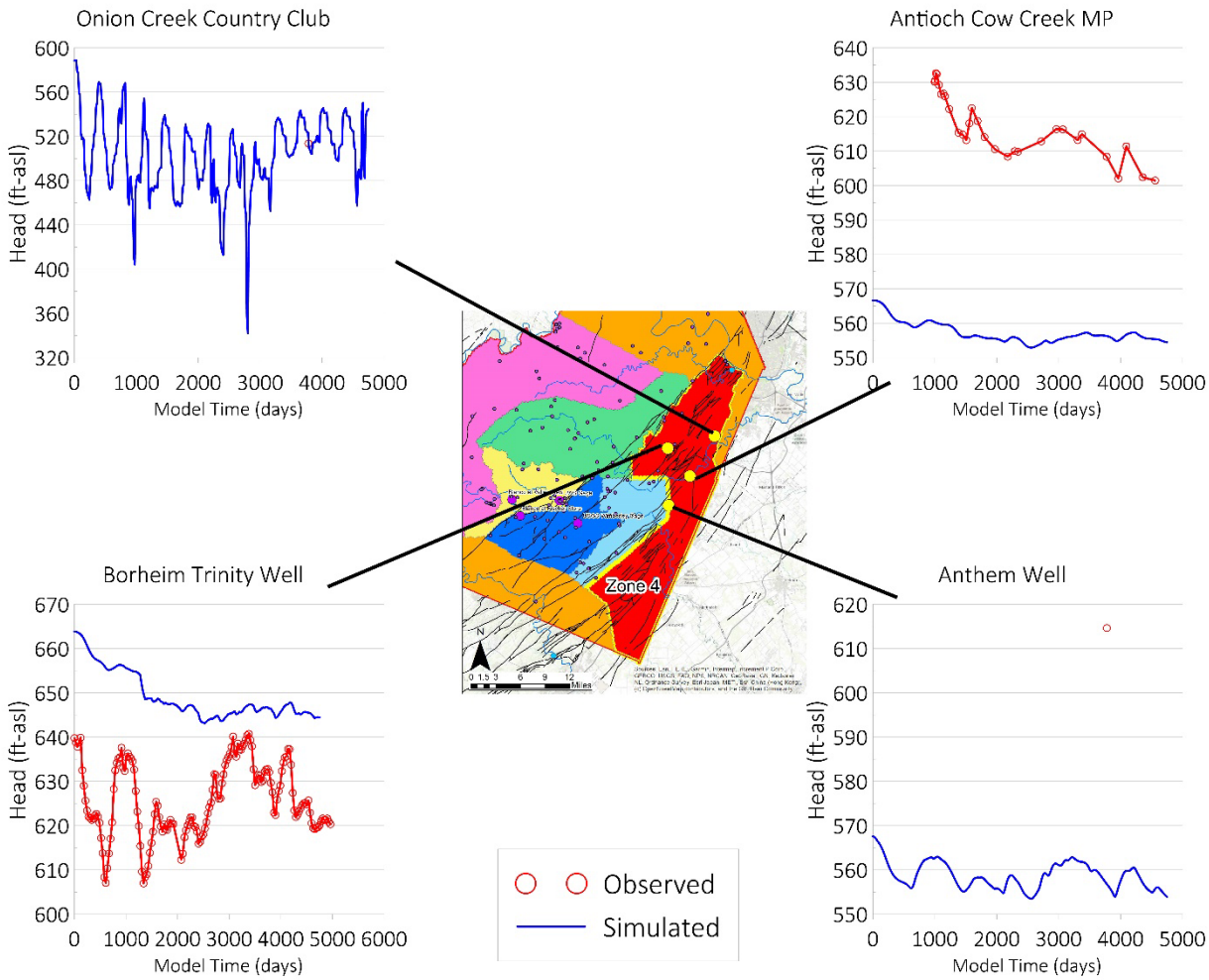

Figure 35. Head calibration targets in hydrostratigraphic Zone 4

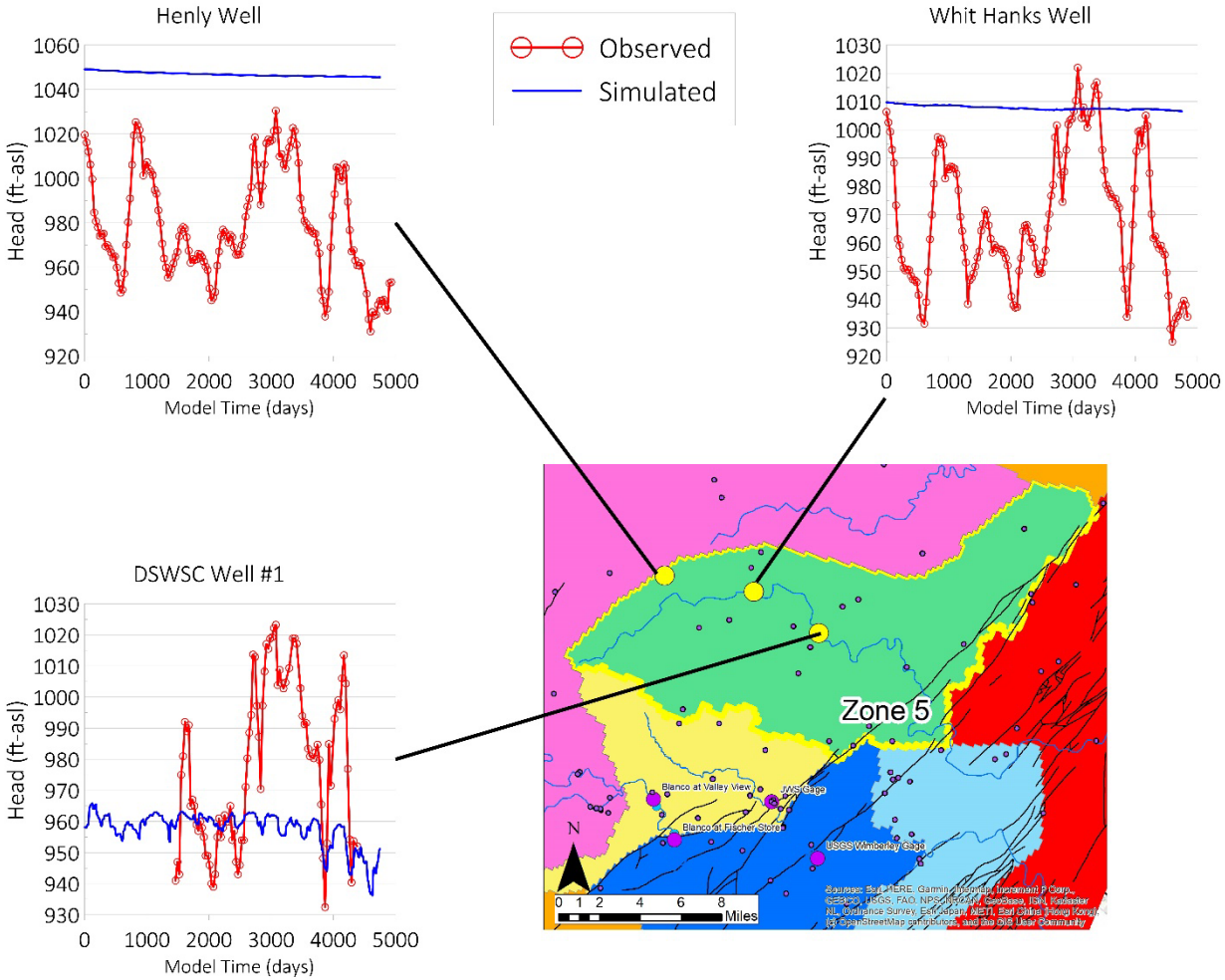

Figure 36. Head calibration targets in hydrostratigraphic Zone 5

Drain Flux Targets (Springflow)

Springflow from JWS and PVS was manually calibrated to simulated drain flux using observed springflow measurements as calibration targets. JWS targets were generated from daily springflow values as reported by the JWS USGS flow gage (ID: 08170990). Daily flow values were averaged to create a monthly average springflow value corresponding to each monthly stress period in the 13-year calibration period. PVS calibration targets were generated using a combination of all available manual measurements (2012-2020) and inferred low-flow values from the USGS Blanco River at Wimberley gage (ID: 08171000). For these inferred values, it was assumed that Blanco River flow at the Wimberley gage is equal to PVS flow when monthly average flow reported by the gage was below 15 cfs.

During manual calibration of spring drains, low-flow stress periods were generally given more weight for calibration efforts than high-flow stress periods. This is because a primary modeling goal was to emphasize better model performance during drought periods, which are of key interest for groundwater management planning purposes. Manual calibration of spring flux targets was performed concurrently with head calibration, and often improvement of springflow target matching was achieved at the cost of poorer matching of head targets elsewhere in the model domain. Possible approaches for reconciling springflow and head target calibration for future modeling efforts include:

- Increasing model grid resolution in key areas of the domain in the vicinity of major spring outlets
- Implementing the MODFLOW Connected Linear Network module to more accurately simulate conduit flow processes and head gradients in the highly karstified portion of the model domain in the vicinity of the springs.

Simulated JWS flow generally agreed with observed flows over the 13-year calibration period. Especially during low-flow (drought) periods (Figure 37). There was less agreement during higher-flow periods when average monthly flow was >10 cfs. Simulated PVS flow showed less variability than observed flow variability and stayed within a narrow range between 15 to 20 cfs (Figure 37). This caused an overestimation of flow during low-flow periods, underestimation of flow during high-flow periods, and general agreement during average/slightly lower than average periods.

While Park Spring upstream of PVS is included as a drain cell in the model domain, the model did not simulate any flux from this drain cell because simulated heads at this location are below the drain elevation for all stress periods. Future versions of the model may include refinement of this portion of the model domain to more accurately simulate flow from the Park Spring complex. However, average volume of flow from the Park Spring complex is relatively small compared to PVS, and not likely to significantly affect overall modeled springflow volumes.

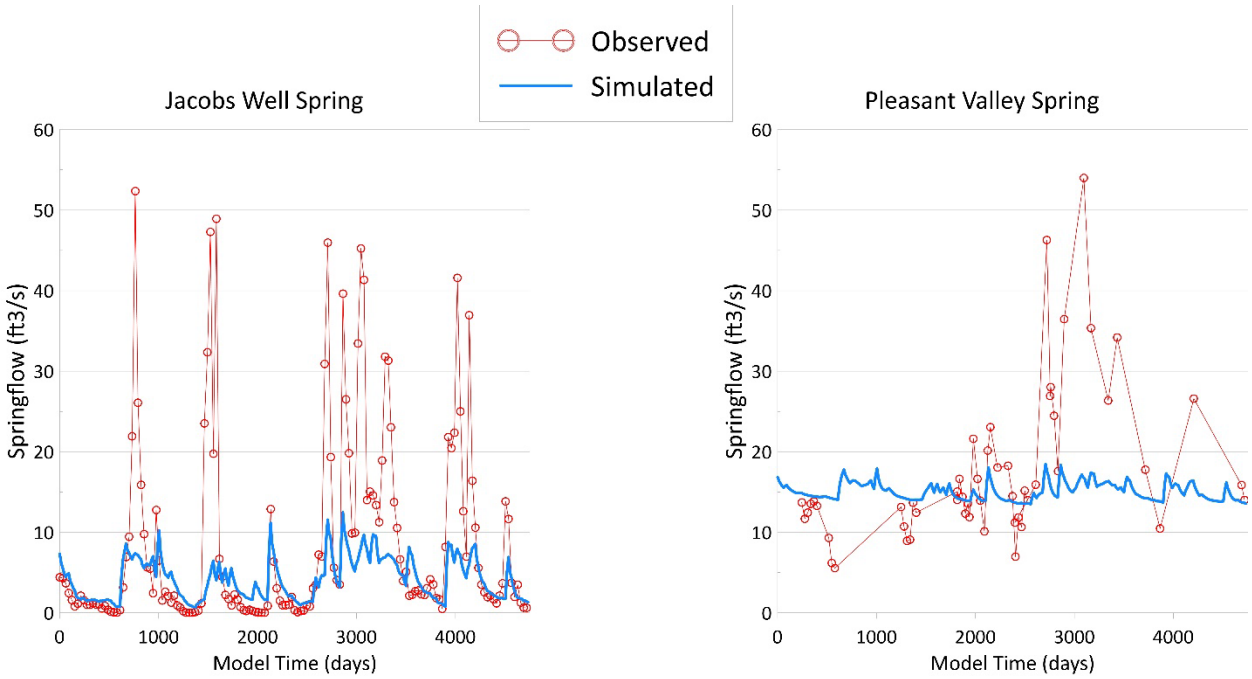

Figure 37. Observed versus simulated spring flow at JWS (left) and PVS (right). JWS observed values are averaged monthly flow from the JWS USGS flow gage (ID: 08170990). PVS observed values are a combination of manual measurements and flow estimates inferred from USGS at Blanco River at the Wimberley gage during low flow periods.

Calibrated Model Water Budget

A summary of the water budget over the 13-year calibration period is presented in Table 17. Summary graphs of water budgets for each stress period of the calibration period within four zones of interest in Layer 3 are presented in Figure 38.

The largest positive flux into the calibrated model simulation was recharge (22,142 acre-ft/yr average). Averaged across the entire recharge domain (Figure 30) this amounts to an average of about 1.1 inches of rainfall per year, or about 4% of average annual precipitation for the study area. This value is below net recharge estimates by Martin et al., (2019), which estimate 6 to 15% net recharge based on an assumed actual evaporation rate of 66-75%. However, this lower net recharge rate is reasonable given that much of the ground surface in the model recharge domain is covered by Upper Glen Rose or Edwards on the surface, and thus not all the recharge entering the subsurface is directly recharging the hydrostratigraphic units of the Middle Trinity Aquifer, which are the units in the TAS model domain.

Storage represents the next largest positive flux and represents about half of the inflow from recharge (10,145 acre-ft/yr average). In MODFLOW USG, a positive storage flux represents a decrease in overall aquifer storage (i.e., water "leaves" aquifer storage and enters the model simulation). Most of this storage decrease came from Layer 1 in the model domain (Table 17). While some observation well data does show an overall downward trend in water levels, a clear downward trend indicating widespread aquifer storage depletion has not been definitively established across the model domain. Thus, this simulated decrease in storage over time should not be assumed to be representative of real-world aquifer conditions.

River leakage represents the last boundary condition with a net inflow into the model domain over the 13-year calibration period and is about an order of magnitude less than the storage inflow (1,363 acre-ft/yr). Given that all river boundary condition cells are on the margins of the model domain and relatively close to GHB outflow boundary cells, it is unlikely that this relatively small water budget component significantly affected the main area of interest within the model domain.

Drains (springflow) represent the largest negative flux over the calibration period with an average of 21,218 acre-ft/yr out of the model domain (29.3 cfs). Total median springflow from both JWS and PVS is 23.4 cfs (Table 5). Given that this observed springflow median does not include flows from Park Spring or springs discharging along the banks of the Pedernales River, the average total drain flux is a reasonable approximation of observed values.

Wells represent the second largest negative flux over the calibration period with an average of 11,726 acre-ft/yr. This simulated pumping is in line with reported non-exempt and estimated exempt pumping values reported in Table 6 (9,995 acre-ft/yr total estimated 2018 pumping).

GHBs represent the smallest negative flux with a simulated average of 705 acre-ft/yr over the calibration period. These GHBs conceptually represents regional lateral inflows/outflows into/out of the model domain. Real-world estimates for the magnitude of these lateral flows are poorly constrained, and thus we do not have good estimates for comparison to simulated values. However, given that regional water inflows/outflows are thought to represent a smaller component of the overall water budget for the study area, the relatively small overall GHB flux simulated by the model seems to be a reasonable approximation of the conceptual model.

Table 17. Summary of water budget inflows/outflows over 13-year calibration period

Entire Model Domain			
Boundary Condition	Total Volumetric Flux (ft3)	Annual Average Flux (acre-ft/yr)	Notes
Storage inflow/outflow	5.74E+09	10,145	
Wells	-6.67E+09	-11,726	
Drains (springs)	-1.21E+10	-21,218	Equals 29.3 cfs average springflow
River Leakage	7.75E+08	1,363	
General Head Boundaries	-4.01E+08	-705	
Recharge	1.26E+10	22,142	1.08 inches/year averaged over recharge domain area
Layer 1			
Type	Total Volumetric Flux (ft3)	Annual Average (acre-ft/yr)	Notes
Storage inflow/outflow	5.54e+09	9,776	
Wells	-3.67E+06	-6	
Drains (springs)	0	0	
River Leakage	-5.72E+08	-1011	
General Head Boundaries	-8.27E+08	-1,461	
Recharge	1.26E-10	22,297	All recharge enters through layer 1
Layer 2			
Type	Total Volumetric Flux (ft3)	Annual Average (acre-ft/yr)	Notes
Storage inflow/outflow	2.88E+07	55	
Wells			
Drains (springs)			
River Leakage	6.74E+08	1,290	
General Head Boundaries	2.13E+08	407	
Recharge			
Layer 3			
Type	Total Volumetric Flux (ft3)	Annual Average (acre-ft/yr)	Notes
Storage inflow/outflow	1.73E+08	330.13	
Wells	0.00E+00	0.00	
Drains (springs)	-6.67E+09	-12757.23	
River Leakage	-1.21E+10	-23083.73	
General Head Boundaries	6.73E+08	1288.07	
Recharge	2.13E+08	407.44	

Zone 1 encompasses gaining portions of the Blanco River basin, including portions of the model domain immediately upgradient of PVS and JWS (Figure 38). Inflows were dominated by vertical leakage from Layer 2, which showed distinctive peaks and valleys across the 13-year calibration period following high and low recharge stress periods. Outflows were dominated by simulated springflow from the JWS and PVS drain cells. Simulated springflow mirrored the peaks and valleys of Zone 1 inflow, displaying relatively

rapid responses to recharge events. The overall magnitude of Zone 1 fluxes were almost an order of magnitude higher than other zone fluxes, despite zone being smaller than the other zones evaluated.

Zones 2, 3, and 4 represent an approximate west-to-east cross-section of Layer 3 with the shallower Cow Creek to the west, traversing the BFZ, and the deeper, more confined, Cow Creek to the east. Zone 4 is coincident with BSEACD jurisdictional boundaries where present in the model domain. Pumping represents the largest outflow in Zone 2 and approximately half of the outflow, depending on the stress period, in Zone 3. Lateral outflow represents the other half of negative flux from Zone 3, with most of that outflow being transmitted downgradient to Zone 4. This lateral outflow is in agreement with the conceptual model, which states that a significant portion of the deeper confined Middle Trinity water budget comes from shallower upgradient regional inflow.

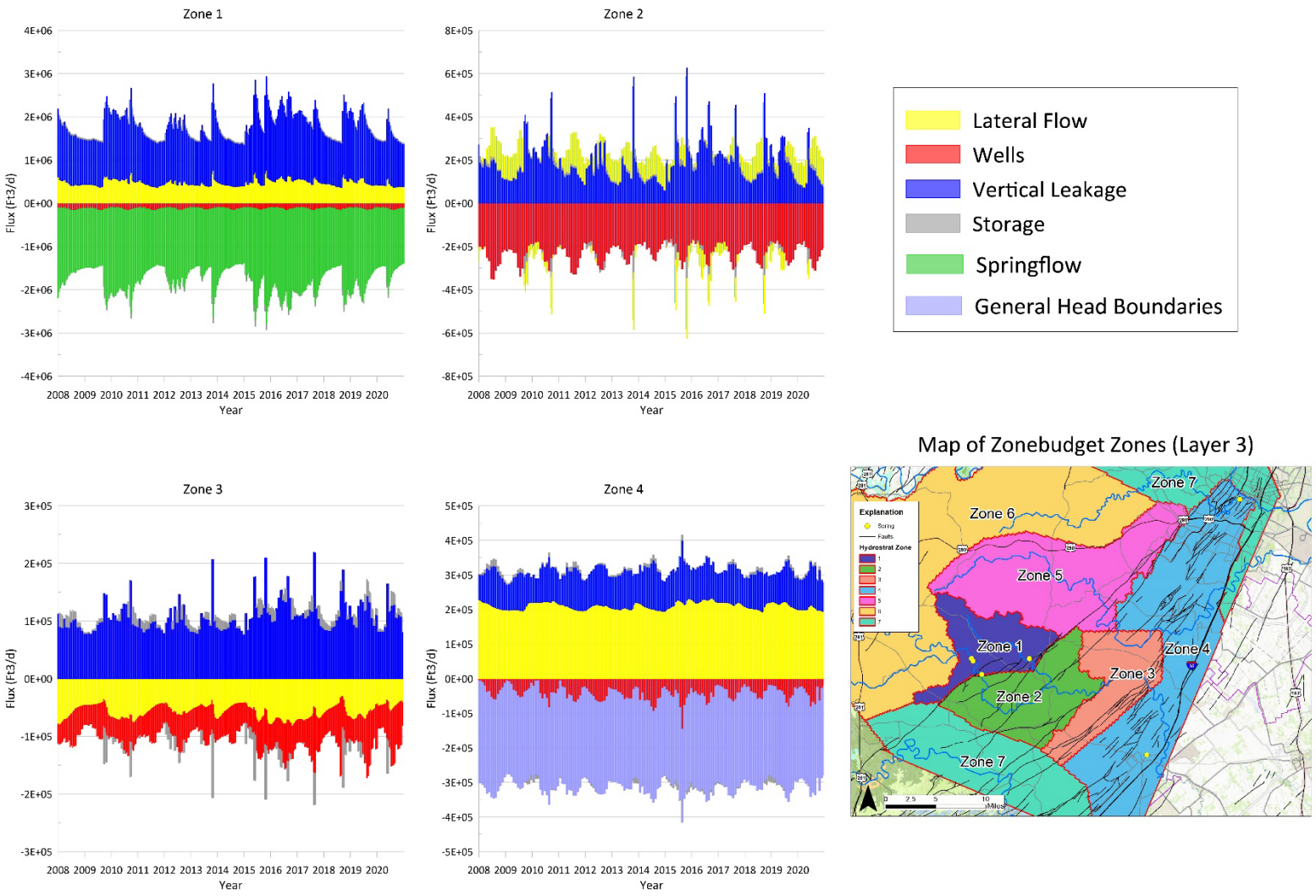

Figure 38. Transient water budget fluxes for each model stress period over the 13-year calibration period for four key zones of interest in Layer 3 of the TAS. Note that each zone figure has a different vertical axis scale.

Parameter Sensitivity Analysis

Sensitivity analyses were performed on various model parameters using the autosensitivity function in Groundwater Vistas 8 to evaluate how varying sensitivity parameters changed target head residuals. For parameters without discreet reaches or zones, such as Kh and Kz, parameters were varied within delineated hydrostratigraphic zones: seven zones in Layer 3, and one zone each representing Layer 2 and Layer 1. A summary of the sensitivity analysis is presented in Table 18. A map of the Layer 3 hydrostratigraphic zones is presented in Figure 39. Horizontal hydraulic conductivity (Kh), general head boundary (GHB) head, and recharge were the most sensitive of the parameters evaluated. Layer 1 Kh had the most influence on residual head of the zones tested, with Layer 1 exhibiting the largest absolute residual mean range (Table 18 and Figure 39). Head elevations for GHB Reach 0 (NW upgradient) and GHB Reach 2 (SE downgradient) exhibited the most sensitivity, with Reach 1 (northeast downgradient) exhibiting the least sensitivity of the three GHBs in the TAS.

Not all parameters tested exhibited the best statistics for parameter values associated with the calibrated model; in particular, Kh in Layer 1 and recharge. However, it should be noted that these quantitative sensitivity analyses only considered simulated head residuals, and do not account for manual calibration of the JWS and PVS spring flow flux targets. During the calibration process, improvement of spring flow target matching sometimes came at the cost of head target matching, and vise-versa. Thus, we do not expect minimization of head target residuals for each of the parameters tested.

Table 18. Summary of sensitivity analysis results by parameter. A map of Layer 3 hydrostratigraphic zones used for the sensitivity analysis can be found in Figure 39.

Parameter	Multiplier [number of runs]	Abs Residual Mean range [% variability from base]	Notes
Kh	0.5-1.5 [5]	34.7-43.8 [25%]	Varied by hydrostratigraphic zone
Kz	0.8-1.2 [5]	35.15-35.28 [0.4%]	Varied by hydrostratigraphic zone
Ss	0.5-1.5 [5]	35.22-35.24 [.05%]	Varied by storage zone
Sy	0.5-1.5 [5]	35.16-35.27 [0.3%]	Varied by storage zone
GHB Conductance	0.8-1.2 [5]	35.23-35.23 [0%]	Parameter varied by layer
GHB Head	0.8-1.2 [5]	35.14-42.60 [21%]	Parameter varied by layer
Drain Conductance	0.5-1.5 [5]	35.21-35.26 [0.1%]	Parameter varied by drain reach
Drain head	-2 to +2 feet [5]	35.03-35.57 [1.5%]	Only reach 1 (JWS) and reach 2 (PVS) varied
HFB Conductance	0.5-1.5 [5]	34.97-35.76 [2.3%]	Varied by HFB reach
Recharge	0.8-1.2 [5]	35.06-38.54 [9.9%]	

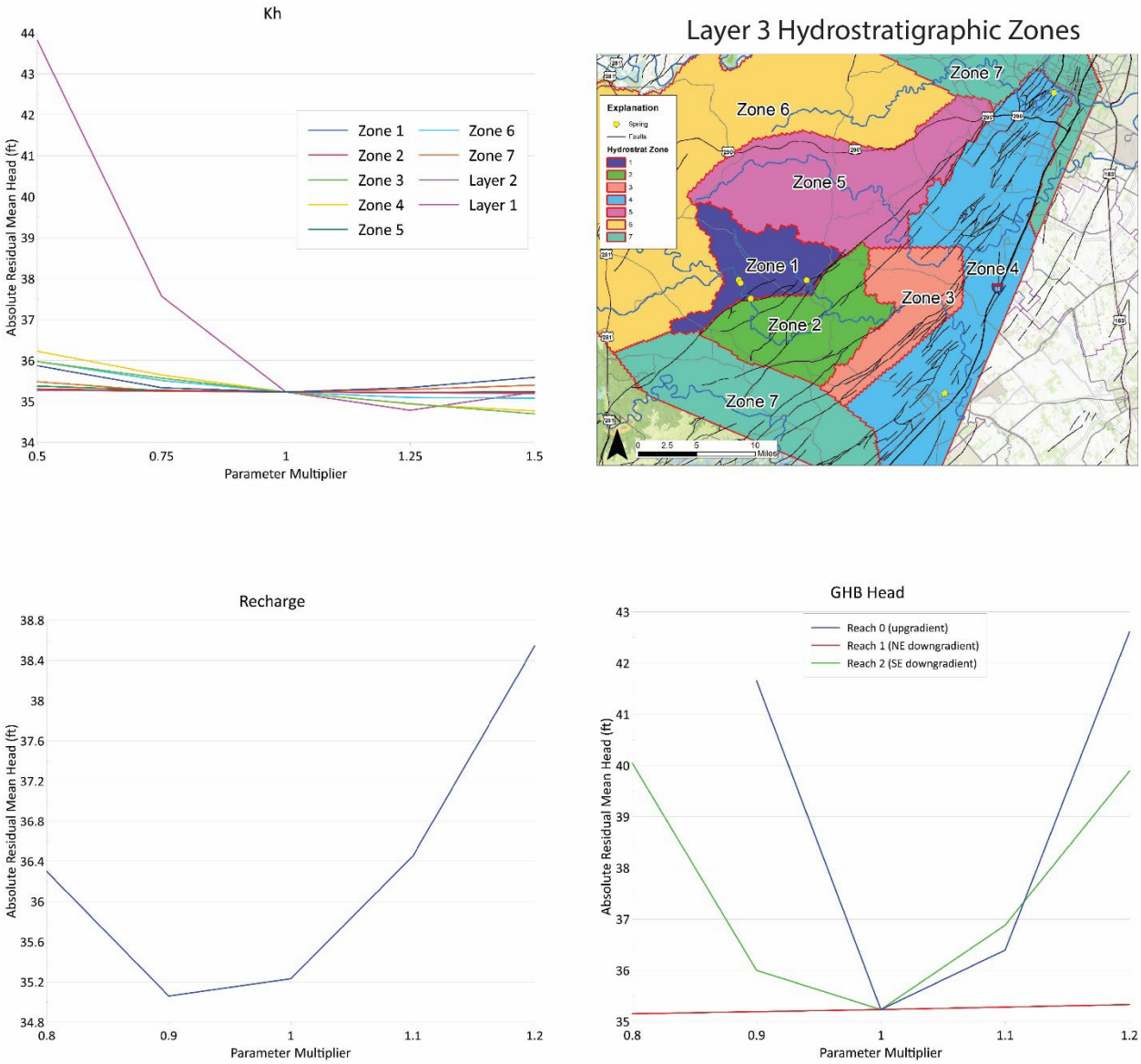

Figure 39. Summary of the three most sensitive parameters identified from sensitivity analysis. Map of hydrostratigraphic zones used for Kh analysis is presented top-right.

Predictive Model Construction and Results

This section outlines a series of predictive model scenarios which were developed from the calibrated model to test simulated Middle Trinity Aquifer behavior in response to varying model stressors (pumping and recharge). An experimental approach to scenario testing was implemented in which two "baseline" models were constructed: BL1) a 50-year model run with recharge and pumping conditions derived from the 2008-2020 calibration period, and BL2) a 10-year model run designed to approximate pumping and recharge conditions from the 1950s drought of record. Experimental scenario models were then built from the baseline models by varying individual model inputs such as recharge or pumping. Results of experimental model runs were then compared to the baseline model runs by calculating the difference in modeled head and/or springflow between the experimental and baseline model. This approach eliminates a substantial amount of uncertainty from model forecasting, because it isolates and tests individual stressors, such as an increase in pumping, and any error associated with simulated absolute values in head or springflow for a single model run will be comparable for both scenarios being tested, and thus canceled out in the calculated difference between them. For the purposes of the following discussion, the difference in head between baseline and experimental model scenarios will be referred to as "drawdown". Positive drawdown is defined as a lowering of hydraulic head (e.g. a mean drawdown of 50 feet for a given scenario means that mean head for the experimental scenario was 50 feet lower than the baseline scenario).

Simulated drawdowns from the predictive model runs are summarized on Table 19. Simulated reductions in springflow between baseline and experimental scenarios are summarized and Table 20. Results for individual scenarios are discussed in more detail below.

Table 19. Summary of mean and maximum drawdown (baseline scenarios minus experimental scenarios) for BSEACD and HTGCD.

Baseline Scenario	Experimental scenario	GCD	Mean Drawdown (ft)	Max Drawdown (ft)
BL1	Scen A (BSEACD Well Field)	BSEACD	15.0	232.7
		HTGCD	5.4	167.9
BL1	Scen B (Regional Growth)	BSEACD	40.6	91.4
		HTGCD	14.64	92.0
Scen BL2 (no pumping)	Scen C1 (DOR-2020 pumping)	BSEACD	15.5	52.4
		HTGCD	4.7	45.1
Scen BL@ (no pumping)	Scen C2 (DOR regional growth)	BSEACD	51.8	111.5
		HTGCD	15.0	98.7

Table 20. Summary of simulated springflow (flux) reduction (baseline minus experimental scenarios) for JWS and PVS.

Baseline scenarios	Experimental scenario	JWS Avg cfs Flux Reduction	JWS Total Volume Flux reduction (%)	PVS Avg cfs Flux Reduction	PVS Total Volume Flux Reduction (%)
Scen BL1	Scen A (BSEACD Well Field)	1.5	39.5	0.0	0.3
Scen BL1	Scen B (Regional Growth)	1.6	43.3	0.6	4.3
Scen BL2 (no pumping)	Scen C1 (DOR-2020 pumping)	2.1	42.8	0.3	1.9
Scen BL2 (no pumping)	Scen C1 (DOR regional growth)	4.1	82.6	1.1	7.2

Scenario BL1: 50-year Baseline Simulation

Scenario BL1 is a 50-year baseline simulation. The general goal in development of Scenario BL1 was to approximate modern pumping and climatic conditions in a 50-year predictive model. In order to achieve this, recharge and pumping inputs from the calibrated model 2008-2020 calibration period were cycled repeatedly to fill the 50-year simulation period. Recharge stress periods from the calibrated model were repeated (13 years, 156 stress period cycle) until the end of the 50-year simulation period was reached. While not a perfect representation of the central Texas climatic cycle, the 13-year calibration period recharge dataset, which was derived from historic PRISM precipitation data, covers both a significant period of drought (2009-2015), and an extended period of above average rainfall (2015-2020). Thus, cycling of the 13-year calibration period over the 50-year baseline simulation results in cycling of the model through wet and dry climatic extremes as the model simulation progresses.

Non-exempt pumping from 2020, the most recent year in the calibration period, was repeated using 12-month stress periods 50 times to fill the 50-year baseline simulation period. Exempt pumping, as represented by constant flux analytic element polygons, was also repeated on a 12-month stress period cycle until the end of the 50-year simulation was reached.

Scenario A: 50-year Simulation with 2.5 MGD Well Field

Scenario A was built on top of the Scenario BL1 baseline scenario and was designed to forecast Middle Trinity Aquifer head and springflow responses to large-scale pumping in the BFZ Middle Trinity portion of the model domain. It is identical to Scenario BL1, except for the addition of a hypothetical large-capacity wellfield in the vicinity of the Rolling Oaks neighborhood, located in central Hays County on the east side of the HTGCD/BSEACD boundary. The well field consists of six wells with a cumulative constant pumping rate of 2.5 million-gallons-per-day (MGD) split evenly between the six wells.

Scenario A Results

Modeled drawdowns (Scenario BL1 baseline minus Scenario A) showed significantly lower water levels in response to hypothetical well field pumping (maximum drawdown=232.7 feet; Table 19). Predictably, the largest drawdowns were simulated closest to the wellfield and drawdowns decreased with distance from the well field (Figure 40). The simulated area of impact from wellfield pumping was widespread, with the 5-ft difference contour extending well into Travis County to the north and crossing the TCFZ barrier and extending west into HTGCD territory.

Scenario A simulated significantly less flux (springflow) from the JWS drain cell than baseline, with a total flux reduction of 39.5% and an mean flux reduction of 1.6 cfs over the duration of the 50 year simulation period (Figure 41, Table 20). The frequency and duration of low/no-flow events at JWS were higher in Scenario A relative to baseline. The difference between Scenario A and baseline modeled JWS springflow generally increased over the duration of the simulation period, reaching a maximum of 6.7 cfs in stress period 490 (year 40.9 of simulation) (Figure 41). In contrast to JWS, the PVS modeled springflow was relatively unchanged from baseline BL1 to Scenario A and showed <1% reduction in total flux over the simulation period (Table 20).

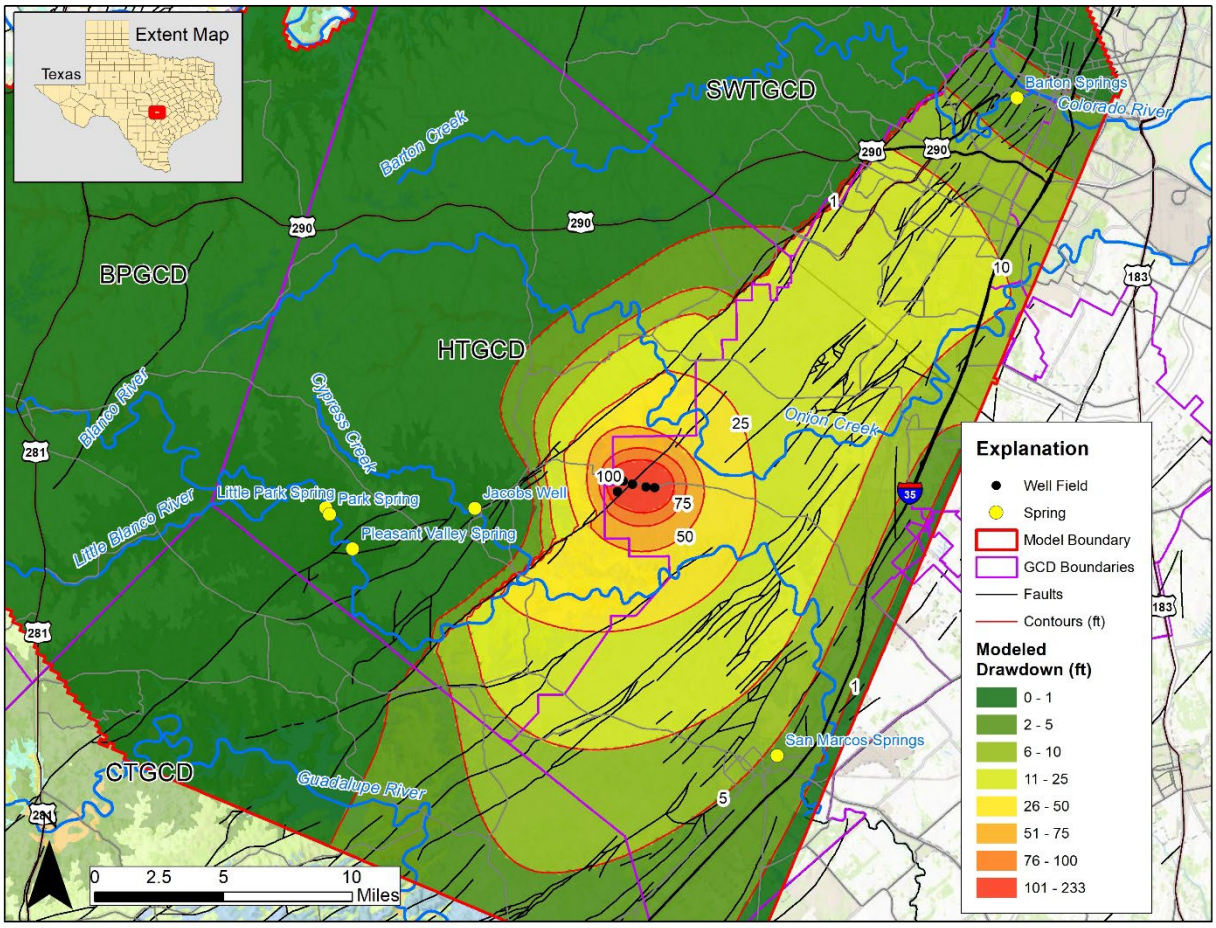

Figure 40. Modeled drawdown map (baseline BL1 minus scenario A) for 50-year simulation of a high capacity well field pumping 2.5 MGD. Drawdowns are from stress period 600 at the end of the 50-year simulation period.

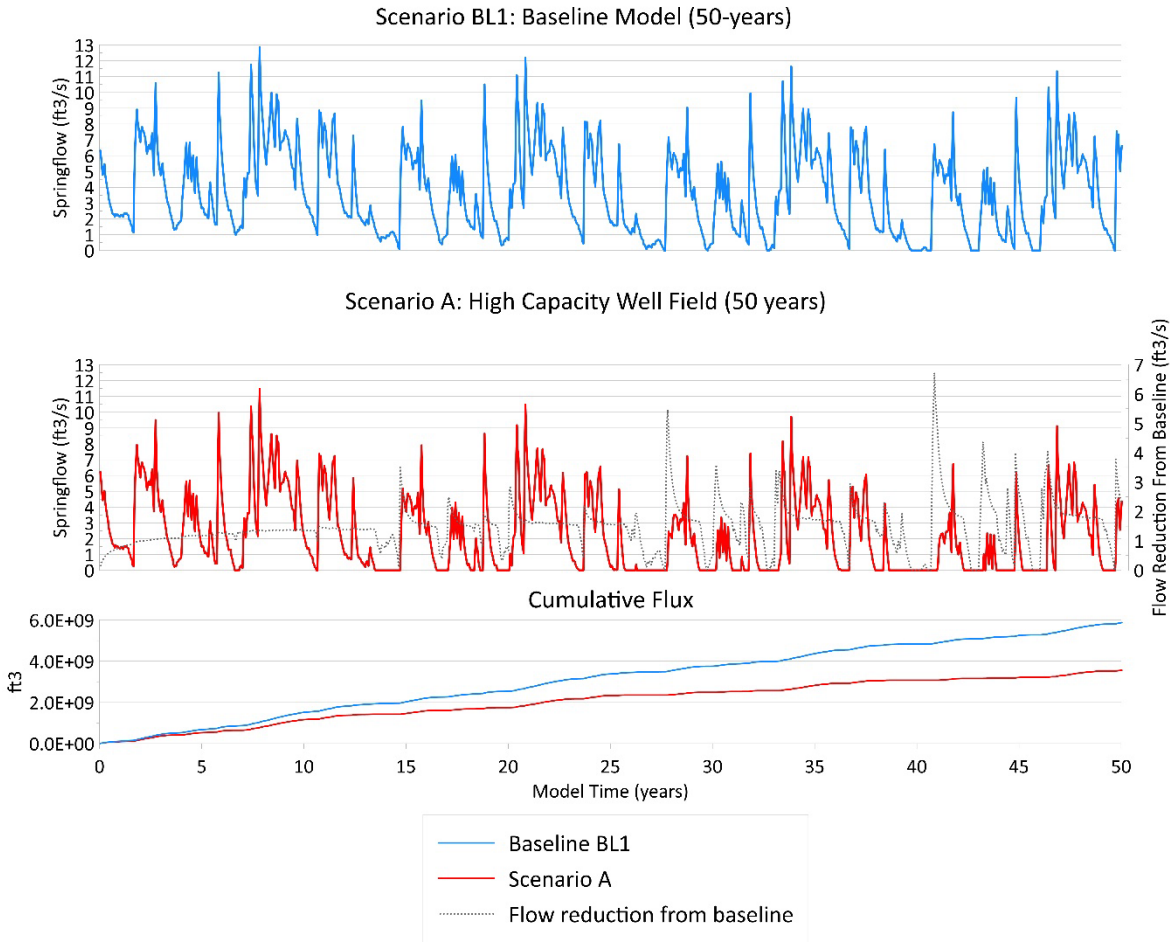

Figure 41. Simulated JWS flow for Scenario A (high-capacity wellfield) for baseline scenario BL1 (above) and scenario A (below). Additional pumping from the high-capacity wellfield causes a simulated reduction in the magnitude of JWS springflow and an increase in the frequency and duration of no-flow events.

Scenario B: 50-year simulation with pumping increase due to projected regional water demand growth

This regional demand growth scenario was created by applying county-level projected water demand estimates from the 2022 state water plan (TWDB 2022) to estimate pumping increases in BSEACD and HTGCD. These projected pumping increases were applied uniformly within the respective districts by creating constant flux analytic element polygons using the Groundwater Vistas software. For BSEACD, a new polygon was drawn approximately following the distribution of known existing Trinity domestic wells (Figure 42) in the SW of BSEACD shown in Figure 11. This area approximates where new increases in pumping are likely to occur because Middle Trinity well productivity and water quality are generally higher and drilling is more economically feasible due to shallower depths to aquifer-bearing strata in SW BSEACD. For HTGCD, simulated pumping was applied to the original exempt pumping polygon established in the calibrated model (i.e., simulated pumping increases are distributed evenly across approximately the entire HTGCD).

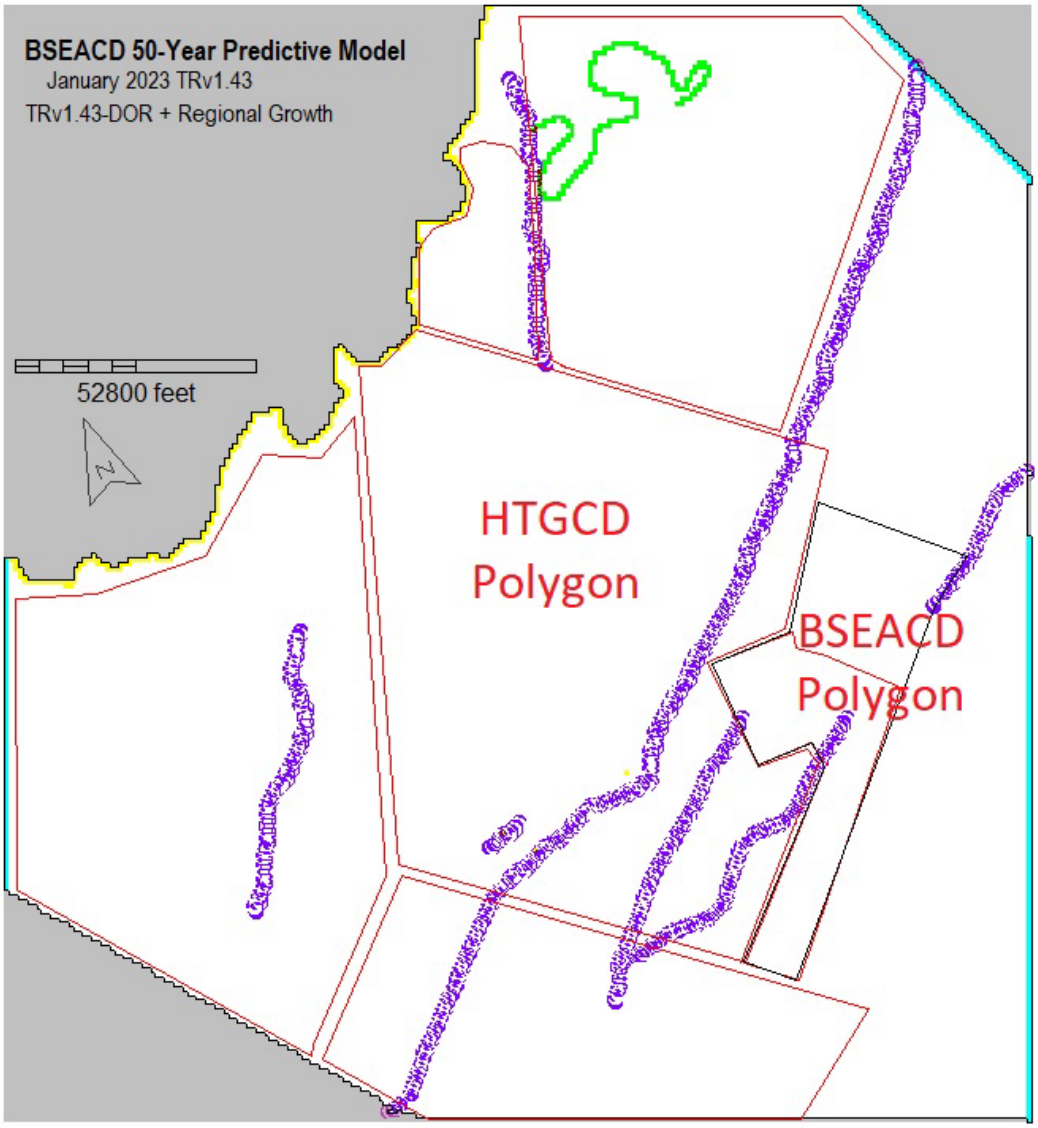

Figure 42. Constant flux polygons over which regional demand growth pumping was applied for the demand growth scenario (Scenario B).

Projected increases in pumping from 2020-2070 (end of simulation period) was calculated as follows for BSEACD and HTGCD:

$$P_{growth2070} = (P_{total2020} * 2.6) - P_{total2020}$$

Where $P_{total2020}$ is total estimated exempt and non-exempt pumping reported in the 2020 fiscal year annual reports of both GCDs (BSEACD 2020; HTGCD 2020). $P_{growth2070}$ represents the net increase in pumping (both exempt and non-exempt) from 2020-2070. The 2.6 factor comes from the TWDB state water plan, which estimates a 2.6X increase in water demand for Hays County in the year 2070 (TWDB 2022). Once calculated, $P_{growth2070}$was divided by the amount of years in each predictive simulation, and further subdivided for each month of the year, using the same monthly/seasonal pumping percentage weighting which was applied to the exempt constant flux polygons in the calibrated model (Table 13). Thus, simulated pumping increases linearly each year of the simulation until projected 2070 demand growth pumping is reached, and a monthly/seasonal variation in pumping is also applied to the simulation within each year. Pumping growth increases were not applied to the other GCDs within the model domain outside of Hays County.

Scenario B Results

Scenario B modeled drawdown (Scenario BL1 baseline minus Scenario B) showed significant and widespread decreases in water levels across most of Hays County. Within the BSEACD portion of the model domain, drawdown also extended north into Travis County with the 10-ft contour almost reaching the Colorado River (Figure 43). BSEACD had the drawdowns in the model domain, with an average of 40.6 ft across the District. The largest drawdowns occurred in western BSEACD (max: 91.4 ft) (Table 19).

Scenario B simulated significantly lower JWS drain flux (springflow) than the baseline Scenario BL1, with a total volume flux reduction of 43.3% and an average flux reduction of 1.6 cfs (Table 20, Figure 44). JWS flow reductions from Scenario B to baseline and the frequency and duration of low/no flow events increased with time over the 50-year simulation period. This reflects increasing annual pumping over time being applied to the regional growth constant flux polygons. During the latter half of the simulation period simulated flux from the JWS drain became more infrequent, with no-flow conditions being more prevalent than flow conditions. Total PVS flow volume difference was higher for Scenario B than Scenario A, but still relatively small (4.3%-Table 20) overall.

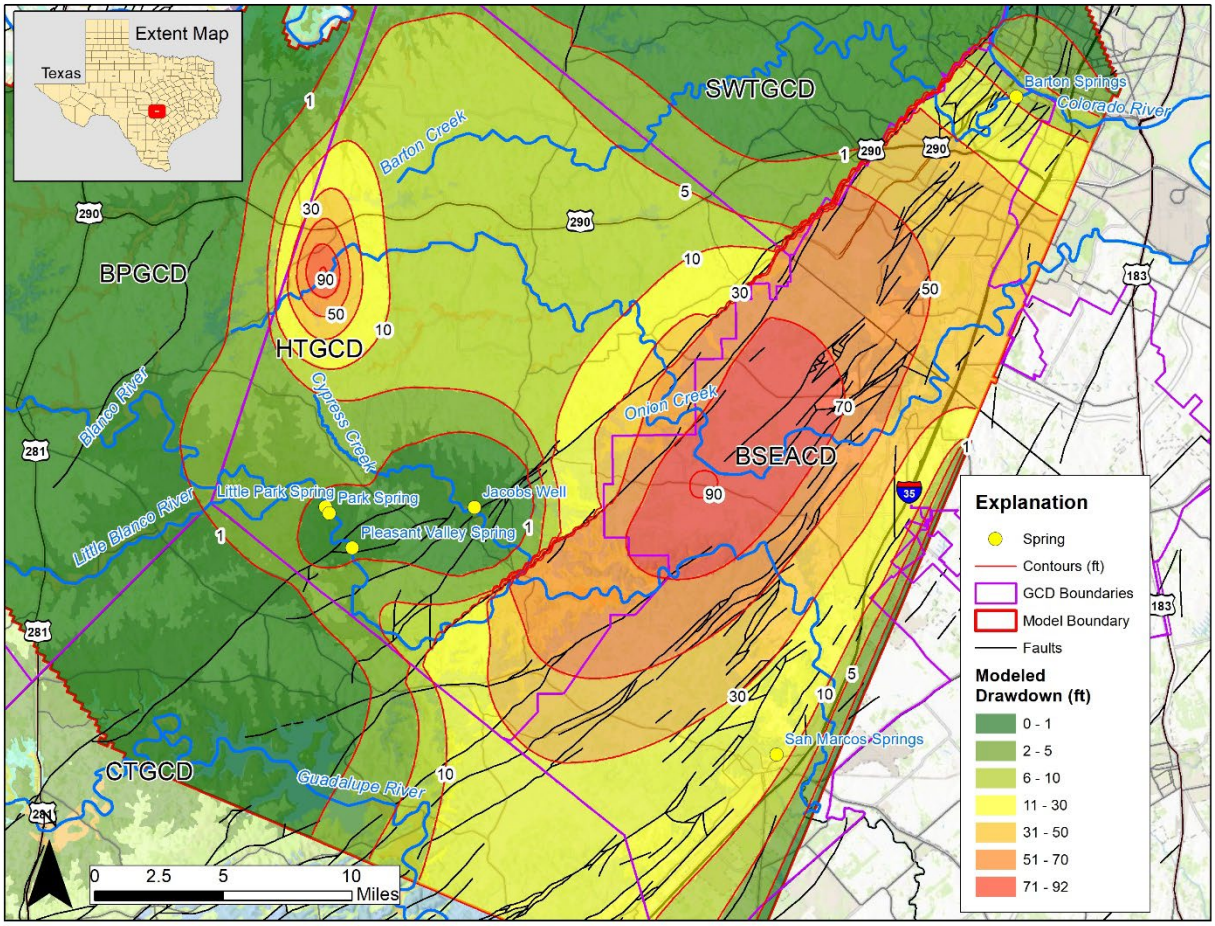

Figure 43. Modeled drawdown map for Scenario B (baseline BL1 minus Scenario B head). Drawdowns are from stress period 600 at the end of the 50-year simulation period.

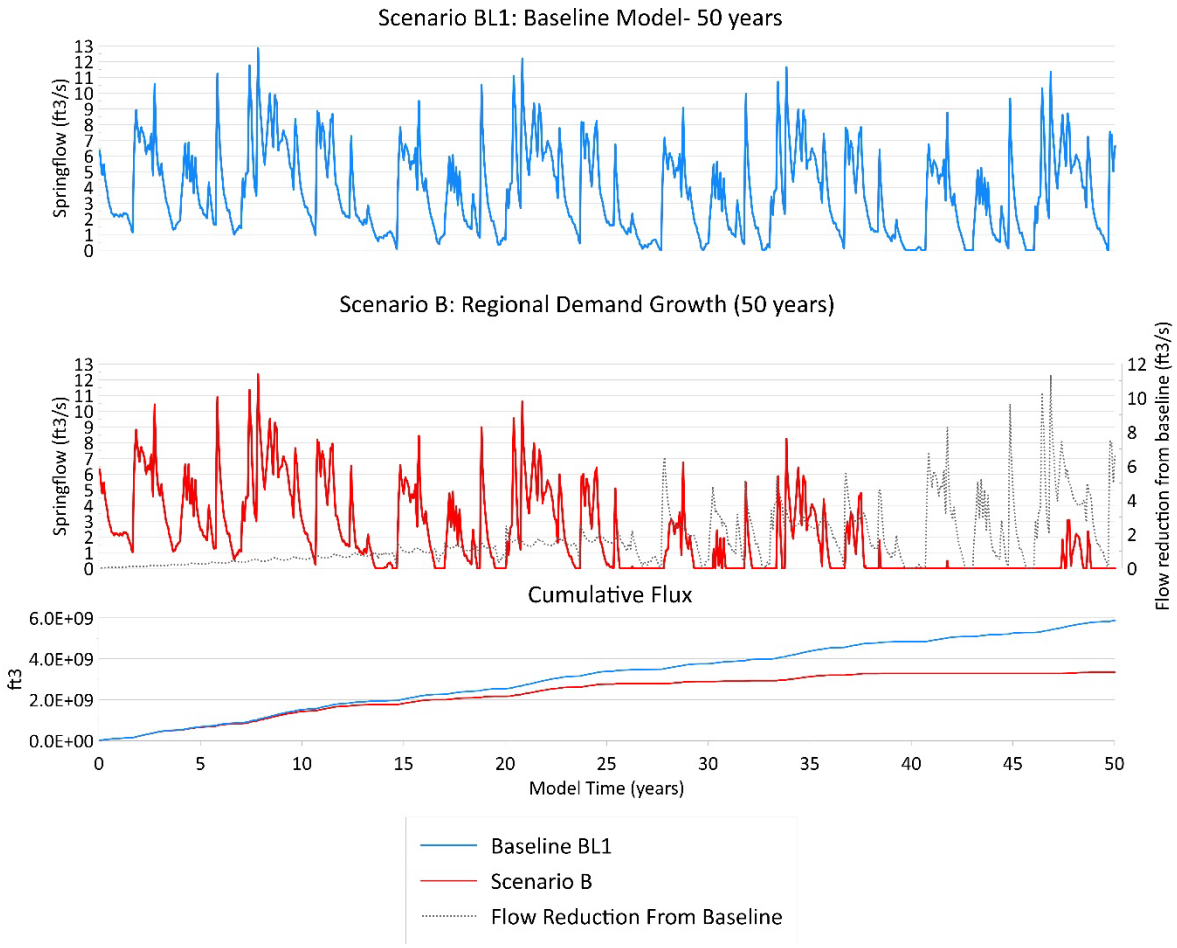

Figure 44. Simulated JWS Springflow for the baseline model (above) and regional pumping growth Scenario B (below).

Scenario BL2: Drought of Record Baseline-10-year Simulation

A drought of record (DOR) baseline scenario was constructed to simulate the impact of the recurrence of a historic 1950's Texas DOR to Trinity Aquifer heads and springflow under different pumping conditions. The DOR recharge dataset was created from gridded PRISM monthly historic precipitation data (PRISM 2022). For the purposes of this modeling experiment, the historic DOR was defined as starting in April 1947 and ending in April 1957 (10 years, 120 stress periods). Historic monthly average Blanco River flow from the USGS Wimberley gage (USGS gage ID: 08171000) was available over this time period, and thus it was possible to use Blanco River flow to apply high or low recharge coefficients to each recharge zone for a given stress period following the same methodology used to generate the calibrated model recharge dataset. The same recharge zones and high/low coefficients from the calibrated model (Table 11) were applied to PRISM precipitation values to generate recharge values for each cell in the layer 1 recharge zone and for each stress period. The DOR baseline scenario BL2 does not include any pumping boundary conditions, either from individual wells or from the constant flux polygons established in the calibrated model. Given the general sparsity of population and pumping demand from the 1950s, it is likely a good approximation of historic conditions to assume that pumping was negligible during the 1950s. Scenario BL2 JWS springflow is in reasonable agreement with three historic DOR springflow measurements ranging from 2.4-2.6 cfs in January to March, 1955 (Figure 46). These three measurements appear to represent low-flow conditions during the DOR. A July 1955 DOR measurement of 12.1 cfs was not matched by Scenario BL2 JWS simulated springflow, indicating that Scenario BL2 may be underestimating flow during higher flow DOR months.

Scenario C1: Recurrence of 1950's Drought of Record with 2020 Pumping (10-year simulation)

Scenario C1 was created to simulate a recurrence of the 1950's DOR under approximately modern pumping conditions. Scenario C1 is identical to the DOR baseline model, except non-exempt pumping (discretely modeled permitted wells), and exempt pumping (constant flux polygons) from the first 10 years of the calibrated model (2008-2018) have been superimposed onto the baseline DOR model. Since the DOR baseline model does not include any pumping stresses, differences between Scenario C1 and the Scenario BL2 DOR baseline essentially simulates the impact of modern pumping during historic DOR recharge conditions.

Scenario C1 Results

Significant modeled drawdowns (Scenario C1 minus Scenario BL2 baseline) were simulated across most of BSEACD during the 10-year simulation period (Figure 45). Mean drawdown within BSEACD was 15.5 ft with a max drawdown of 52.4 ft (Table 19). The largest drawdowns were concentrated in northern and western BSEACD, and within the upper Onion Creek basin in HTGCD (Figure 45).

Scenario C1 simulated significantly less total JWS flux (springflow) than baseline, showing a 42.8% reduction in total flux volume from the JWS drain cell, and an average flux reduction of 2.1 cfs relative to baseline (Table 20). Difference in flow between C1 and baseline over the simulation period cycled between approximately 2-2.8 cfs, following seasonal fluctuations in simulated pumping (Figure 46). Similar to Scenarios A and B, PVS flow was relatively unchanged between Scenario C1 and baseline BL2, with a cumulative flux volume reduction of 1.9% (Table 20).

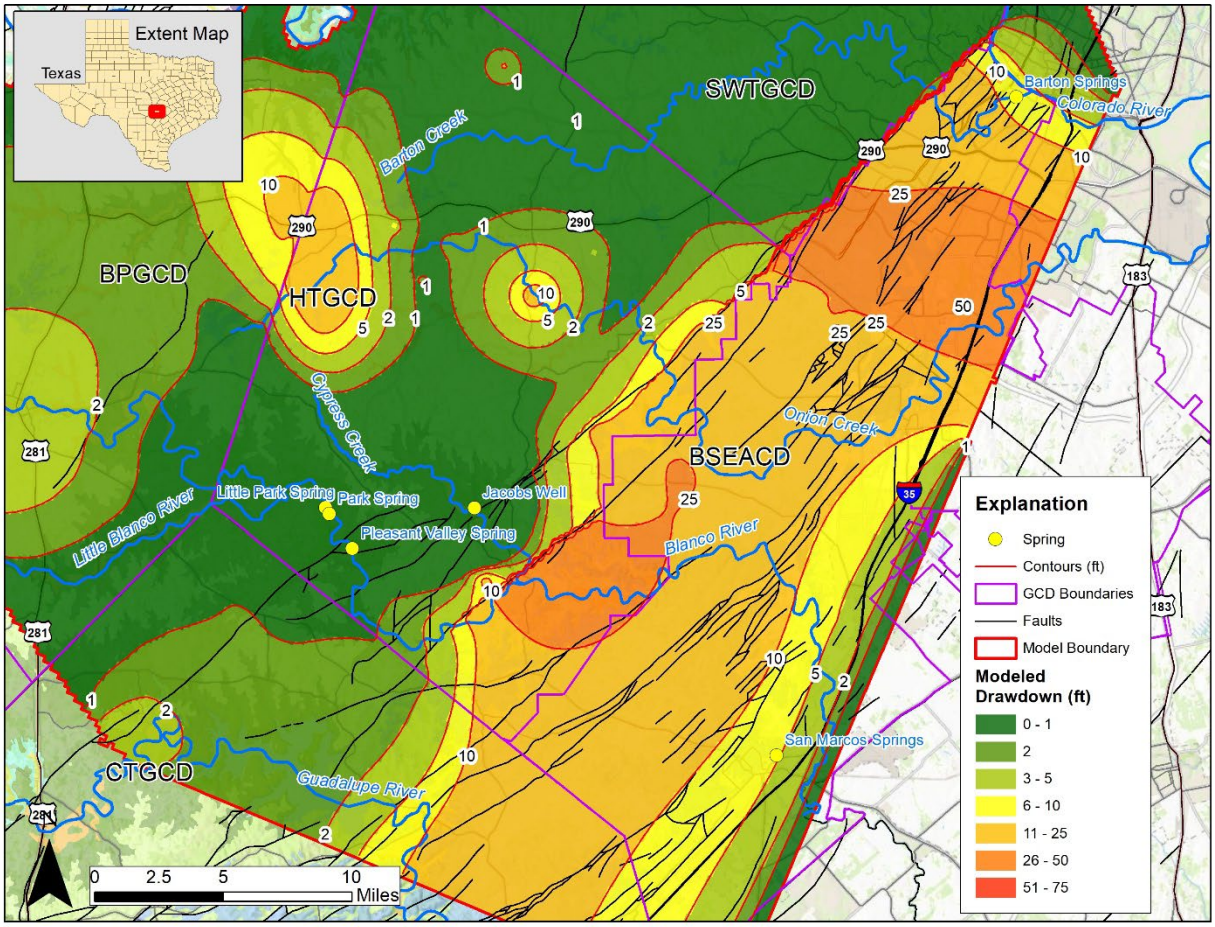

Figure 45. Modeled drawdown map for scenario C1 (recurrence of drought of record) between pumping and no pumping at the end of the 10-year simulation period (stress period 120). Pumping causes significant additional simulated drawdown during a recurrence of drought of record, particularly in the confined, BSEACD portion of the aquifer, and within the upper Onion Creek Basin in HTGCD.

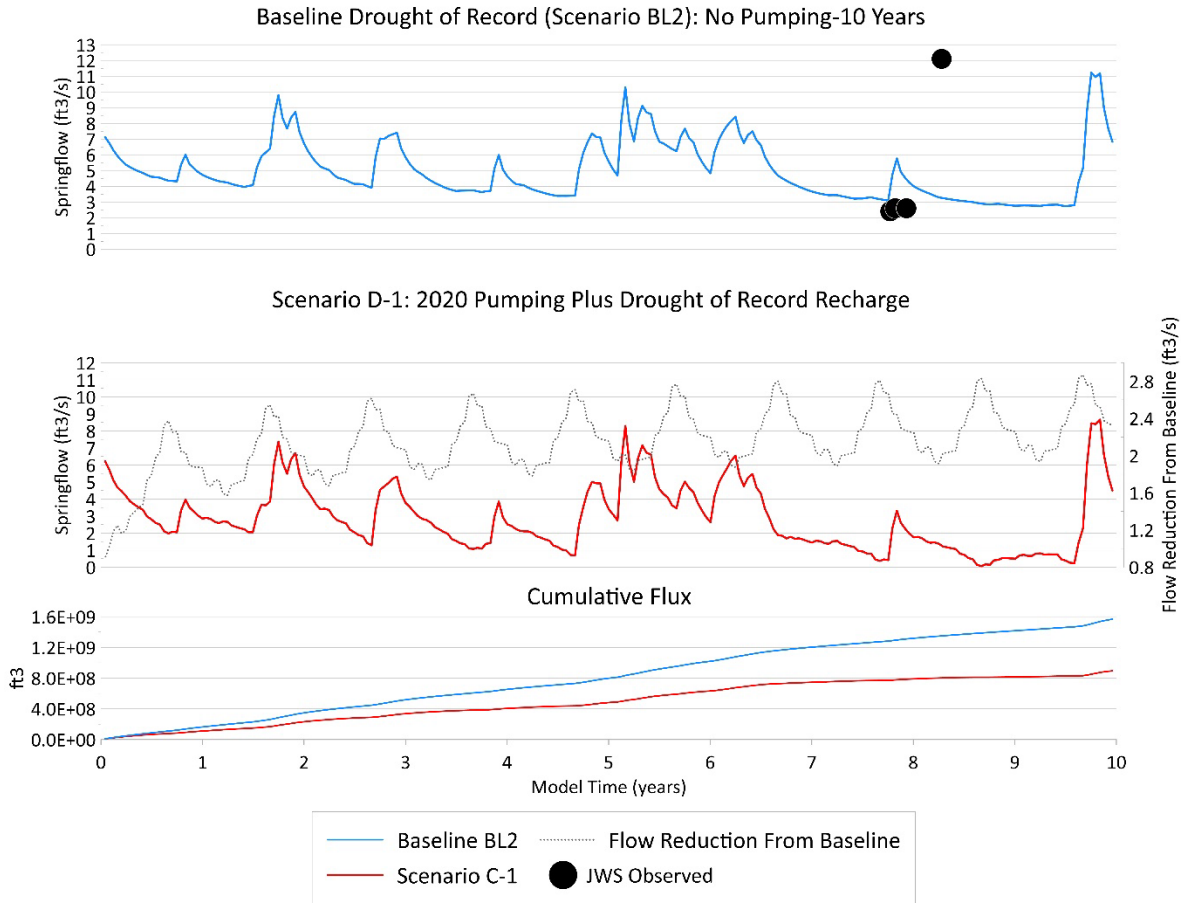

Figure 46. Simulated JWS Springflow for Scenario BL2: Recurrence of drought-of-record recharge with modern-day pumping and without modern-day pumping. JWS observed values are historic measurements from TBWE (1960).

Scenario C2: Recurrence of 1950's Drought of Record with regional projected water demand growth pumping increase (10-year simulation)

Scenario C2 is similar to Scenario C1, but instead of simulating modern pumping conditions from 2008-2018, the regional demand growth pumping increase from Scenario B was superimposed onto DOR recharge conditions. Details on the regional demand growth pumping increase model can be found in the Scenario B section of this report. The final 10 years (2060-2070: 120 stress periods) of the Scenario B constant flux regional pumping boundary conditions (HTGCD and BSEACD constant flux polygons) were added to Scenario C1 to model increased pumping from regional increases in water demand.

Scenario C2 Results

Modeled drawdown values (Scenario C2 minus Scenario BL2 baseline) were large across most of BSEACD at the end of the 10-year simulation period, with the largest drawdowns occurring in the western portion of the district (Figure 47). Mean drawdown within BSEACD was 51.8 feet, with a maximum of 111.5 feet (Table 19). Scenario C2 mean drawdown within BSEACD was the largest of the four scenarios presented in this report.

Scenario C2 simulated significantly less total JWS drain flux (springflow) than baseline, showing an 82.6 percent decrease in total flow volume and an average flux reduction of 4.1 cfs over the 10 year simulation period (Table 20). More than half of the Scenario C2 stress periods simulated no flux from the JWS drain cell, with a maximum flow reduction of 11 cfs compared to baseline occurring toward the end of the simulation period (Figure 48).

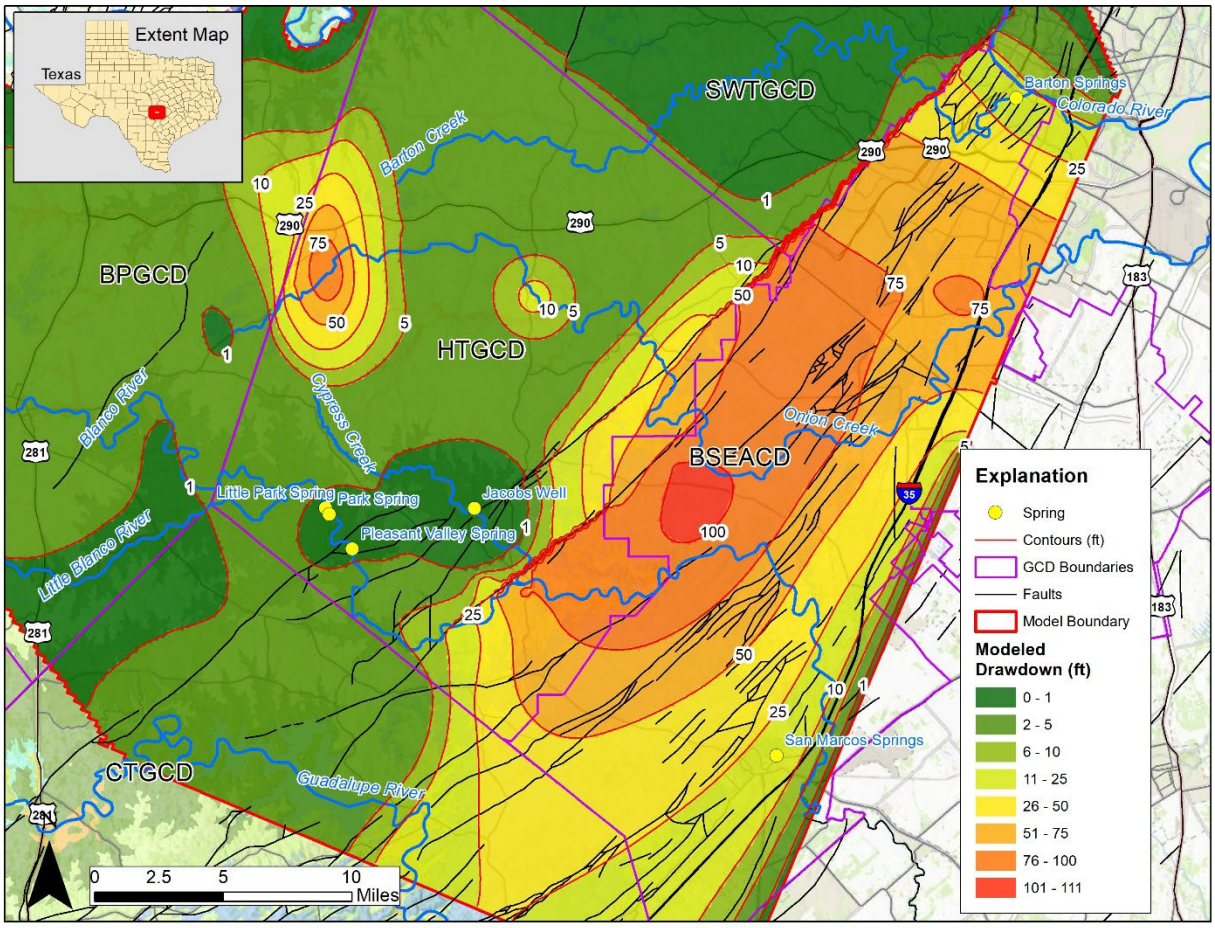

Figure 47. Modeled drawdown map for Scenario C2 at the end of the 10-year simulation period (stress period 120). (Recurrence of drought of record plus scenario B regional growth pumping increase: simulation years 2060-2070).

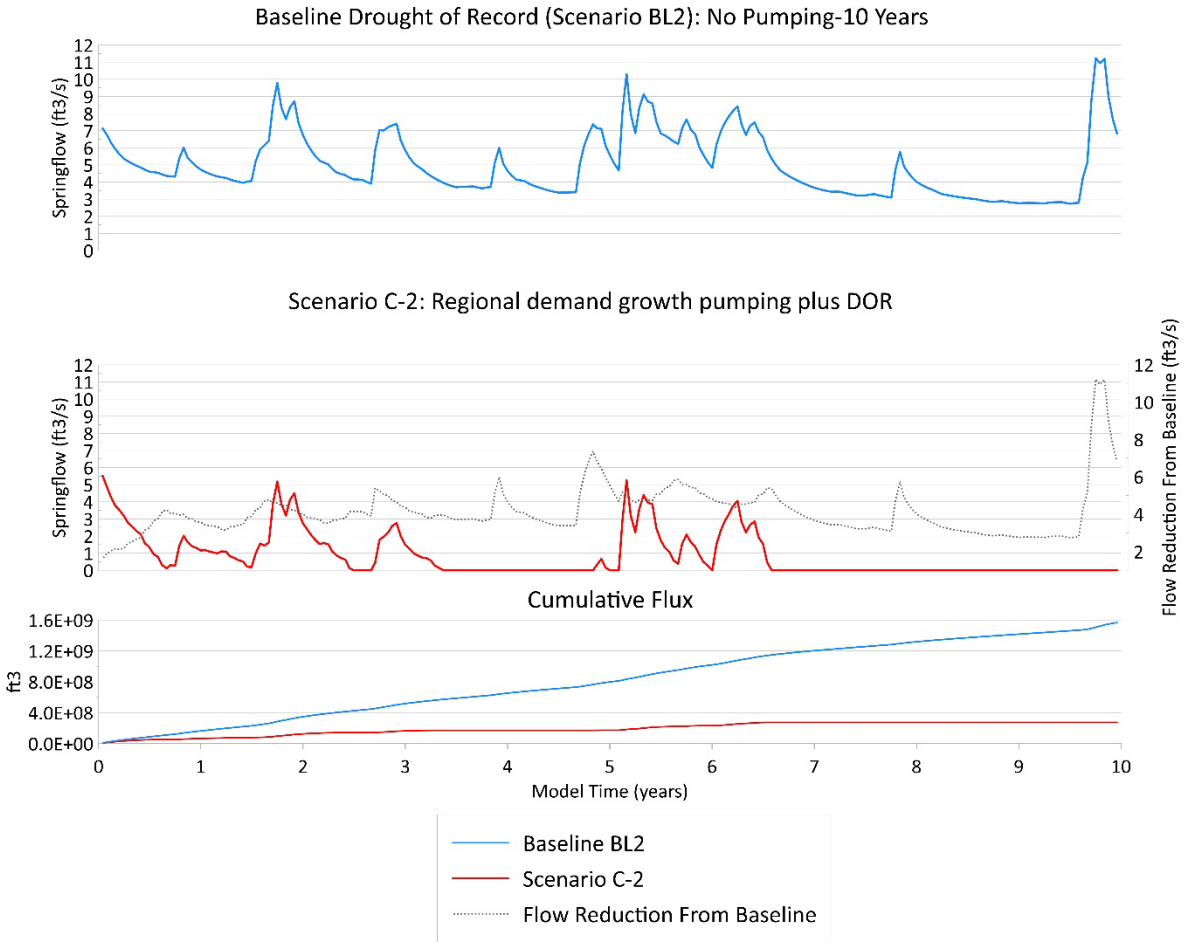

Figure 48. Simulated JWS Springflow for drought of record no pumping (Scenario BL2) versus drought of record plus regional pumping growth _(Scenario C1).

Discussion of Predictive Modeling Results

Head (water levels)

All predictive modeling scenarios presented in this report demonstrated significant modeled drawdowns in response to pumping increases. Mean drawdowns within BSEACD ranged from 15.0 (Scenario A) to 51.8 feet (Scenario C2) (Table 19). The maximum drawdown came from Scenario A (232.7 feet), which simulated a hypothetical wellfield of six wells pumping at a constant rate of 2.5 MGD. Predictably, maximum drawdowns for Scenario A were close to the wellfield pumping center (Figure 40). However, Scenario A mean drawdowns were almost three times lower than Scenario B (Regional Growth Scenario).

These results demonstrate the importance of pumping distribution and magnitude when evaluating the potential impacts of pumping on aquifer heads. Scenario A had significantly less overall annual pumping volume than the final stress period of Scenario B, but a more concentrated distribution of pumping (a localized wellfield). This resulted in larger localized drawdowns in the vicinity of the wellfield than any localized drawdowns in Scenario B, which distributed a higher volume of pumping over a larger area.

All predictive model scenarios simulated higher mean drawdowns in BSEACD than HTGCD (Table 19). These simulated results agree with trends in observed water level data, which show generally larger fluctuations in water levels between wet and dry conditions, and larger drawdowns in response to pumping in the BFZ Middle Trinity (Gary et al., 2019). This difference in aquifer head response is mainly due to the lower hydraulic conductivity in the BFZ Middle Trinity than upgradient portions of the aquifer. The BSEACD jurisdictional boundaries fall entirely within the BFZ Middle Trinity Aquifer. Thus, BSEACD stakeholders and policymakers can anticipate generally larger drawdowns in response to pumping within BSEACD than the upgradient HTGCD portion of the Trinity.

Upgradient of the BFZ, head fluctuations and modeled drawdown in response to pumping are generally more muted than the downgradient confined portion of the Middle Trinity Aquifer. This is particularly true in the Blanco Basin in the vicinity of JWS and PVS, where major spring outlets connected to large conduits provide a "pressure relief valve" for hydraulic head (Gary et al., 2019). This hydraulic characteristic of the aquifer in the vicinity of JWS and PVS generally anchors aquifer heads to within several feet of spring outflow elevation, and mutes head responses to pumping and recharge events. In the TAS, this behavior in head response was achieved by manually adjusting Kh to be very high in the vicinity of spring drain cells, which propagates the influence of the spring drain cells to cells further away from the spring drain. This amounts to an equivalent porous media (EPM) approximation of the JWS and PVS karst conduit/spring drain system, in which turbulent flow occurring in subsurface aquifer conduits is being approximated as a porous material with very high hydraulic conductivity. While not effective for simulating transport processes or more localized flow paths, the EPM approach has been shown to be effective for simulating springflow volume and regional hydraulic heads in karst systems (Scanlon et al., 2003). Another consequence of the "pressure relief valve" hydraulic characteristic of the Middle Trinity in the vicinity of JWS and PVS described above is that significant capture of springflow from pumping is possible despite the same pumping causing relatively modest reductions in aquifer head (i.e. relatively small impacts to water levels can be associated with relatively large reductions in springflow in the vicinity of springs). Springflow impacts are discussed in more detail below.

Both DOR scenarios (C1 and C2) simulated significant modeled drawdowns in both HTGCD and BSEACD in response to pumping during a recurrence of DOR recharge conditions. This indicates that drought, especially a recurrence of the 1950s DOR, has a significant impact on water levels in the Trinity.

Comparison of Scenario C2 to Scenario B (regional demand growth scenario) provides an evaluation of how the Middle Trinity Aquifer might respond when the impacts of greatly increased pumping due to regional growth in water demand are superimposed on the impacts of a recurrence of the 1950s DOR. Scenario C2 had a significantly larger mean and max modeled drawdown than Scenario B, which has the same pumping stressors over the final 10 years of the 50-year simulation (Table 19). Thus, these models predict that drawdown due to pumping is much more pronounced during periods of extended drought.

Springflow (JWS and PVS Drain Cells)

All of the predictive scenarios showed significant reductions in JWS springflow relative to baseline, with an average flow reduction of 1.5-4.1 cfs and a total flow volume reduction of 39.5-82.6% over the simulation periods (Table 20). Despite these significant impacts to modeled springflow, modeld drawdowns in the vicinity of JWS were relatively small (<1ft) for all modeling scenarios tested, suggesting that relatively small head reductions can result in large simulated springflow impacts. These model results are in agreement with the general conceptual model, and historic observational data, for JWS; which is thought to have a relatively small spring recharge catchment and has been observed to respond directly to pumping from nearby public water-supply system wells despite showing minimal hydraulic aquifer head fluctuations over time (Gary et al., 2019).

Simulated pumping impacts to springflow in Scenario B (2.5 MGD well field) suggest that pumping in the BFZ Middle Trinity has the potential to capture springflow in the upgradient shallower Trinity, with a total springflow volume reduction of 39.5% (Table 20). This volumetric springflow reduction to JWS agrees with the earlier steady state version of the model, which simulated a 39% volumetric reduction from the same hypothetical well field (Hunt and Smith, 2020). The hypothetical well field is approximately 6 miles from JWS along a west-to-east transect that extends across the TCFZ and other mapped faults that are thought to act as hydraulic barriers to groundwater flow. In the current model construction, a relay ramp structure described by Hunt et al., (2015), has been conceptualized as HFB reach #2 (Figure 19), a reach in the TCFZ with higher conductivity than adjacent reaches, which allows more groundwater to bypass the fault and travel downgradient into the BFZ Middle Trinity. Without this relay ramp conceptualization, it is likely that the influence of the hypothetical wellfield on JWS springflow would be reduced as there would be less hydraulic connection between them. However, previous versions of the model which excluded the relay ramp conceptualization had generally poorer agreement with head targets, especially in the BFZ Middle Trinity.

Some uncertainty remains as to the location and geometry of relay ramp structures in the BFZ, and to what extent they may provide a pathway for groundwater flow from the JWS area to deeper confined portions of the Trinity. As such, caution should be taken in assuming that the Scenario A prediction of JWS springflow capture from downgradient pumping within BSEACD is an accurate prediction. Further investigation is needed to more accurately quantify the ability of relay ramp structures to transmit groundwater across the BFZ barrier faults, and to what extent they can transmit hydraulic impacts from downgradient pumping into upgradient portions of the Trinity within HTGCD. Also, it should be noted that increased pumping in the upper Blanco/Cypress Creek catchment within HTGCD will likely cause much more JWS springflow capture than any more distal downgradient confined pumping due to the closer proximity to the spring outlet.

The relay ramp portion of the model domain is an excellent location to focus further refinement of the TAS. As new hydrogeologic data such as downhole geophysical logs, monitoring well hydrographs, and

aquifer test data become available, TAS model cells and hydraulic parameters should be adjusted to reflect this new data. This refinement would make the TAS model a more effective tool for hypothesis testing related to the BFZ relay ramp structures because it would allow simulation of groundwater hydraulics using various fault barrier arrangements and geometries for matching with real-world data.

In contrast to JWS, modeled PVS flow was generally more resilient to increases in pumping in the predictive scenarios, with an average flux (springflow) reduction of 0.0-1.1 cfs, and a total volume flux reduction of 0.3-7.2% as compared to baseline models (Table 20). This is likely a result of the distribution of hypothetical pumping centers in the predictive scenarios. For example, if the hypothetical well field in scenario B had been placed upgradient of the PVS spring outlet, modeled PVS springflow capture likely would have been significantly increased. Further pumping scenarios with different pumping distributions in the upper Blanco Basin could be built to evaluate potential impacts to PVS.

Conclusions

This report documents the first phase of development of the TAS, a transient numerical groundwater model constructed in MODFLOW USG that simulates hydraulic head and spring discharge in the Middle Trinity Aquifer. Completion of the TAS fills a key technical demand for guiding the BSEACD Trinity Sustainable Yield policymaking project by allowing quantitative evaluation of the impact of different pumping and recharge scenarios on aquifer levels and spring discharge. The predictive model scenarios presented in this report show that significant increases in pumping in Hays County is likely to result in significant impacts to water levels and springflow in the Middle Trinity Aquifer in Hays County.

However, it is important to acknowledge the limitations of the TAS model, and indeed numerical groundwater models more generally. Groundwater models are only as good as the data and conceptual models used to build them, and the Trinity Aquifer is an inherently complex system with limited available data to inform the conceptual model. As of publication date of this report, the authors believe that the model presented here is the best available tool for quantitative evaluation of water level and springflow impacts from pumping. However, there is still much work that could be done to refine the model and reduce uncertainty in model predictions. If new hydrogeologic data and studies emerge which change our conceptual model of the Trinity Aquifer, it will be important to update the TAS to reflect these changes. It will also be important to validate the model by running it with the most recent rainfall and pumping datasets to ensure that model simulations of head and springflow are aligning with real Trinity Aquifer behavior. The following is a list of some potential areas of work for improving the TAS:

- Development of predictive scenarios that reflect potential changes in aquifer recharge due to climate change.
- Incorporation of the MODFLOW USG Connected Linear Network (CLN) module to better simulate karstic groundwater flow.
- Refinement of model parameters to better match head responses in the BFZ Middle Trinity.
- Implementation of finer resolution nested cell grids in key areas of the model domain, such as in the vicinity of large pumping centers or spring outlets.
- Refinement of exempt pumping spatial distribution, particularly within HTGCD jurisdictional boundaries.

Acknowledgments

Development of the TAS would not have been possible without the hard work of countless geologists who developed the datasets and analyses that provide the foundation for the conceptual groundwater model from which the TAS was developed. Thank you to all who participated in our technical advisory committee and provided technical review and comment on our model files and modeling report (a list of participants is provided below). Brian Hunt deserves special acknowledgement for developing the steady-state numerical model which preceded the TAS. Thanks also to Nick Martin for advising us during development of the TAS, and for providing PYTHON scripts and guidance for accessing and downloading PRISM rainfall datasets.

Technical Advisory Committee Members

Roberto Anaya (Texas Water Development Board)

Paul Bertetti (Edwards Aquifer Authority)

Radu Boghici (Hays Trinity Groundwater Conservation District)

Dr. Marcus Gary (Edwards Aquifer Authority)

Jevon Harding (Texas Water Development Board)

Brian Hunt (Bureau of Economic Geology)

Bill Hutchinson (Private groundwater modeling consultant)

Ian Jones (Texas Water Development Board)

Dr. Robert Mace (Meadows Center for Water and the Environment)

Nick Martin (Southwest Research Institute)

Dr. Jack Sharp (University of Texas Professor Emeritus)

Doug Wierman (Meadows Center for Water and the Environment)

References

Abusaada, M. and M. Sauter. 2013. Studying the flow dynamics of a karst aquifer system with an equivalent porous medium model. Ground Water. 51(4). pp. 641-50. doi: 10.1111/j.1745- 6584.2012.01003.x

Anderson, M.P., W.W. Woessner, and R.J. Hunt, 2015, Applied Groundwater Modeling, 2nd Edition. Elsevier Inc. 564 p.

Ashworth, J.B., 1983, Ground-water availability of the Lower Cretaceous formations in the Hill Country of south-central Texas: Texas Department of Water Resources Report 273, 173 p.

Austin, B., D. Thomas, R. Burns, and M. Sansom, 2001, Volumetric Survey of Canyon Lake, TWDB Report. Prepared for: Guadalupe-Blanco River Authority In cooperation with the United States Army Corps of Engineers. November 9, 2001. 48 p. https://www.twdb.texas.gov/hydro_survey/Canyon/2001-11/Canyon2000_FinalReport.pdf

Broun, A. S., B. B. Hunt, J. A. Watson, and D. A. Wierman, 2020, A Reevaluation of the Lithostratigraphy and Facies of the Lower Cretaceous Hensel Sand–Lower Glen Rose Transition, Comanchean Shelf, Blanco and Hays Counties, Central Texas. GCAGS Journal, v. 9 (2020), p. 76–92. http://www.gcags.org/Journal/2020.GCAGS.Journal/2020.GCAGS.Journal.v9.05.p76-92.Broun.et.al.pdf

Barton Springs Edwards Aquifer Conservation District (BSEACD), 2017, Hydrogeologic Setting and Data Evaluation: 2016 Electro Purification Aquifer Test, Cow Creek Well Field: Hays County, Texas. Barton Springs Edwards Aquifer Conservation District, Technical Memo 2017-1010, 39 p.

Barton Springs Edwards Aquifer Conservation District (BSEACD), 2018a, Aquifer Parameter Estimation for the EP Well Field, Hays County, Texas. Barton Springs Edwards Aquifer Conservation District, Technical Memo 2018-0213, 28 p.

Barton Springs Edwards Aquifer Conservation District (BSEACD), 2018b, Evaluation of the Potential for Unreasonable Impacts from the EP Well Field, Hays County, Texas. BSEACD Technical Memo 2018-0219. February 2018. 13 p.

Barton Springs Edwards Aquifer Conservation District (BSEACD), 2020, Annual Report Fiscal Year 2020, < https://bseacd.org/uploads/12.10.2020-Annual-Report-with-App-A-and-B.pdf>

Cockrell, L., Hunt, B.B., Gary, R., and B.A. Smith, 2018, Regional Geologic Geodatabase Project, Central Texas: Barton Springs/Edwards Aquifer Conservation District Data Series Report 2018-1211, December 2018, 14 p.

Environmental Simulations Incorporated (ESI), 2017a, Guide to Using Groundwater Vistas Version 7. 427 p.

Environmental Simulations Incorporated (ESI), 2017b, Tutorial guide for Groundwater Vistas Version 7. 331 p.

Gary, M.O., B. B. Hunt, B. A. Smith, J. A. Watson, and D. A. Wierman, 2019, Evaluation for the Development of a Jacob's Well Groundwater Management Zone Hays County, Texas. Technical Report prepared for the Hays Trinity Groundwater Conservation District, Hays County, Texas. Meadows Center for Water and the Environment, Texas State University at San Marcos, TX. Report: 2019-05. July 2019. 58 p.

Hays Trinity Groundwater Conservation District (HTGCD), 2020, 2020 Annual Report, < https://haysgroundwater.com/wp-content/uploads/2022/01/2020-Annual-Report.pdf>

Hill, R.T., and T. W. Vaughan., 1898, Geology of the Edwards Plateau and Rio Plain adjacent to Austin and San Antonio, Texas, With Reference to the Occurrence of Underground Waters, U. S. Geological Survey, Annual Report 18, p. 193-321.

Hoff, S.Z., and A.R. Dutton, 2017, Beyond the Bad-Water Line—A Model for the Occurrence of Brackish Water in the Upper Coastal Plain Aquifers in Texas. GCAGS Journal, v. 6 (2017), p. 135–149.

Hunt, B. B., B. A. Smith, and J. Beery, 2007, Potentiometric Maps for Low to High Flow Conditions, Barton Springs Segment of the Edwards Aquifer, Central Texas, Barton Springs Edwards Aquifer Conservation District Report of Investigations 2007-1201, 64 p.

Hunt, B.B., B.A. Smith, J. Kromann, D. A. Wierman, and J. Mikels, 2010, Compilation of Pumping Tests in Travis and Hays Counties, Central Texas: Barton Springs Edwards Aquifer Conservation District Data Series report 2010-0701, 12 p. + appendices.

Hunt, B.B., and B.A. Smith, 2010, Spring 2009 Potentiometric Map of the Middle Trinity Aquifer in Groundwater Management Area 9, Central Texas: Barton Springs Edwards Aquifer Conservation District Report of Investigations 2010-0501, 26 p.

Hunt, B.B., B.A. Smith, R. Slade Jr., R.H. Gary, and W.F. Holland, 2012, Temporal Trends in Precipitation and Hydrologic Responses Affecting the Barton Springs Segment of the Edwards Aquifer, Central Texas: Gulf Coast Association of Geological Societies Transactions, 62nd Annual Convention, October 21-24, 2012, Austin, TX.

Hunt, B.B., C. Norris, M.O. Gary, D.A. Wierman, A.S. Broun, and B.A. Smith, 2013, Pleasant Valley Spring: A Newly Documented Karst Spring of the Texas Hill Country Trinity Aquifer. Geological Society of America Abstracts with Programs. Vol. 45, No. 3, p. 92.

Hunt, B.B., B.A. Smith, A. Andrews, D.A. Wierman, A.S. Broun, and M.O. Gary, 2015, Relay ramp structures and their influence on groundwater flow in the Edwards and Trinity Aquifers, Hays and Travis Counties, Central Texas, Sinkhole Conference, October 5-10, 2015, Rochester, Minnesota

Hunt, B.B., A.S. Broun, D.A. Wierman, D.A. Johns, and B.A. Smith, 2016a, Surface-water and groundwater interactions along Onion Creek, Central Texas: Gulf Coast Association of Geological Societies Transactions, v. 66, p. 261–282.

Hunt, B.B., A. Andrews, and B.A. Smith, 2016b, Hydraulic Conductivity Testing in the Edwards and Trinity Aquifers Using Multiport Monitor Well Systems, Hays County, Central Texas. Barton Springs/Edwards Aquifer Conservation District Report of Investigations. BSEACD RI 2016-0831, August 2016, 39 p. https://bseacd.org/uploads/Hunt-et-al.-2016_Slug-Testing_FINAL.pdf

Hunt, B.B. and B.A. Smith, 2016c, Evaluation for Unreasonable Impacts: Needmore Water, LLC, Well D Permit Application. Barton Springs/Edwards Aquifer Conservation District. Technical Memo 2016-1115. 26 p. https://bseacd.org/uploads/GM_Preliminary-DecisionBinder_112216.pdf

Hunt, B.B., B.A. Smith, M.O. Gary, A.S. Broun, and D.A. Wierman, 2017a, An Evolving Conceptual Model of the Middle Trinity Aquifer, Hays County, Central Texas. Geological Society of America Abstracts with Programs. Vol. 49, No. 1, South-Central Section Meeting, San Antonio, Texas, March 2017.

Hunt, B.B., B.A. Smith, M.O. Gary, A.S. Broun, D.A. Wierman, J. Watson, and D.A. Johns, and 2017b, Surface-water and Groundwater Interactions in the Blanco River and Onion Creek Watersheds: Implications for the Trinity and Edwards Aquifers of Central Texas. South Texas Geological Society Bulletin, v. 57, no. 5, January 2017, p. 33-53.

Hunt, B.B, B.A. Smith, M.O. Gary, J.A. Watson, A.S. Broun, D.A. Wierman, and R. Fieseler, 2018, Technical Review and Comments: Conceptual Model Update for the Hill Country Portion of the Trinity Aquifer. Letter dated August 31, 2018. 22 p.

Hunt, B.B., B.A. Smith, R. Gary, and J. Camp, 2019a, March 2018 Potentiometric Map of the Middle Trinity Aquifer, Central Texas. BSEACD Report of Investigations2019-0109. 28 p.

Hunt, B.B., B.A. Smith, and N.M. Hauwert, 2019b, Barton Springs segment of the Edwards (Balcones Fault Zone) Aquifer, central Texas, in Sharp, J.M., Jr., Green, R.T., and Schindel, G.M., eds., The Edwards Aquifer: The Past, Present, and Future of a Vital Water Resource: Geological Society of America Memoir 215, p. 1–XXX, https://doi.org/10.1130/2019.1215(07).

Hunt, B.B., L.P. Cockrell, R.H. Gary, J.M. Vay, V. Kennedy, B.A. Smith, and J.P. Camp, 2020, Hydrogeologic Atlas of Southwest Travis County, Central Texas. BSEACD Report of Investigations 2020-0331, March 2020, 80 p. + digital datasets. https://repositories.lib.utexas.edu/handle/2152/81562

Hunt, B.B. and B. Smith, 2020, Development of a Steady-State Numerical Model, Middle Trinity Aquifer, Central Texas, BSEACD Technical Memo 2020-0930, September 2020.

Jones, I.C., R. Anaya, and S.C. Wade, 2011, Groundwater Availability Model: Hill Country Portion of the Trinity Aquifer of Texas. Texas Water Development Board Report 377. June 2011. 175 p. http://www.twdb.texas.gov/publications/reports/numbered_reports/doc/R377_HillCountryGAM.pdf

Mace, R., A. Chowdhury, R. Anaya, and S. Way, 2000, Groundwater Availability of the Trinity Aquifer, Hill Country Area, Texas: Numerical Simulations through 2050: Texas Water Development Board, 172 p. Country Area, Texas: Numerical Simulations through 2050: Texas Water Development Board, 172 p.

Lindgren, R.J., A.R. Dutton, S.D. Hovorka, S.R.H. Worthington, and S. Painter, 2004, Conceptualization and simulation of the Edwards aquifer, San Antonio region, Texas, U.S. Geological Survey, Scientific Investigations Report 2004-5277. 143p. https://pubs.er.usgs.gov/publication/sir20045277.

Martin, N.M., R. T. Green, K.D. Nicholaides, S.B. Fratesi, R.R. Nunu, and M.E. Flores, 2019. Blanco River Aquifer Assessment Tool: A Tool to Assess How the Blanco River Interacts with Its Aquifer: Creating the Conceptual Model. Technical Report prepared for the Meadows Center for Water and the Environment. Texas State University at San Marcos, Texas. 136 p. + attachments.

Oliver, W., and J. Pinkard, 2018, Recalibration and Predictive Simulations of the Analytical Element Tool to Evaluate the Trinity Aquifer in Hays County, Texas. Intera Technical Memorandum. April 16, 2018. 29 p.

Panday, S., 2023, MODFLOW-USG-Transport Version 2.10: Transport and Other Enhancements to MODFLOW-USG : GSI Environmental , Jan 2023 < http://www.gsi-net.com/en/software/free-software/USG-Transport.html>

PRISM Climate Group (PRISM),2022, Daily and monthly gridded precipitation data, Oregon State University, accessed online 24 August, 2022 <https://prism.oregonstate.edu> .

Rumbaugh, J. O. and D. B. Rumbaugh, 2020, Guide to Using Groundwater Vistas Version 8, Environmental Simulations Inc., Leesport, PA, 523 p., <http://www.groundwatermodels.com>.

Scanlon, B. R., Mace, R. E., Barrett, M. E., and B. Smith, 2003, Can we simulate regional groundwater flow in a karst system using equivalent porous media models? Case study, Barton Springs Edwards aquifer, USA., Journal of Hydrology: v. 276, pp. 137-158.

Singh, A., S. Mishra, R.J. Hoffpauir, A.S. Lavenue, N.E. Deeds, and C.S. Jackson, 2010, Analyzing Uncertainty and Risk in the Management of Water Resources for the State of Texas. Texas Water Development Board Report. July 2010. 106 p.

Smith, B.A., B.B. Hunt, and S.B. Johnson, 2012, Revisiting the Hydrologic Divide Between the San Antonio and Barton Springs Segments of the Edwards Aquifer: Insights from Recent Studies: Gulf Coast Association of Geological Societies Journal Vol. 1, 62nd Annual Convention, October 21-24, 2012, Austin, TX.

Smith, B.A., B.B. Hunt, A.G. Andrews, J.A. Watson, M.O. Gary, D.A. Wierman, and A.S. Broun, 2015, Hydrologic Influences of the Blanco River on the Trinity and Edwards Aquifers, Central Texas, USA, in Hydrogeological and Environmental Investigations in Karst Systems, (Eds) B. Andreo, F. Carrasco, J. Duran, P. Jimenez, and J. LaMoreaux, Environmental Earth Sciences, Springer Berlin Heidelberg, Volume 1, pp 153-161.

Smith, B.A., B.B. Hunt, D.A. Wierman, and M.O. Gary, 2018, Groundwater Flow Systems of Multiple Karst Aquifers of Central Texas. In I.D. Sasowsky, M.J. Byle, and L. Land (Eds). Proceedings of the 15th Multidisciplinary Conference on Sinkholes and the Engineering and Environmental Impacts of Karst and the 3rd Appalachian Karst Symposium, National Cave and Karst Research Institute (NCKRI) Symposium 6, p 17-29. <https://bseacd.org/uploads/Smith-et-al.-2018-GW-Flow-Systems-in-Multiple-Karst-Aquifers-Sinkhole-Conference.pdf>

Smith, B.A., and B. B. Hunt, 2019, Multilevel monitoring of the Edwards and Trinity Aquifers, in Sharp, J.M., Jr., Green, R.T., and Schindel, G.M., eds., The Edwards Aquifer: The Past, Present, and Future of a Vital Water Resource: Geological Society of America Memoir 215, p. 1–6, <https://doi.org/10.1130/2019.1215(25).>

Strategic Mapping Program (StratMap), 2023, Central Texas Lidar, 2017-01-01, accessed online April 2022 < https://tnris.org/stratmap/elevation-lidar/>

(TBWE) Texas Board of Water Engineers, 1960, Channel Gain and Loss Investigations Texas Streams 1918-1958: Bulletin 5807 D, 270p. http://www.twdb.texas.gov/ publications/reports/bulletins/doc/B5807D.pdf

Texas Water Development Board (TWDB), 2022, 2021 Regional Water Plan Water Demand Projections by County for 2020-2070 in Acre-Feet, accessed online April 30, 2022 <https://www3.twdb.texas.gov/apps/reports/Projections/2022%20Reports/demand_county>

Texas Water Development Board (TWDB), 2023, Automated Groundwater Level Wells, accessed online April 2022 < https://www.waterdatafortexas.org/groundwater>

US Geological Survey, (USGS), 2005, Geologic Map Database of Texas, Data Series 170 <https://pubs.er.usgs.gov/publication/ds170>

US Geological Survey, (USGS), 2022, personal communication via e-mail. Received November 1, 2022.

UT Austin, 2019, Surface Water-Groundwater Interaction and Water Quality of the Guadalupe River Basin and the Trinity aquifer in Western Comal County, Texas. Class Project Report. University of Texas at Austin Geology Class Geo377K/391K. Dr. Marcus Gary, Adjunct Assistant Professor. December 9, 2019. 78 p. <https://24db2da5-3e88-4566-8846-75cfa9ee8996.filesusr.com/ugd/e62693_fb415e070e394f8da3d5f13ac625e688.pdf>

Watson, J.A., B.B. Hunt, M.O. Gary, D.A. Wierman, and B.A. Smith, 2014, Potentiometric Surface Investigation of the Middle Trinity Aquifer in Western Hays County, Texas: BSEACD Report of Investigations 2014-1002, October 2014, 21 p.

Watson, J.A., A.S. Broun, B.B. Hunt, B.A. Smith, D.A. Johns, J. Camp, and D.A. Wierman, 2018, Summary of Findings: Upper Onion Creek Dye Trace, Hays County, Texas, Winter 2017. Interagency Memo. May 18, 2018. 19 p. http://bseacd.org/uploads/Upper-Onion-trace-memo_05182018.pdf

Wet Rock Geosciences (WRGS), 2017, Hydrogeologic Report of the Electro Purification, LLC Cow Creek Well Field, Report of Findings WRGS 17-001, WRGS Project No. 100-002-16. 80 p. plus appendices.

Wong, C.I., J.S. Kromann, B.B. Hunt, B.A. Smith, and J.L. Banner, 2014, Investigation of Flow Between Trinity and Edwards Aquifers (Central Texas) Using Physical and Geochemical Monitoring in Multiport Wells. Vol. 52, No. 4–Groundwater–July-August 2014 (pages 624–639).

Wierman, D.A., A.S. Broun, and B.B. Hunt (Eds), 2010, Hydrogeologic Atlas of the Hill Country Trinity Aquifer, Blanco, Hays, and Travis Counties, Central Texas: Prepared by the Hays-Trinity, Barton Springs/Edwards Aquifer, and Blanco Pedernales Groundwater Conservation Districts, July 2010, 17 plates + DVD.

Wierman, D.A., and B.B. Hunt, (2018). Groundwater Level Monitoring Results for HTGCD Transducer Wells and Wimberley Valley Public Water Supply Wells, Hays County, TX. Meadows Center for Water and the Environment, Texas State University at San Marcos, TX. https://bseacd.org/uploads/Wierman-and-Hunt-2018-TSU-Water-Levels_revised.pdf

Wierman, D.A., Walker, J., and T.S. Udita, 2019, How Much Water is in the Guadalupe? A Baseflow Analysis, Meadows Center for Water and the Environment, Texas State University at San Marcos, TX. 52 p. https://gato-docs.its.txst.edu/jcr:c39ea6a9-6537-4d16-bd82-8f323b5f6c76